Supporting Information

Multi-site esterification: A tunable, reversible strategy to tailor therapeutic peptides for delivery

Mark S. Bannon[1], Jeffrey F. Ellena[2], Aditi S. Gourishankar[1], Spencer R. Marsh[3], Dilza T. Silva,[4] Nicholas E. Sherman,[4] L. Jane Jourdan[3], Robert G. Gourdie[3], and Rachel A. Letteri[1]*

[1]Department of Chemical Engineering, University of Virginia, Charlottesville, VA, 22903, USA
[2]Biomolecular Magnetic Resonance Facility, School of Medicine, University of Virginia, Charlottesville, VA, 22903, USA
[3]Fralin Biomedical Institute at Virginia Tech Carillion School of Medicine, Roanoke, VA, 24016, USA
[4]Biomolecular Analysis Facility, School of Medicine, University of Virginia, Charlottesville, VA, 22903, USA

Table of Contents

Section S1: Fischer Esterification of αCT11

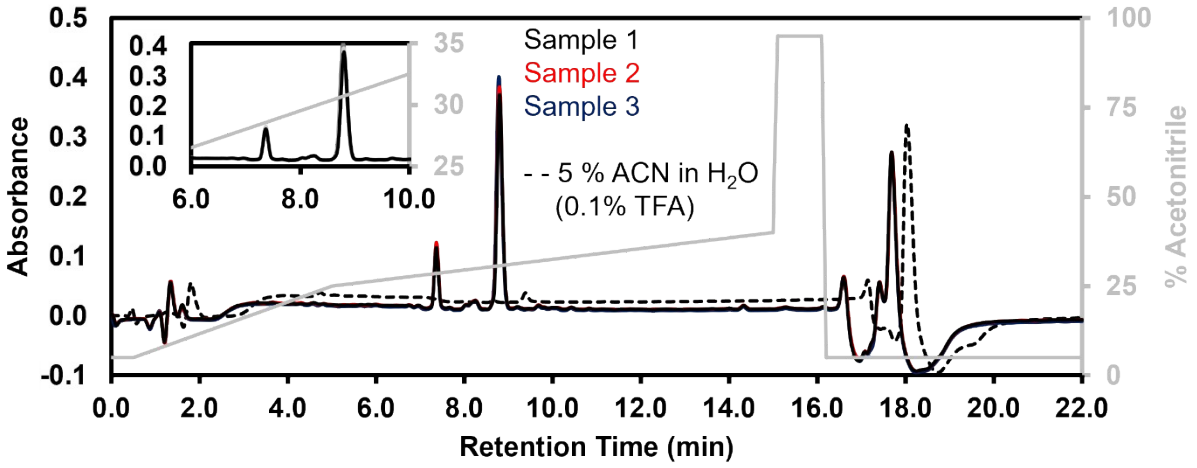

Figure S1. RP-HPLC chromatograms of αCT11 Fischer esterification replicates, showing 3 independently set up reaction mixtures. The peptide eluted between 25% and 40% acetonitrile (ACN) in each different reaction, with the produced peaks overlapping each other. Mobile phase composition (% ACN, gray) is plotted against normalized retention time in each RP-HPLC chromatogram.

Table S1. RP-HPLC mobile phase gradient

Mobile Phase Stages	Time (min)		Mobile Phase Composition	
	Analytical	Preparative	% Water + 0.1% TFA (A)	% Acetonitrile + 0.1% TFA (B)
Warm up	0	0	95	5
Ramp up	0.5	2.6	95	5
Elution	5	25.2	77	23
Purge	15	50.2	74	26
	15.1	50.7	5	95
	16.1	60.0	5	95
Equilibration	16.2	60.6	95	5
	22	70.0	95	5

In this study, our RP-HPLC mobile phase gradients had five stages. First was the warm-up stage, where the system was equilibrated for 30 s with a mobile phase composition of 95% water + 0.1% trifluoroacetic acid (TFA) (mobile phase A) and 5% acetonitrile + 0.1% TFA (mobile phase B). During the ramp-up stage, the % B in the mobile phase was increased linearly to 23% over 4.5 min. In the elution stage, the % B was further increased linearly to 26% over 10 min to elute the sample from the column. To remove any bound solute from the column, we then increased the % B to 95% linearly and held at that composition for 1 min, in the purge phase of the elution. Finally, the equilibration phase

was used to prepare the system for the next injection, where the % B was reset to 5% and held there until the end of the run. The flowrates of mobile phase in the analytical and preparative-scale RP-HPLC systems were 1 mL/min and 25.52 mL/min, respectively.

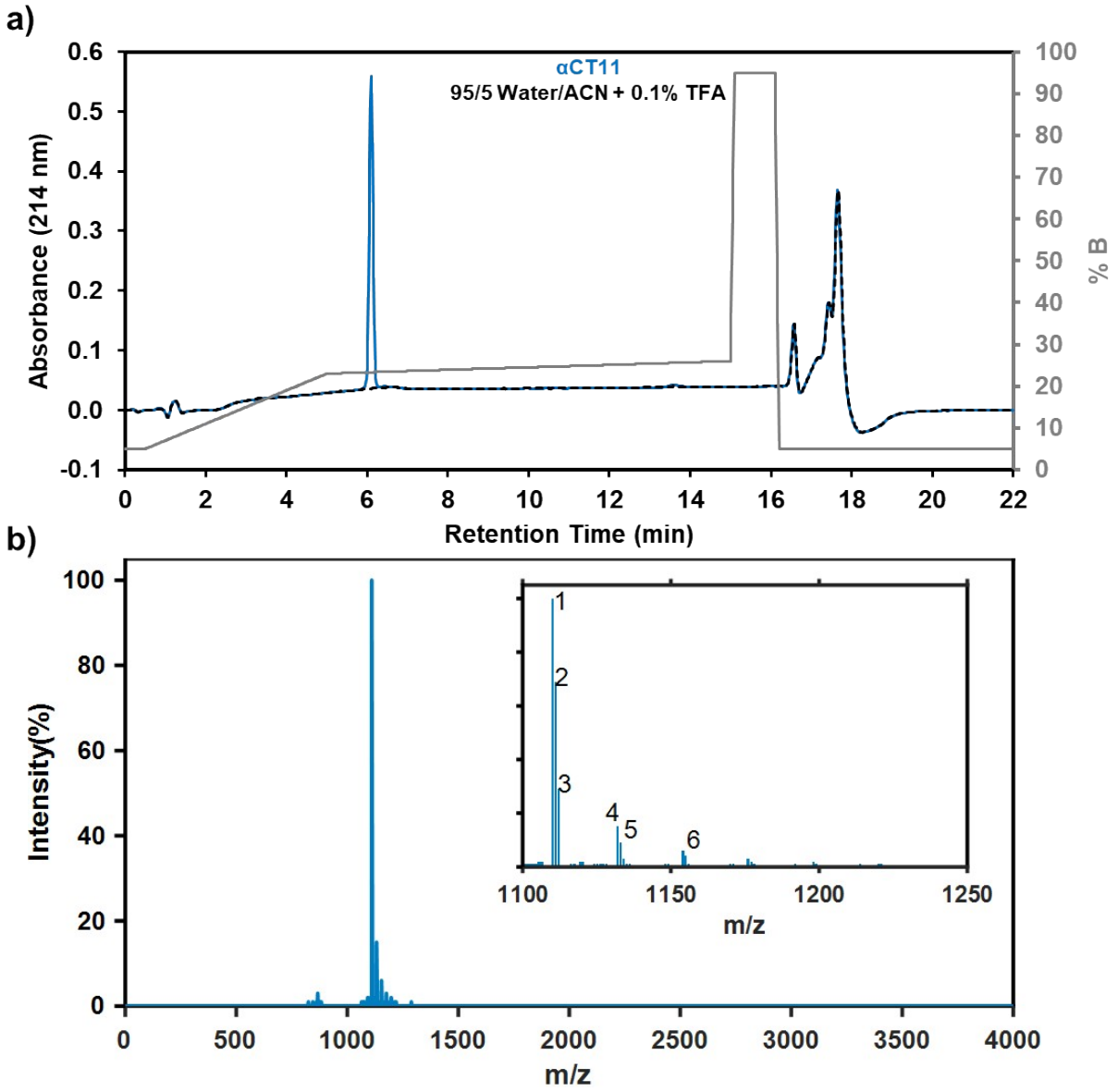

label	Mass (Da)	Intensity (%)	Species
1	1110	100	[αCT11 + H]+
2	1111.1	69	
3	1112.1	29	
4	1132.1	15	[αCT11 + Na]+
5	1133.1	9	
6	1154.1	6	[αCT11 + 2Na - H]+

Figure S2. a) RP-HPLC chromatogram and **b)** MALDI-TOF MS of αCT11. In MALDI-TOF, $[\alpha CT11+2Na-H]^+$ indicates that one of the originally protonated carboxylic acids now carries a sodium counterion.

Table S2. Installed methyl ester number and position, normalized retention times of the products in each gradient, and percent peak area of αCT11 and its esterified products

αCT11 Product	# of methyl esters installed	Esterified Residues	COOH Residues	Normalized Retention Time (τ)	Percent Peak Area
αCT11	0	N/A	D5, D6, E8, I9	0	N/A
2OMe	2	*Not Determined		0.22	1
3OMe(A)	3	D5, D6, E8	I9	0.35	19
3OMe(B)	3	D5, D6, I9	E8	0.69	4
3OMe(C)	3	D6, E8, I9	D5	0.70	
3OMe(D)	3	D5, E8, I9	D6	0.74	
4OMe	4	D5, D6, E8, I9	N/A	1.00	74

*Ester positions were not able to be determined by ^{1}H NMR spectroscopy (insufficient amounts isolated)

Table S3. Calculated molecular mass of αCT11 with various numbers of esters, charge (z) = 1

Sample:	**αCT11**	**αCT11-1OMe**	**αCT11-2OMe**	**αCT11-3OMe**	**αCT11-4OMe**
Exact Mass:	1109.6	1123.6	1137.6	1151.6	1165.7
[M + H]+	1110.6	1124.6	1138.6	1152.6	1166.7
[M + Na]+	1132.6	1146.6	1160.6	1174.6	1188.7
[M + K]+	1148.6	1162.6	1176.6	1190.6	1204.7
[M + 2Na - H]+	1154.6	1168.6	1182.6	1196.6	
[M + K + Na - H]+	1170.6	1184.6	1198.6	1212.6	
[M + 1 imide + H]+	1092.6	1106.6	1120.6	1134.6	
[M + 1 imide + Na]+	1114.6	1128.6	1142.6	1156.6	
[M + 1 imide + K]+	1130.6	1144.6	1158.6	1172.6	
[M + 2 imide + H]+	1074.6	1088.6	1102.6		
[M + 2 imide + Na]+	1096.6	1110.6	1124.6		
[M + 2 imide + K]+	1112.6	1126.6	1140.6		
[M + 3 imide + H]+	1056.6	1070.6			
[M + 3 imide + Na]+	1078.6	1092.6			
[M + 3 imide + K]+	1094.6	1108.6			

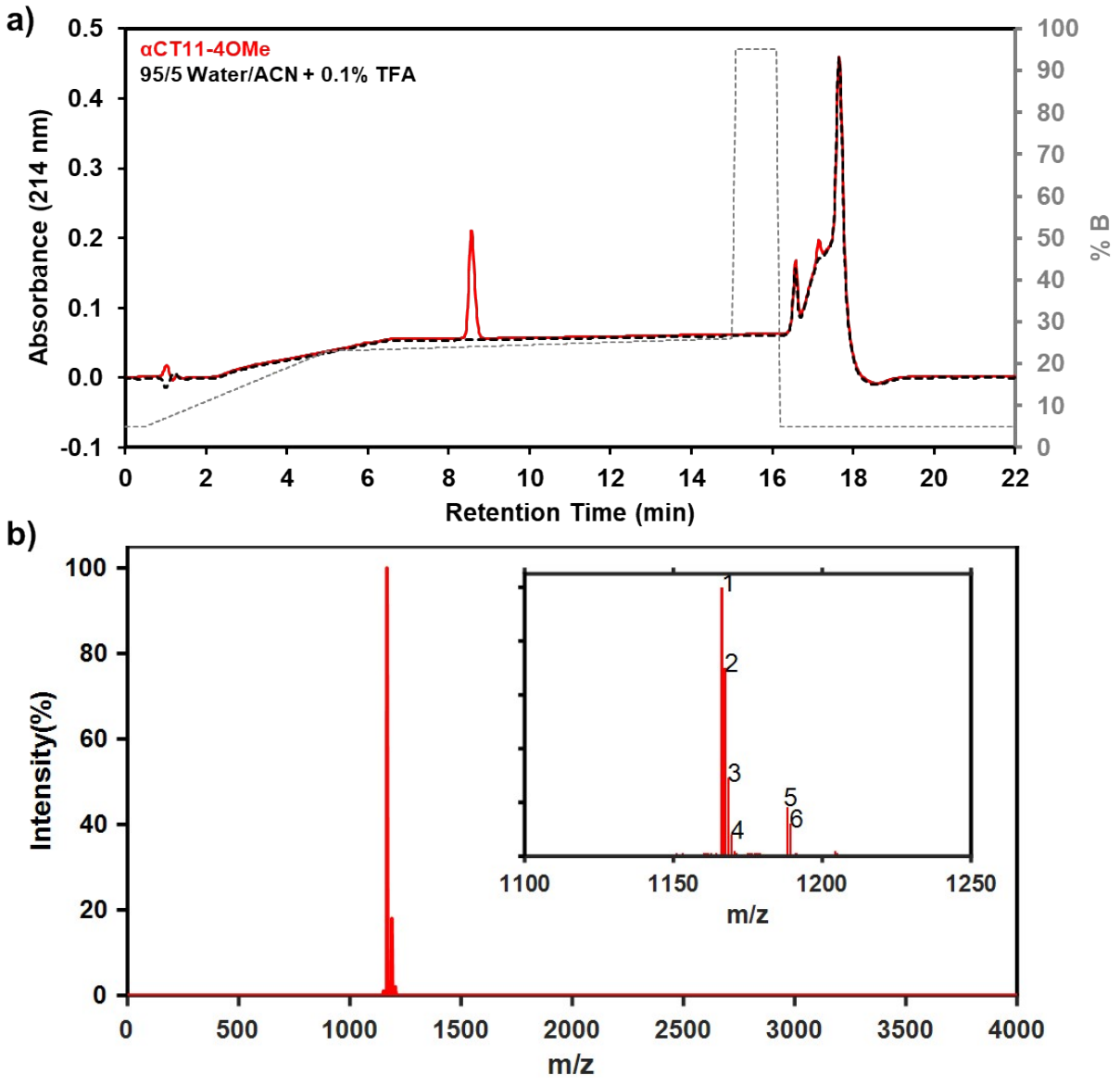

label	Mass (Da)	Intensity (%)	Species
1	1166.3	100	[αCT11-4OMe + H]+
2	1167.3	70	
3	1168.4	29	
4	1169.4	8	
5	1188.3	18	[αCT11-4OMe + Na]+
6	1189.3	12	

Figure S3. a) RP-HPLC chromatogram and **b-c)** MALDI-TOF MS of αCT11-4OMe.

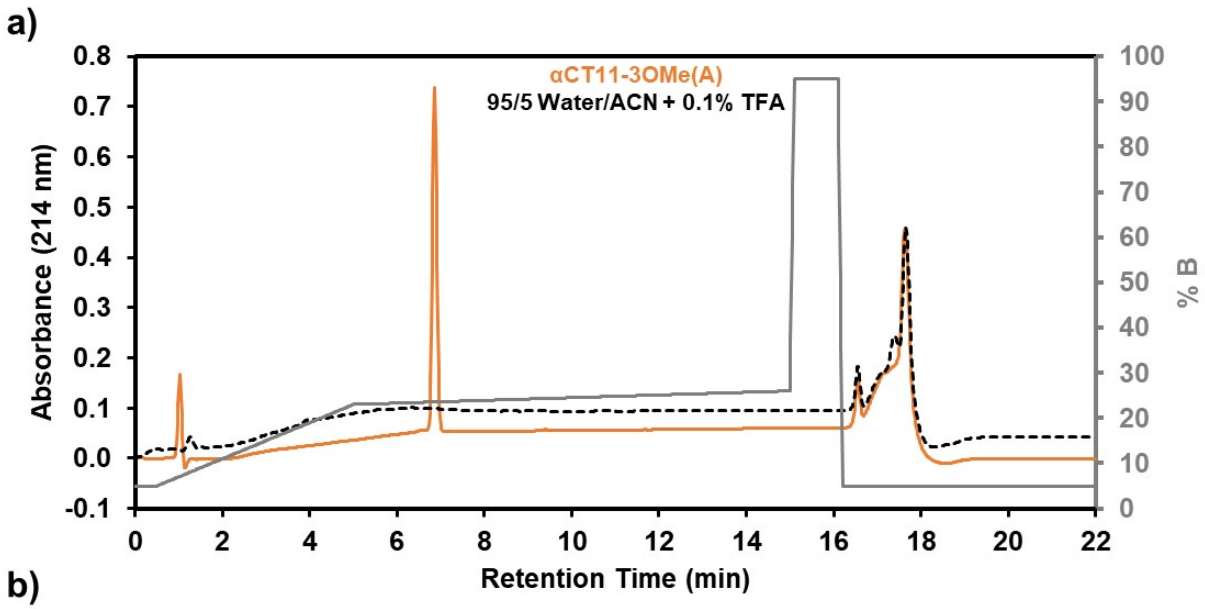

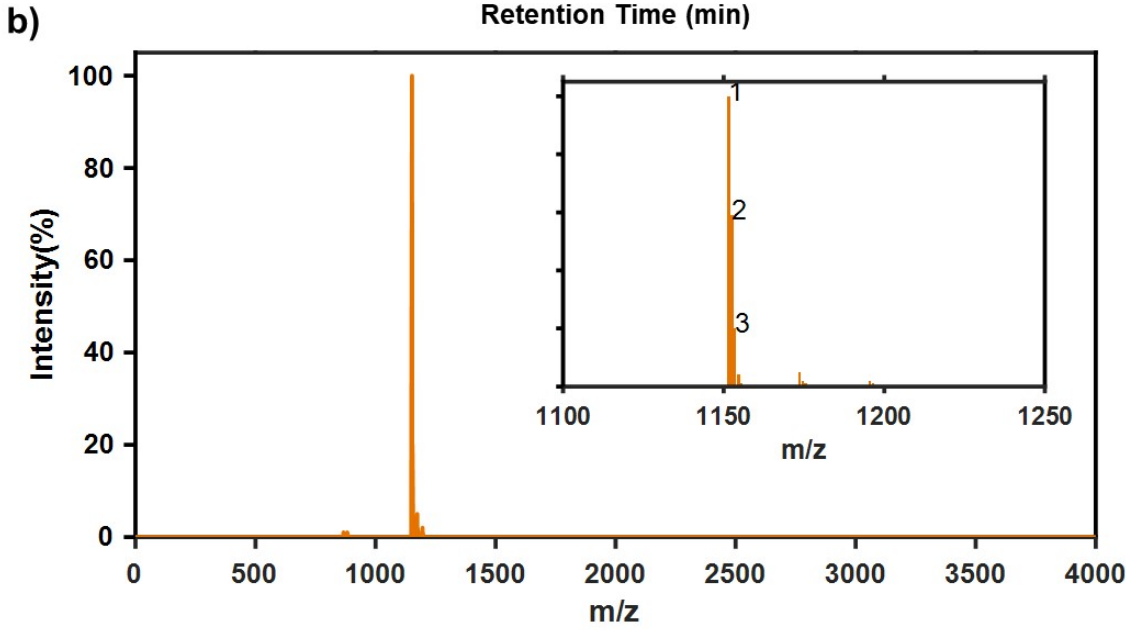

label	Mass (Da)	Intensity (%)	Species
1	1151.6	100	[αCT11-3OMe + H]+
2	1152.6	59	[αCT11-3OMe + H]+
3	1153.6	20	[αCT11-3OMe + H]+

Figure S4. a) RP-HPLC chromatogram and **b)** MALDI-TOF MS of αCT11-3OMe(A), with $[3OMe+2Na-H]^+$ indicating that one of the originally protonated carboxylic acids now carries a sodium counterion.

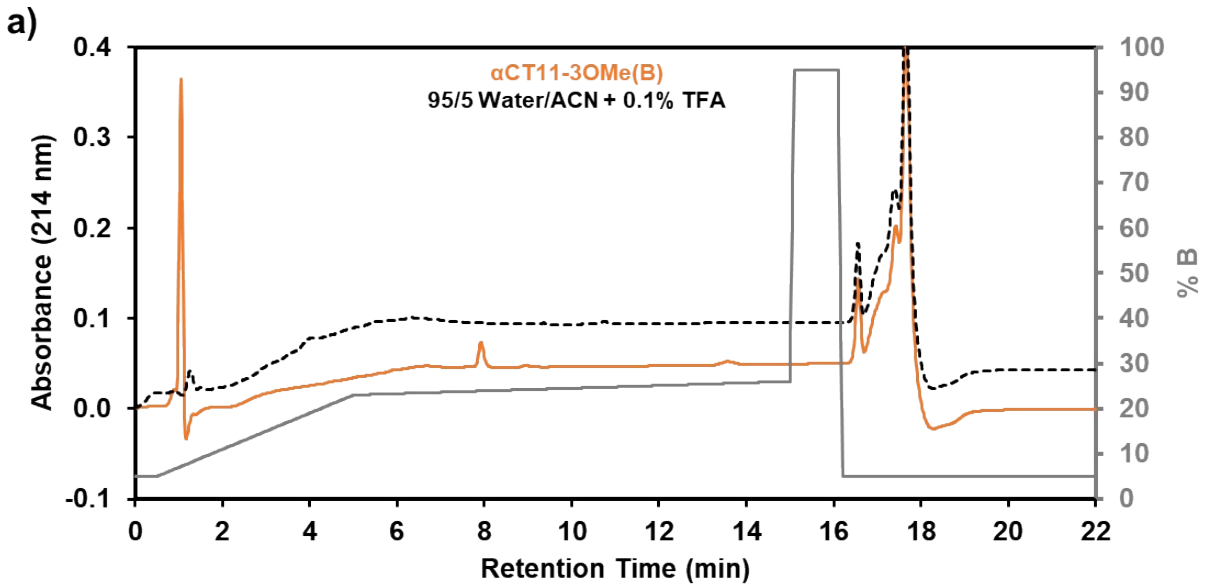

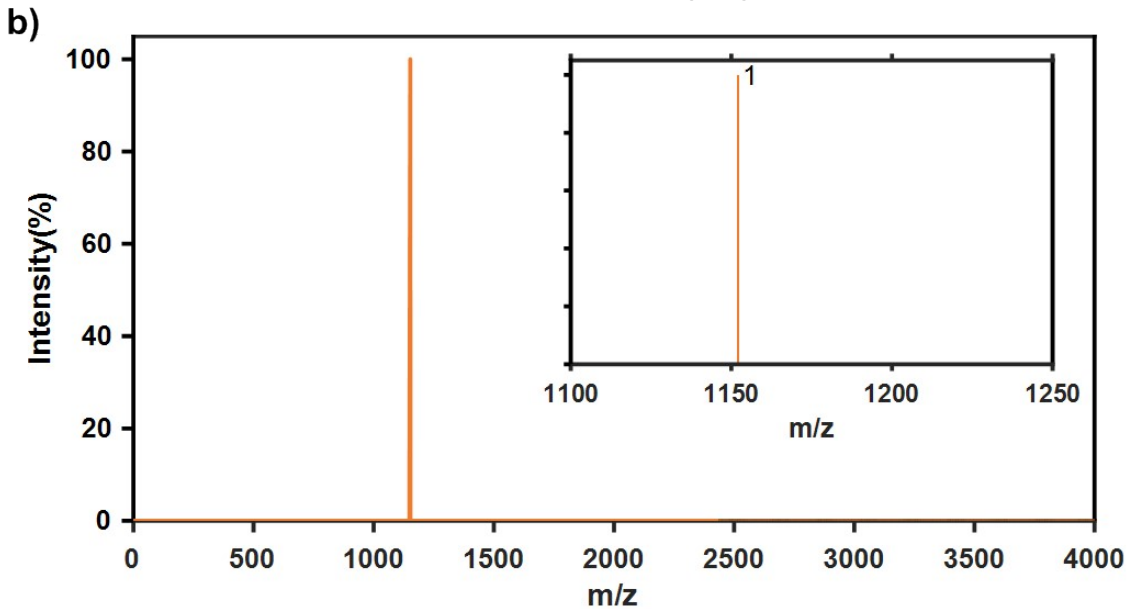

label	Mass (Da)	Intensity (%)	Species
1	1152.2	100	[αCT11-3OMe + H]+

Figure S5: a) RP-HPLC chromatogram and **b)** MALDI-TOF MS of αCT11-3OMe(B)

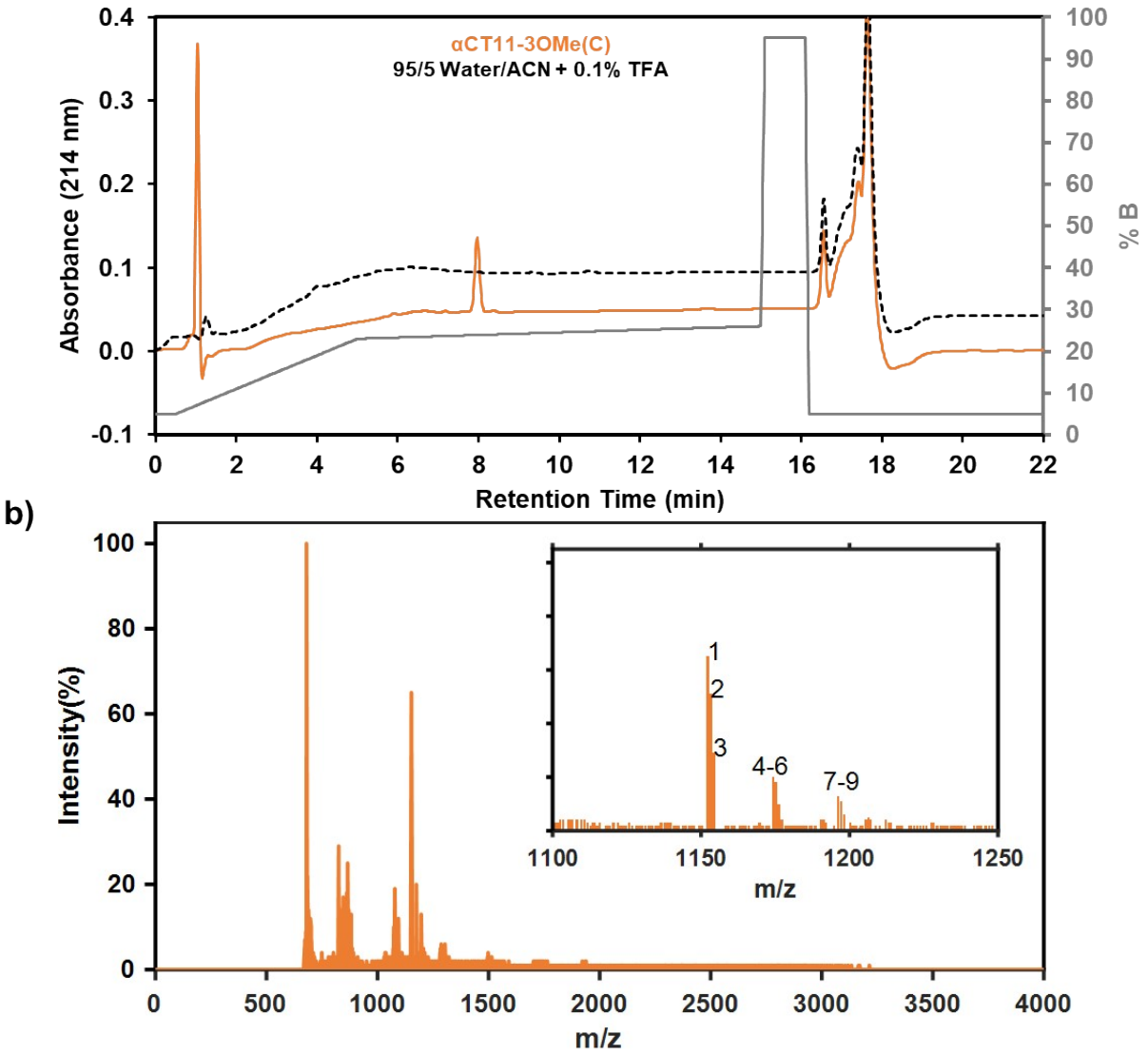

label	Mass (Da)	Intensity (%)	Species
1	1152.3	65	[αCT11-3OMe + H]+
2	1153.3	51	
3	1154.3	29	
4	1174.4	20	[αCT11-3OMe + Na]+
5	1175.2	18	
6	1176.2	10	
7	1196.3	13	[αCT11-3OMe + 2Na - H]+
8	1197.2	11	
9	1198.2	6	

Figure S6: a) RP-HPLC chromatogram (gradient 2) and **b)** MALDI-TOF MS plot of αCT11-3OMe(C).

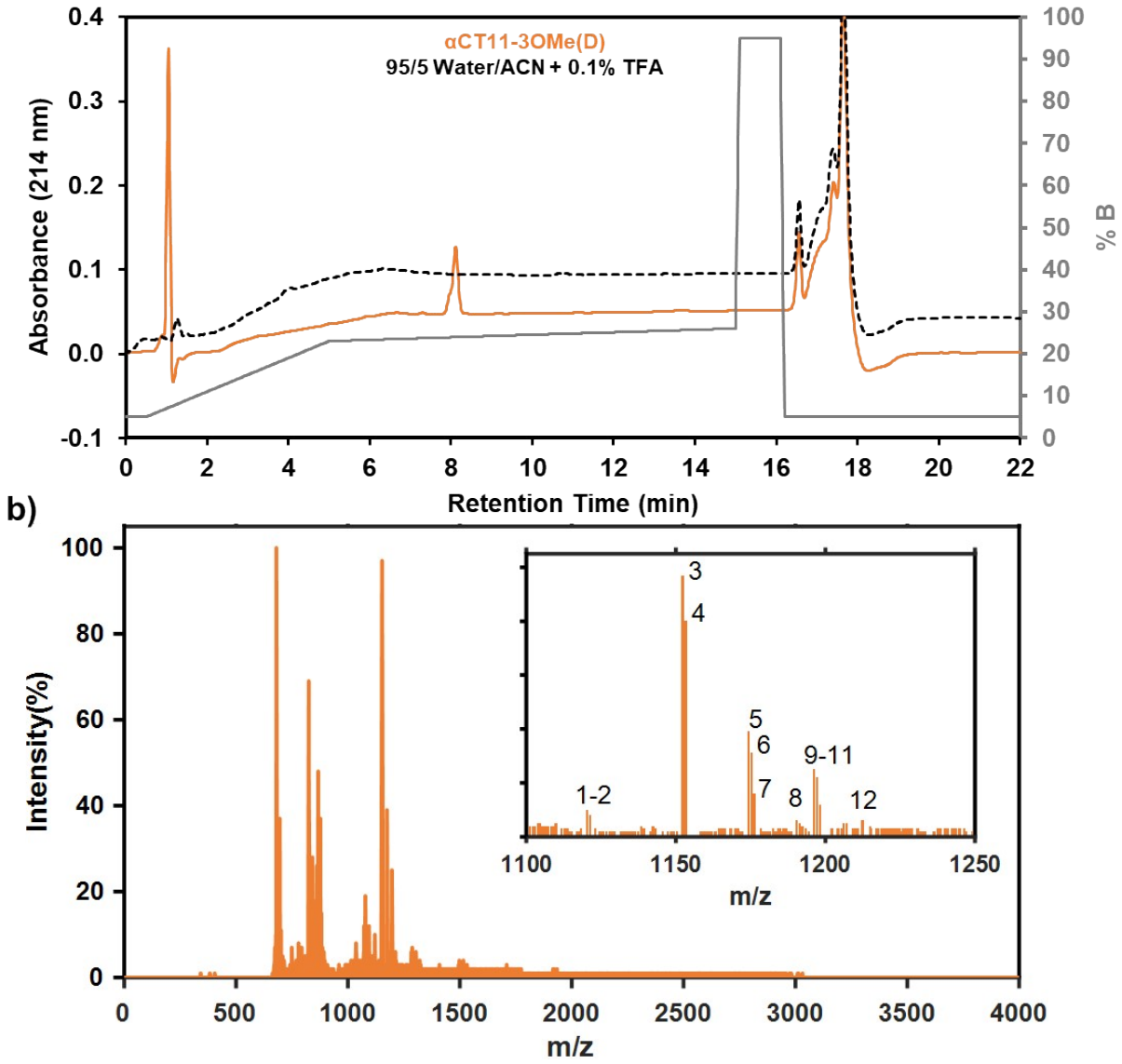

label	Mass (Da)	Intensity (%)	Species
1	1120.3	10	[αCT11-2OMe + 1 imide + H]+
2	1121.3	8	
3	1152.3	97	[αCT11-3OMe + H]+
4	1153.3	80	
5	1174.4	39	[αCT11-3OMe + Na]+
6	1175.3	31	
7	1176.2	16	
8	1190.3	6	[αCT11-3OMe + K]+
9	1196.3	25	[αCT11-3OMe + 2Na - H]+
10	1197.3	22	
11	1198.2	12	
12	1212.4	6	[αCT11-3OMe + K + Na - H]+

Figure S7. a) RP-HPLC chromatogram (gradient 2) and **b)** MALDI-TOF MS of αCT11-3OMe(D).

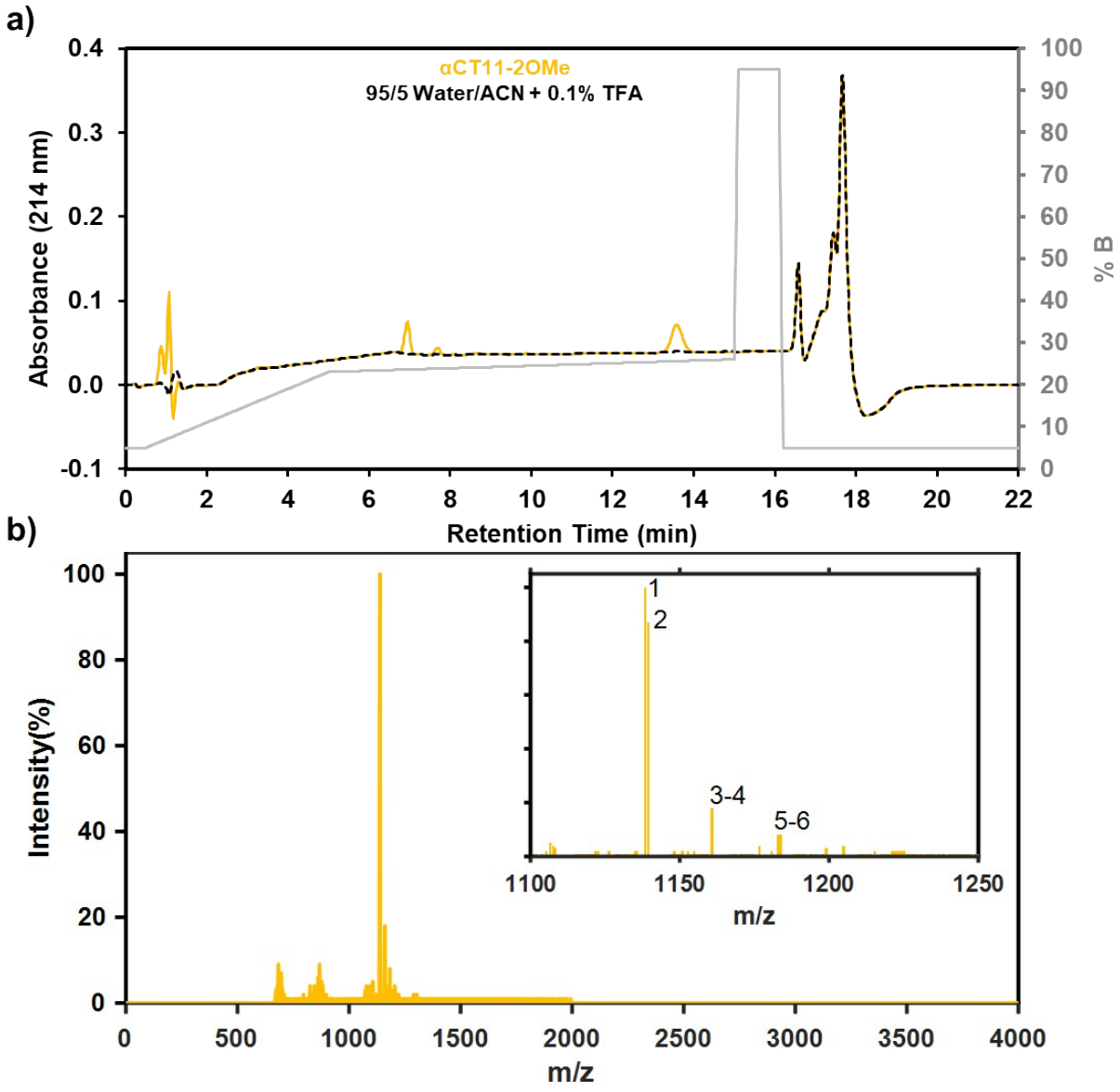

label	Mass (Da)	Intensity (%)	Species
1	1138.5	100	[αCT11-2OMe + H]+
2	1139.5	87	
3	1160.8	18	[αCT11-2OMe + Na]+
4	1161.6	18	
5	1182.8	8	[αCT11-2OMe + 2Na - H]+
6	1183.7	8	

Figure S8: a) RP-HPLC chromatogram and **b)** MALDI-TOF MS of αCT11-2OMe.

Section S2: Establishing ester position with 2D nuclear magnetic resonance (NMR) spectroscopy

To assign the methyl ester αCT11-4OMe protons and carbons (**Figure S9**), we used 1D ^{1}H (**Figure S10-12**) and ^{13}C (**Figure S13**) spectra together with 2D H-H total correlation spectroscopy (TOCSY, **Figures S14-15**), H-H nuclear Overhauser effect spectroscopy (NOESY, **Figure S16**), H-H clean in-phase correlation spectroscopy (CLIP COSY, **Figures S17-20**), and H-C heteronuclear multiple bond correlation (HMBC, **Figures S21-24**). For reference, the H and C chemical shifts and the H integrations and numbers are listed in **Table S4**. Towards assigning the D5 and D6 Cγ, E8 Cδ, and I9 C carbonyls in the ^{13}C spectrum for correlation with the methyl ester proton resonances, we first used TOCSY to separate each H resonance into their individual spin system, which contains all the H resonances connected in a continuous chain of protonated nuclei. For example, the D5 C backbone carbonyl is not bound to a proton and therefore serves as a spin system boundary, separating the D5 and D6 spin systems. Conveniently, the H resonances within a given amino acid are in the same spin system. **Therefore, we assigned some of the amide/amine proton resonances (HN, Hε, 7.7 – 8.3 ppm) as belonging to either a R, D, E, or L/I residue spin system by considering the number of backbone-sidechain correlations with H resonances between 0 – 4.7 ppm** (**Figure S14**). For example, we found the E8 HN (7.91 ppm) to have 4 unique correlations: 1 in the Hα region (4.0 – 4.7 ppm), 1 around the expected shift of the E8 Hγ resonance (2.32 ppm), and 2 around the expected shifts of the E8 Hδ resonances (~1.8 ppm). **However, we were unable to distinguish between R1 and R3, D5 and D6, or L7 and I9 resonances due to the similar number and chemical shifts of these correlations in the TOCSY spectrum. We assigned the R1 HN (8.17 ppm) because the amine-water H exchange caused it to appear as a broad singlet instead of a doublet split by the adjacent Hα. The TOCSY spectrum also showed HN - Hε correlations for both R1 and R3 in the amide/amine region of the spectrum, allowing us to assign the R1 and R3 HN (8.17 and 8.24 ppm) and Hε (7.83 and 7.71 ppm) resonances (Figure S15).**

To assign the D5, D6, L7, and I9 Hs, we next used NOESY, which shows correlations between protons that are close to each other in space, suspecting it would reveal interactions between amide/amine protons on adjacent amino acids. We observed a correlation in the amide/amine (HN and R Hε) region (7.7 – 8.3 ppm) of the NOESY spectrum (**Figure S16**) between what TOCSY showed to be either the D5 or D6 HN and either the L7 or I9 HN. Because D6 is next to L7 in the peptide sequence, this correlation allowed us to assign the D6 and L7 HN, and by the process of elimination D5 and I9 Hs. **In all, NOESY revealed D5-D6, D6-L7, L7-E8, and E8-I9 HN-HN correlations, which allowed us to assign the remaining HN resonances.**

With the HNs and Hε resonances assigned, we next moved to COSY, which displays correlations between protons on adjacent nuclei, with the goal of assigning the I9 Hα (4.17 ppm) and the D5/D6 Hßs (2.57 – 2.75 ppm), which were each 3 bonds away from their respective methyl ester carbonyl Cs, and could therefore be used to assign said carbonyl Cs with selHMBC. To enhance the signal intensities, we used CLIP COSY.

To assign the Hα resonances, we plotted the now assigned *H*N and Hε region (7.7 – 8.3 ppm) against the Hα region (4.0 – 4.7 ppm) (Figure S17), where correlations allowed us to assign the D5 Hα (4.54 ppm), D6 Hα (4.58 ppm), E8 Hα (4.32 ppm), and I9 Hα (4.17 ppm) resonances. We also used CLIP-COSY correlations to assign the D5/D6 Hßs (2.57 – 2.75 ppm) through their respective correlations with the now-assigned Hα region (4.0 - 4.7 ppm) (Figure S18). The D5 and D6 Hα protons split the adjacent Hß resonances, and CLIP-COSY showed each of part of the split D5 and D6 Hß resonances to correlate with the respective Hα resonances. **After assigning the E8 Hα resonance, we were able to assign the E8 Hß resonances (1.8 and 1.90 ppm) (Figure S19) and, subsequently, the E8 Hγ resonance (2.32 ppm) (Figure S20) through their respective correlations.**

Finally, to assign the carbonyl Cs in the ^{13}C spectrum of αCT11-4OMe, we used selHMBC, which measures correlations between protons and carbons separated by 2-4 bonds within a specified region of the spectrum, as HMBC did not offer enough resolution in the ^{13}C dimension to confidently assign each peak, specifically the D5 and D6 Cγ resonances (**Figure S21**). As a reference for the αCT11-4OMe selHMBC spectrum, which was collected only in the carbonyl region (165 – 175 ppm), we used the L7 Hα-carbonyl C correlation (4.25-171.61 ppm) (**Figure S22**). As we had already assigned the relevant I9 Hα resonance, the D5/D6 Hß resonances, and the E_8 Hγ resonances, we used observed correlations in selHMBC to assign the respective carbonyl Cs, specifically the D5/D6 Cγ, E8 Cδ, and I9 Cs. **Plotting the Hα region of the ^{1}H spectrum (4.0 – 4.7 ppm) against carbonyl C region of the ^{13}C spectrum, in which we observed Hα - C correlations, allowed us to assign the D5 C (170.23 ppm), D5 Cγ (170.68 ppm), D6 C (169.75), D6 Cγ (170.68 ppm), and I9 C (171.76) resonances (Figure S23).** The observed methyl ester -OCH_3 - Cγ correlations (**Figure 1i**) allowed us to distinguish the D6 backbone and side chain carbonyls, the former of which was 6 bonds away from the methyl ester -OCH_3, and would not have produced a selHMBC correlation. **We then used the E8 Hγ - Cδ correlation to assign the E8 Cδ resonance (Figure S24).** After assigning all the relevant carbonyl C resonances, we were then able to use their selHMBC correlations with their respective D5, D6, E8, and I9 methyl ester -OCH_3 resonances to assign each singlet in the αCT11-4OMe ^{1}H spectrum (Figure 1i).

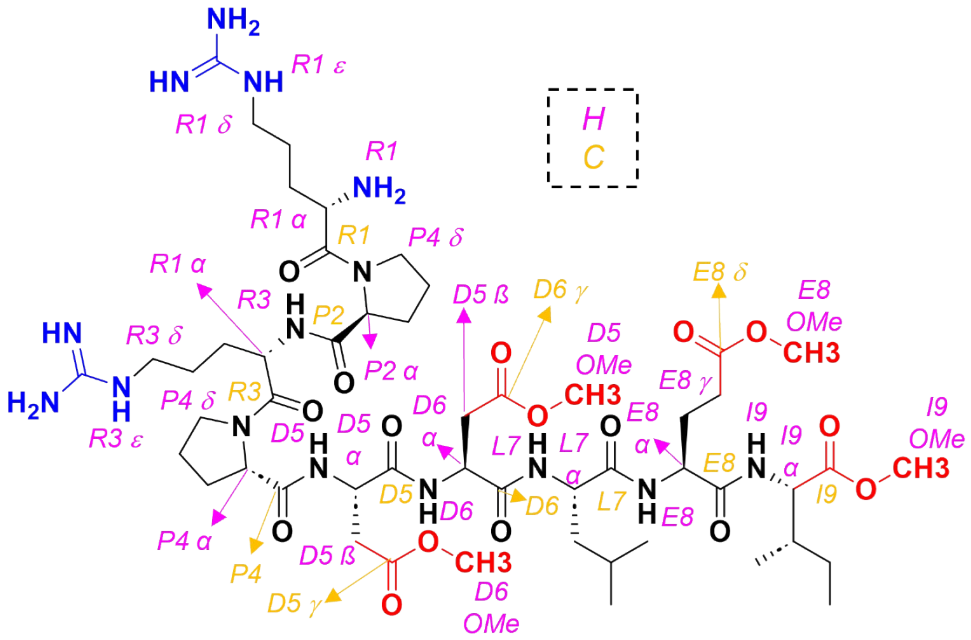

Figure S9. Chemical structure of αCT11-4OMe. Relevant ^{1}H (pink) and ^{13}C (yellow) atoms are labeled within the structure, and ester groups (red) and positively charged groups (blue) are also highlighted.

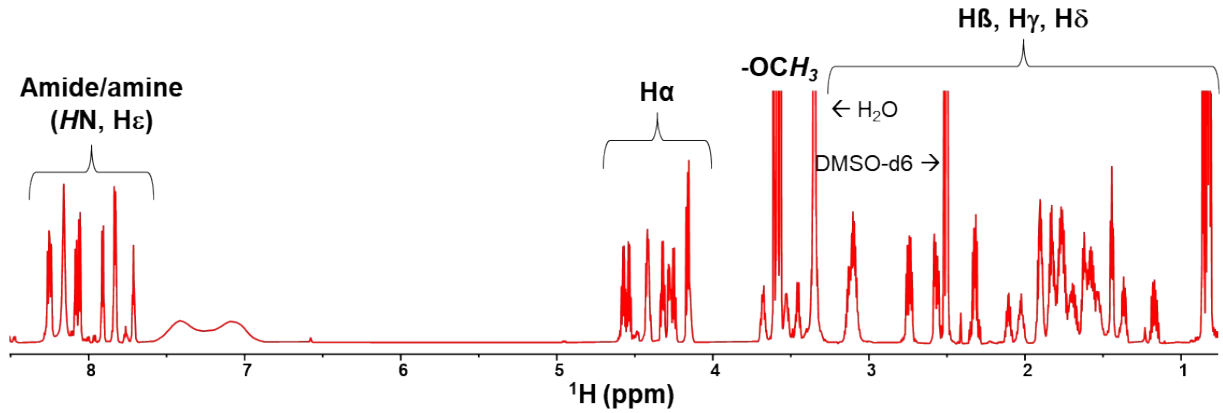

Figure S10. ^{1}H NMR spectrum of αCT11-4OMe (0.75 – 8.50 ppm).

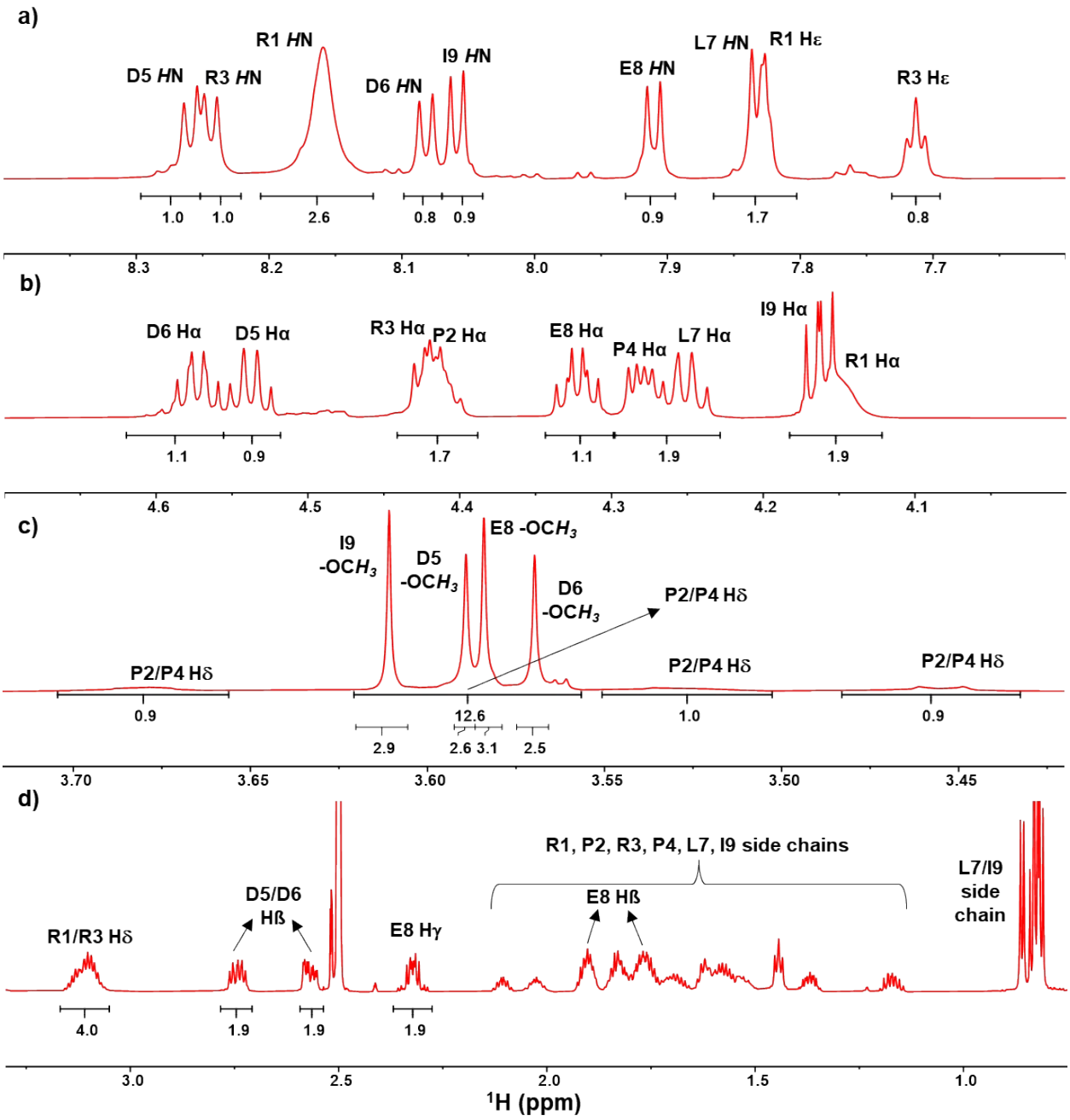

Figure S11. Expanded select regions of the αCT11-4OMe ^{1}H NMR spectrum. The **a)** amide/amine (HN, Hε) (7.6 – 8.4 ppm), **b)** Hα (4.0 – 4.7 ppm), **c)** methyl ester H (-OCH_3) and proline Hδ (3.4 – 3.7 ppm), and **d)** the Hß, Hγ, and Hδ (0.75 – 3.50 ppm) regions are shown.

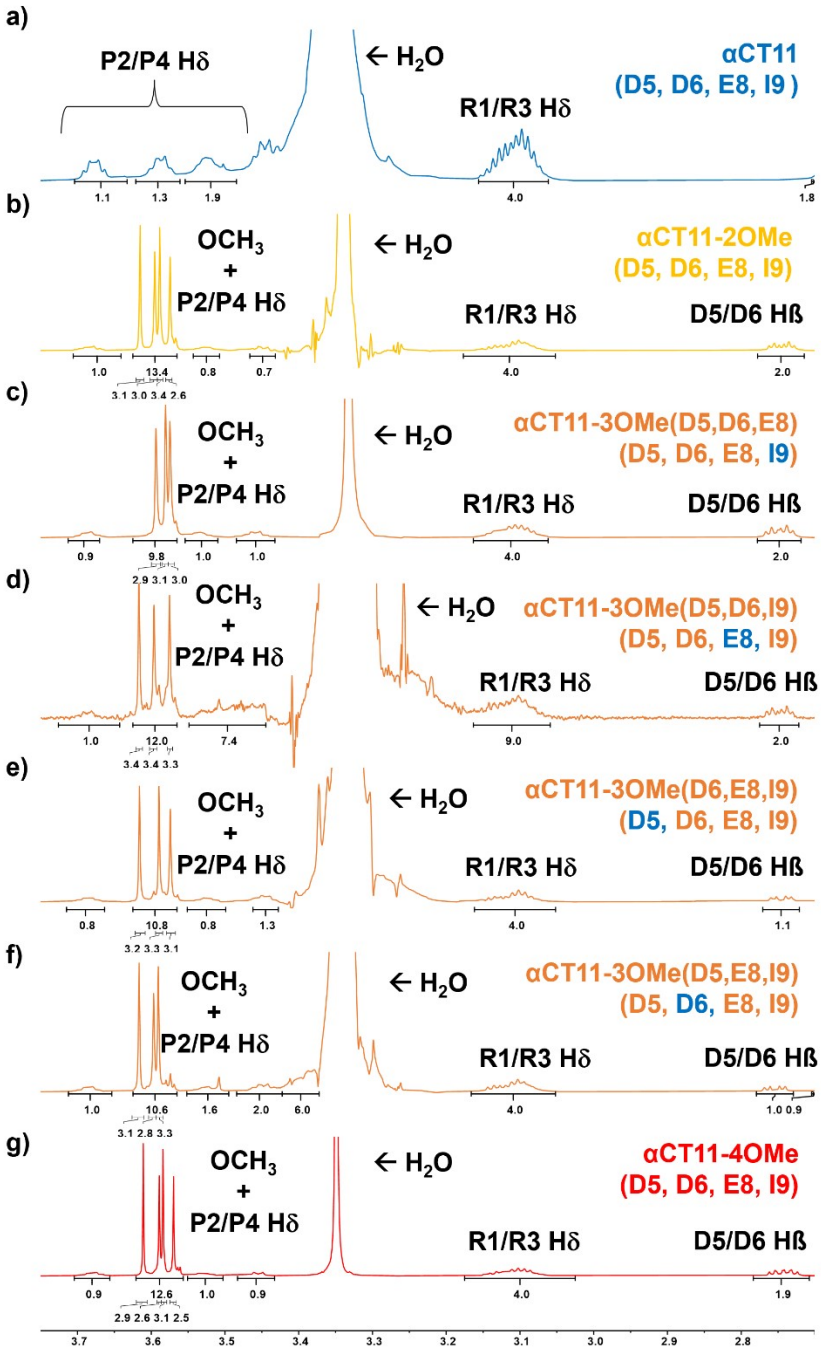

Figure S12. ^{1}H NMR spectrum of αCT11 and esterified variants (2.7 – 3.75 ppm). Only proline Hδ resonances were observed in the region that methyl ester H singlets were observed in the esterified ^{1}H spectra (3.55 – 3.64 ppm). For each esterified spectrum, both the total methyl ester H region and the individual peaks were integrated to show the presence of the proline Hδ proline, which is overlapped by the methyl ester H singlets. All methyl ester peaks integrate to 3 protons; however, in (**d-f**) the αCT11-3OMe samples with an esterified I9 residue, lower concentrations of sample led to higher baseline noise and slightly higher integrals than expected (9 methyl ester Hs + 1 proline Hδ = 10 Hs). The αCT11-2OMe spectrum contained peaks from all the possible esterified methyl esters, suggesting this product is a mixture of αCT11 with different combinations of 2 methyl esters esterified.

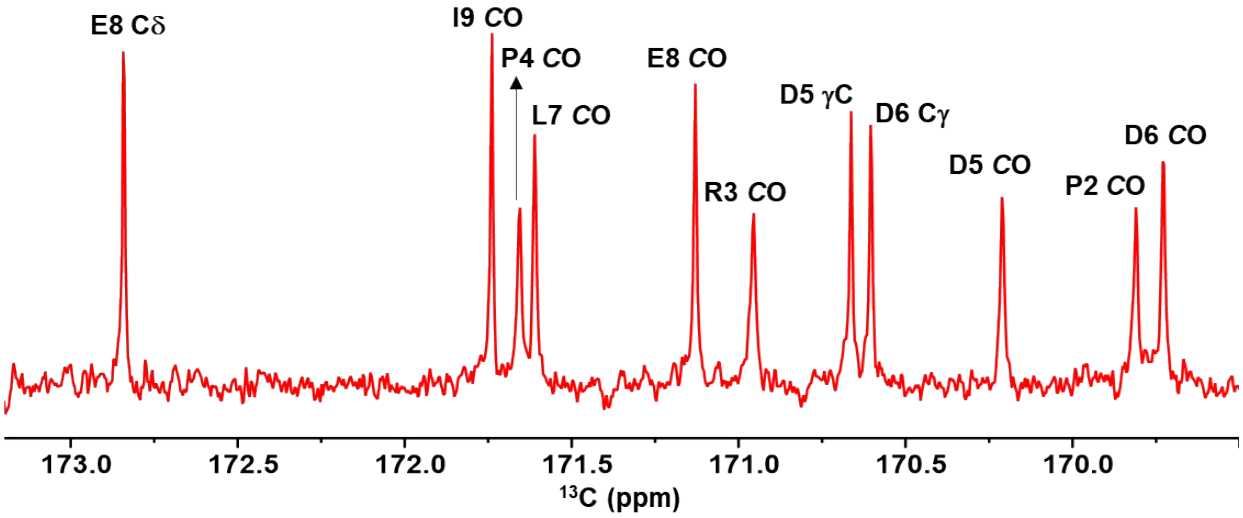

Figure S13. Carbonyl carbon region of the αCT11-4OMe ^{13}C NMR spectrum (169.5 – 173.2 ppm).

Table S4. Chemical shifts of relevant ^{1}H and ^{13}C in αCT11-4OMe

Amino Acid	Atom	Chemical Shift (ppm)	Integral	# of protons
R1	HN	8.17	2.6	3
	Hα	4.17	1.0	1
	Hδ	3.11	2*	
	Hε	7.83	0.9	1
P2	Hα	4.41	0.9	1
	Hδ	3.68 - 3.45	Not isolatable**	2
	CO	169.83	N/A	N/A
R3	HN	8.24	1.0	1
	Hα	4.41	0.9	1
	Hδ	3.11	2*	
	Hε	7.71	0.8	1
	CO	170.98	N/A	
P4	Hα	4.29	1.0	1
	Hδ	3.68 - 3.45	Not isolatable**	2
	CO	171.68	N/A	N/A
D5	HN	4.54	1.0	1
	Hα	4.54	0.9	1
	Hß	2.75	1.0	1
		2.57	1.0	1
	CO	170.23	N/A	
	Cγ	**170.68**	**N/A**	
	OCH_3	**3.59**	**2.6**	**3**
D6	HN	8.08	0.8	1
	Hα	4.58	1.1	1
	Hß	2.75	1.0	1
		2.57	1.0	1
	CO	169.75	N/A	
	Cγ	**170.62**	**N/A**	
	OCH_3	**3.57**	**2.5**	**3**

L7	HN	7.83	0.9	1
	Hα	4.24	1.0	1
	CO	171.63	N/A	
E8	HN	7.91	0.9	1
	Hα	4.32	1.1	1
	Hγ	2.32	1.9	2
	Hß	1.90	Not isolatable***	-
		1.77	Not isolatable***	-
	CO	171.15	N/A	
	Cδ	**172.86**	N/A	
	OCH_3	**3.58**	**3.1**	**3**
I9	HN	8.06	0.9	1
	Hα	4.17	1.0	1
	CO	**171.76**	**N/A**	
	OCH_3	**3.61**	**2.9**	**3**

*Set as the reference integration
**Peak was either not able to be individually assigned (P2/P4 Hδ)
***Peaks were not able to be integrated separately from neighboring peaks (E8 Hß)

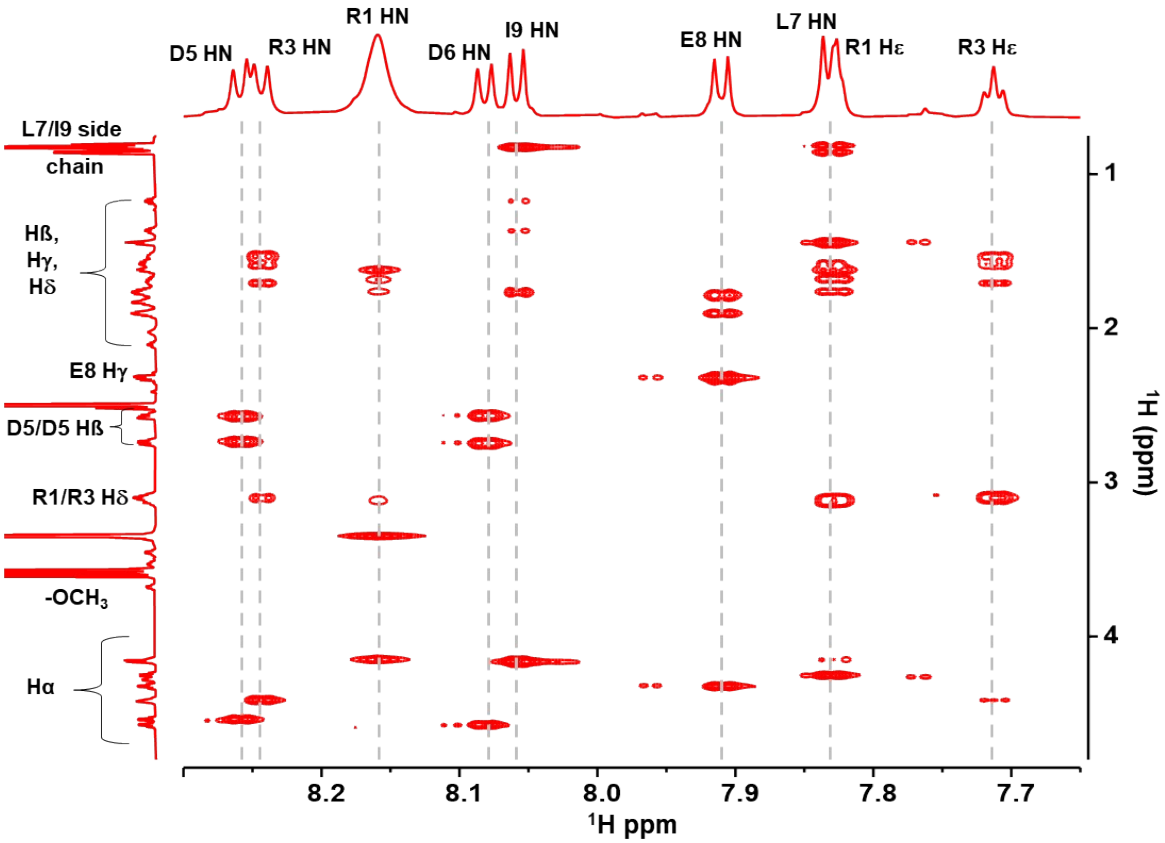

Figure S14. Total correlation spectroscopy (TOCSY) of αCT11-4OMe: HN & Hε region (7.65 – 8.3 ppm) x Hα, Hß, Hγ, Hδ, and methyl ester H region (0.75 – 4.7 ppm). Dashed vertical lines are shown to guide the eye along the spin systems of the peptide, which were used to assign the HN and Hε resonances (x-axis).

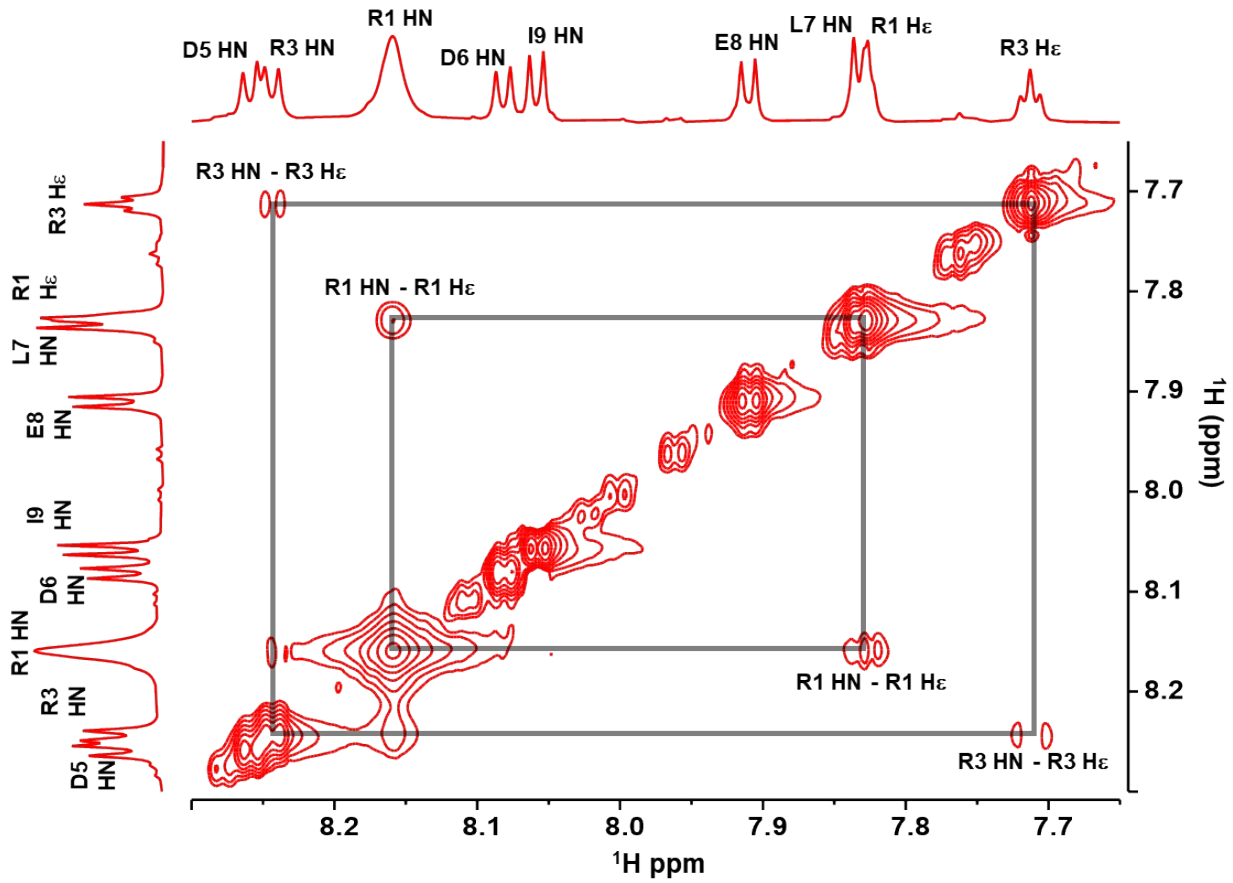

Figure S15. TOCSY of αCT11-4OMe: HN & Hε region (7.65 – 8.30 ppm) x HN & Hε region. Correlations between the R1/R3 HN – Hε correlations were used to assign R1 and R3 HN and Hε resonances.

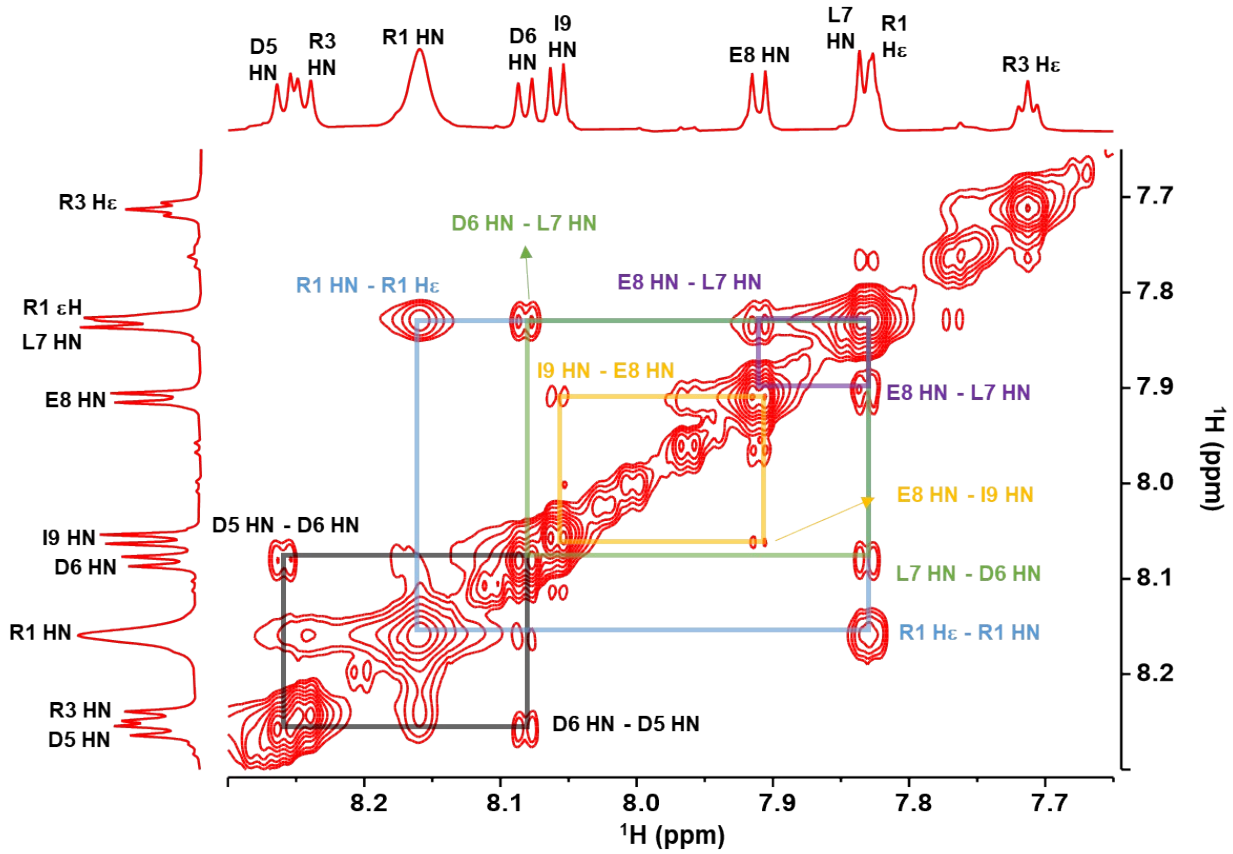

Figure S16. Nuclear Overhauser spectroscopy (NOESY) of αCT11-4OMe: HN & Hε region (7.65 – 8.30 ppm) x HN & Hε region. R1 HN - R1 Hε (blue), D6 HN - L7 HN (green), and D5 HN - D6 HN (black) correlations were observed, with the latter 2 correlations being used assign the D5, D6, L7, and I9 HNs.

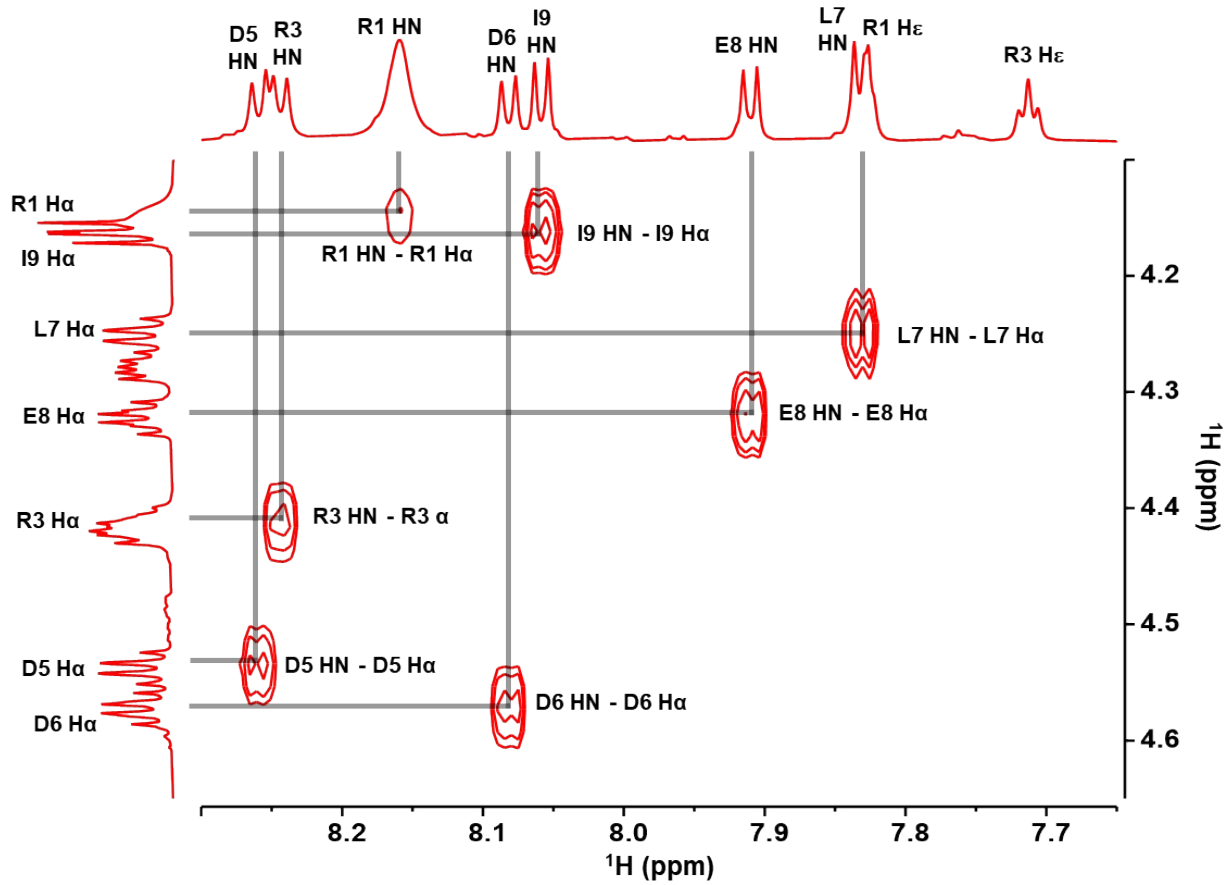

Figure S17. Clean in-phase correlation spectroscopy (CLIP COSY) of αCT11-4OMe: *H*N & Hε region (7.65 – 8.30 ppm) x Hα region (4.10 – 4.65 ppm). *H*N – Hα correlations were used to assign the Hα resonances.

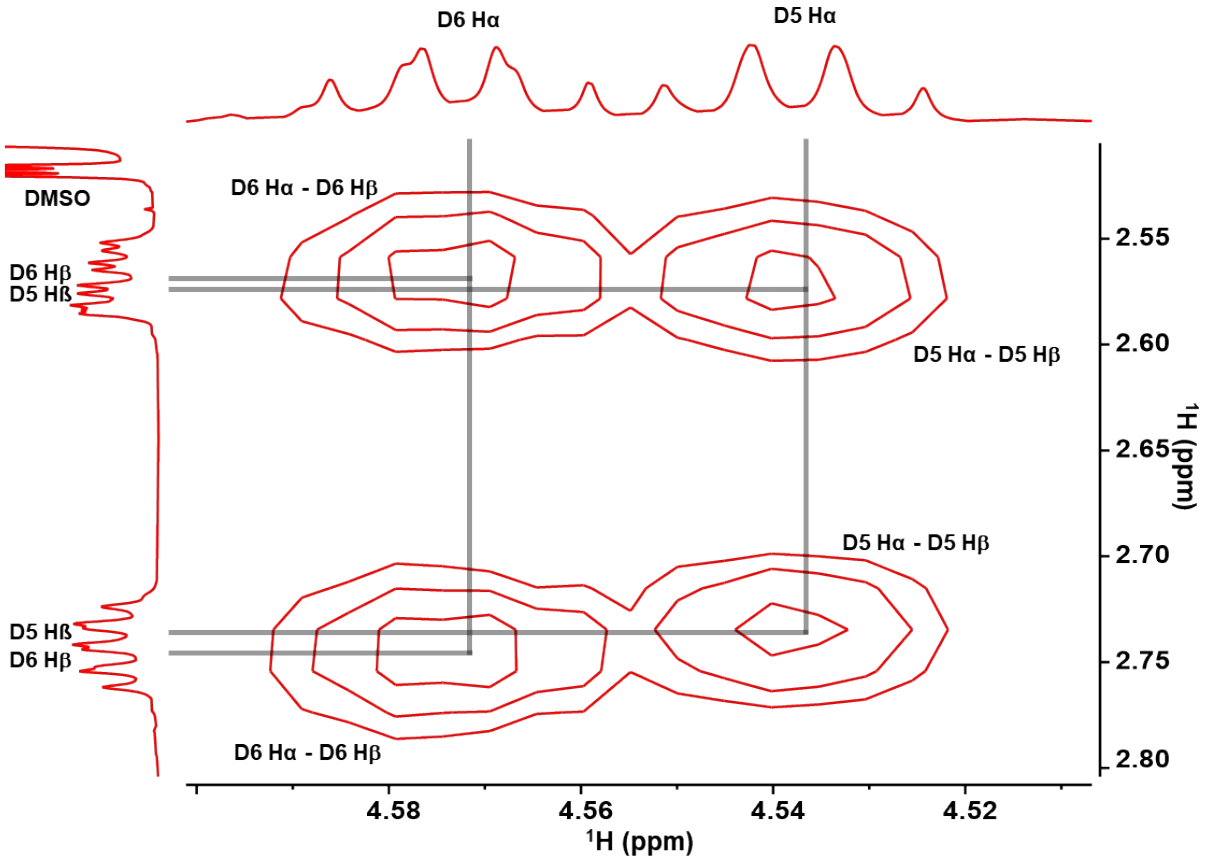

Figure S18. CLIP COSY of αCT11-4OMe: D5 & D6 Hα resonance region (4.5 – 4.6 ppm) x D5 & D6 Hß resonance region (2.5 – 2.8 ppm). The D5 and D6 Hα protons split the adjacent Hß resonances, and this CLIP-COSY spectrum showed each of part of the split D5 and D6 Hß resonances to correlate with the respective Hα resonances.

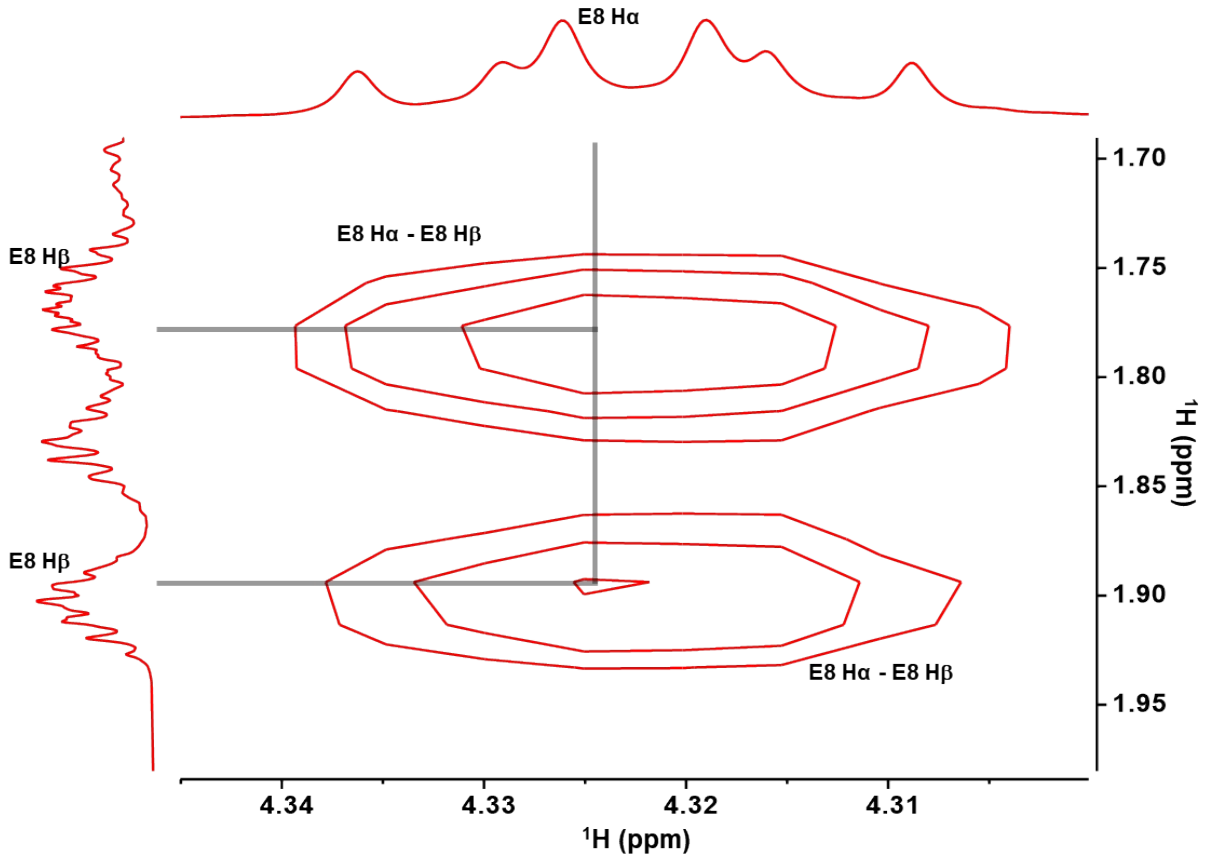

Figure S19. CLIP COSY of αCT11-4OMe: E8 Hα resonance region (4.31 – 4.34 ppm) x the E8 Hß region (1.70 – 1.95 ppm), with E8 Hα – Hß correlations allowing for the assignment of the 2 E8 Hß resonances.

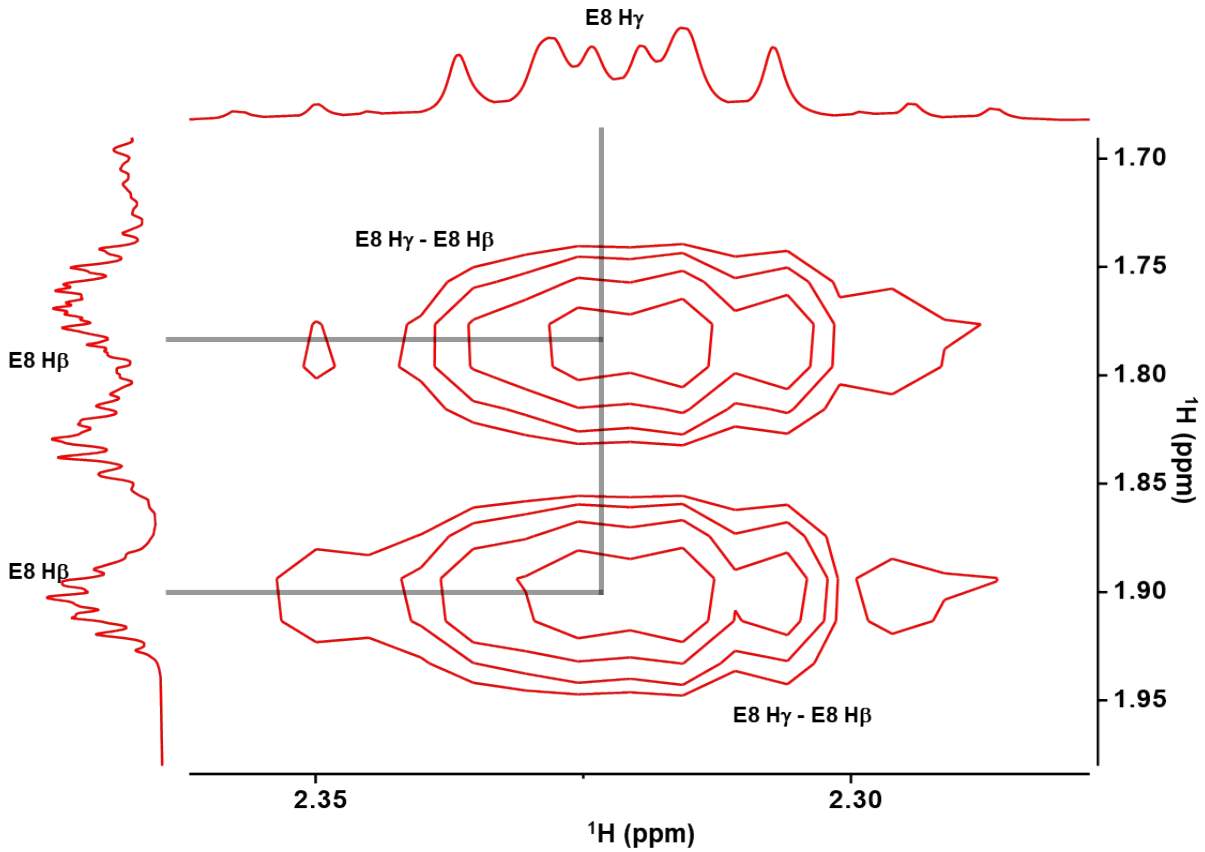

Figure S20. CLIP COSY of αCT11-4OMe: E8 Hγ resonance region (2.30 – 2.35 ppm) x E8 Hß resonance region (1.70 – 1.95 ppm), with the E8 Hγ - Hß correlations allowed for the assignment of the E8 Hγ resonance.

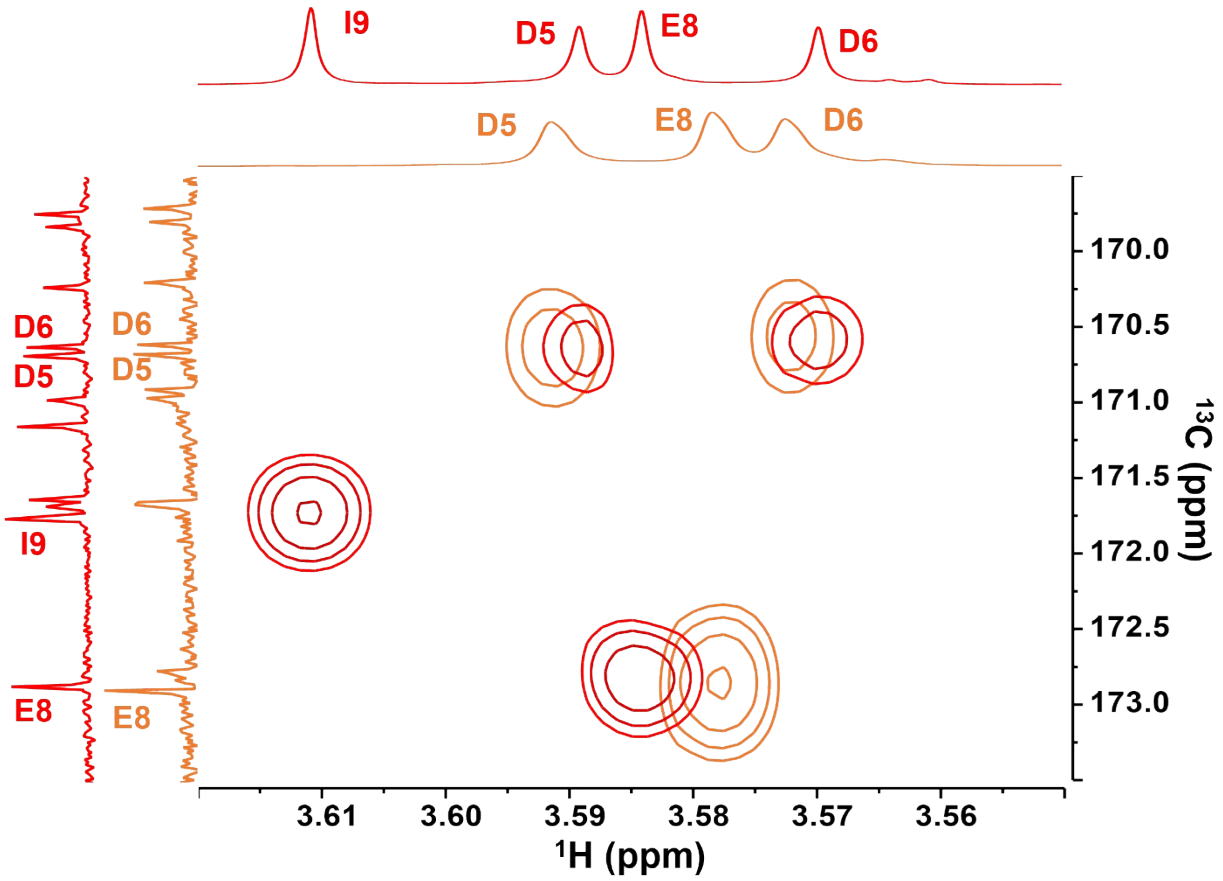

Figure S21. Heteronuclear multiple bond correlation (HMBC) of αCT11-4OMe: methyl ester H singlet region (3.55 – 3.62 ppm) x carbonyl C region (169 – 173 ppm). Correlations did not have high enough resolution in the ^{13}C region to discern between methyl ester H correlations with the D5 and D6 $C\gamma$ resonances.

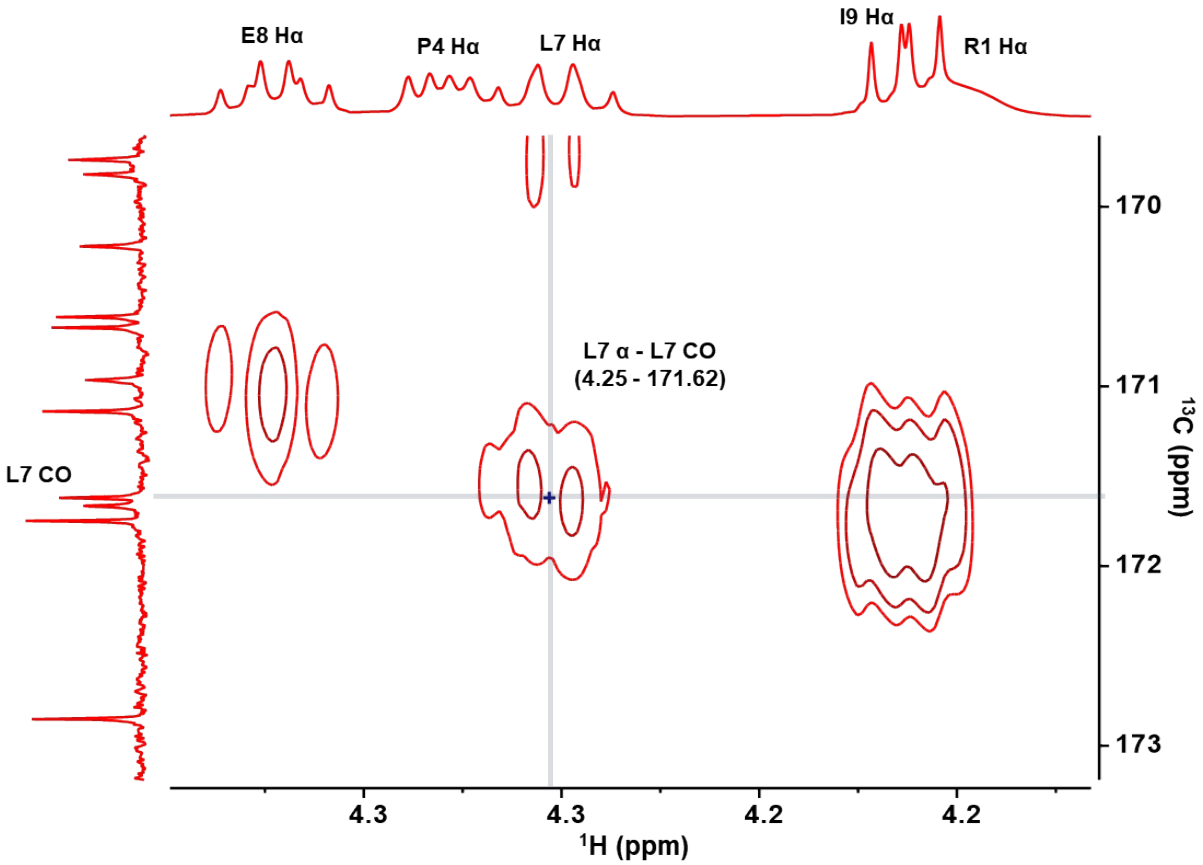

Figure S22. HMBC of αCT11-4OMe: Hα region (4.1 – 4.4 ppm) x carbonyl C region (169 – 173 ppm). The L7 Hα – L7 CO correlation (at 4.25 –171.62 ppm) is highlighted, and was used to reference all of the selective HMBC (selHMBC) spectra.

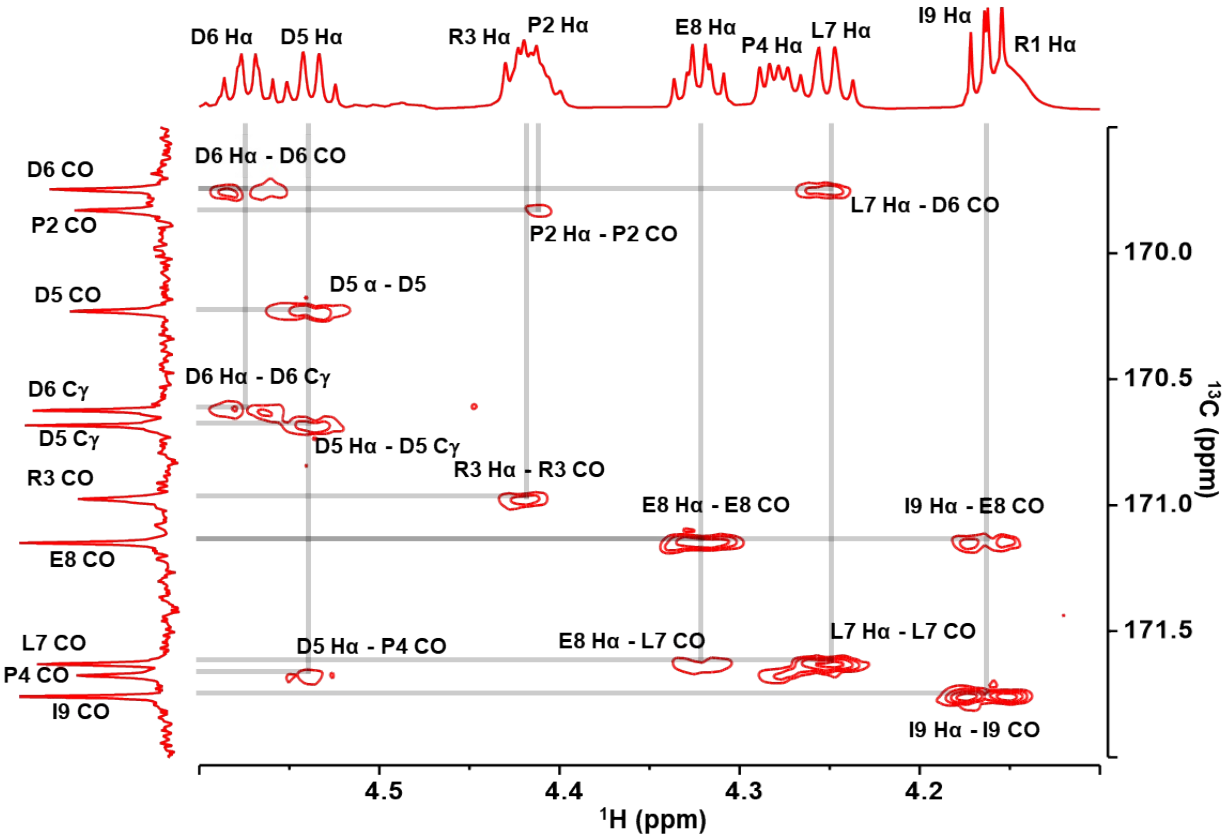

Figure S23. selHMBC of αCT11-4OMe: Hα region (4.1 – 4.6 ppm) x carbonyl C region (169 – 172 ppm). Hα – CO and D5/D6 Hα – Cγ correlations were used to assign relevant CO and Cγ resonances.

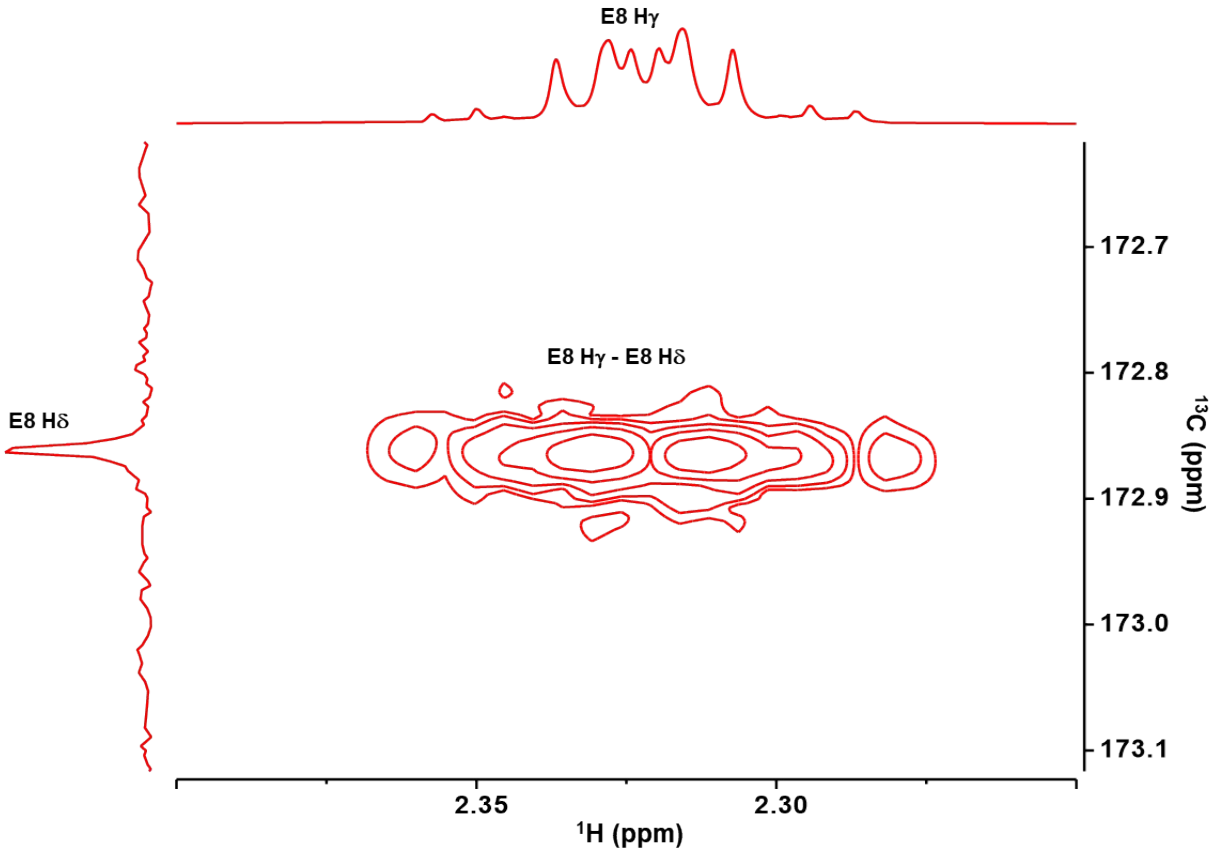

Figure S24. selHMBC of αCT11-4OMe: E8 Hγ resonance region (2.30 – 2.35 ppm) x E8 Cδ region (172.7 – 173.1 ppm), with the E8 Hγ (pink)- Cδ (yellow) correlation used to identify the E8 Cδ resonance.

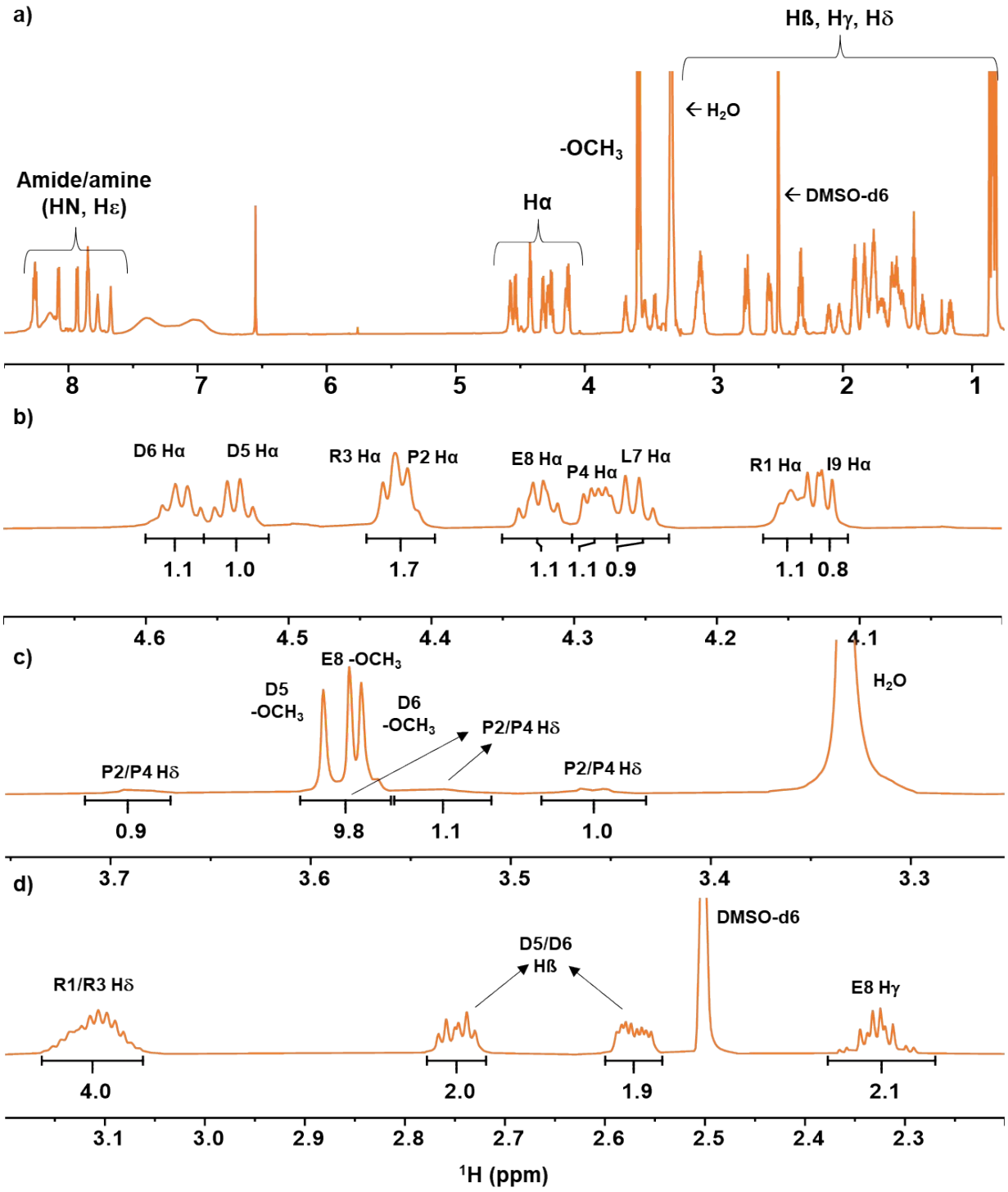

Figure S25. Expanded select regions of the αCT11-3OMe(D5,D6,E8) ^{1}H NMR spectrum. Besides **a)** the full spectrum (0.75 – 8.5 ppm), the **b)** Hα region (4.0 – 4.7 ppm), **c)** methyl ester H and proline Hδ region (3.3 – 3.8 ppm), and **d)** the R1/R3 Hδ, D5/D6 Hß, and E8 Hγ region H (2.2 – 3.2 ppm) regions are expanded with the corresponding resonances labeled.

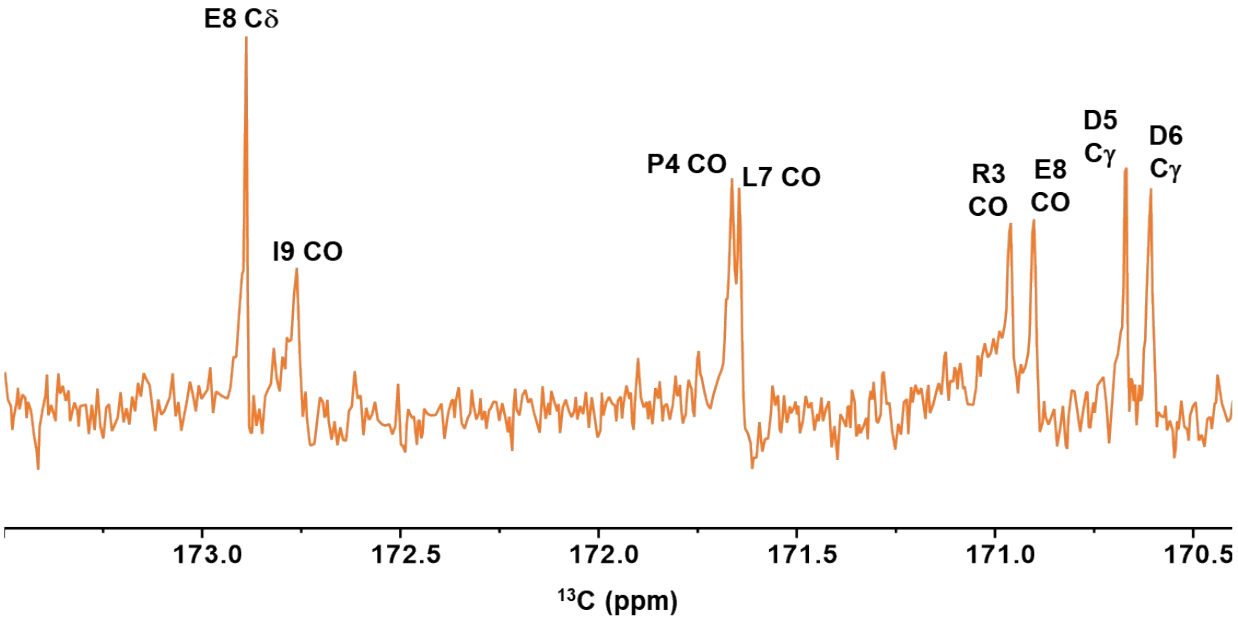

Figure S26. Carbonyl carbon region of the αCT11-3OMe(D5,D6,E8) ^{13}C NMR spectrum (170.4 – 173.5 ppm).

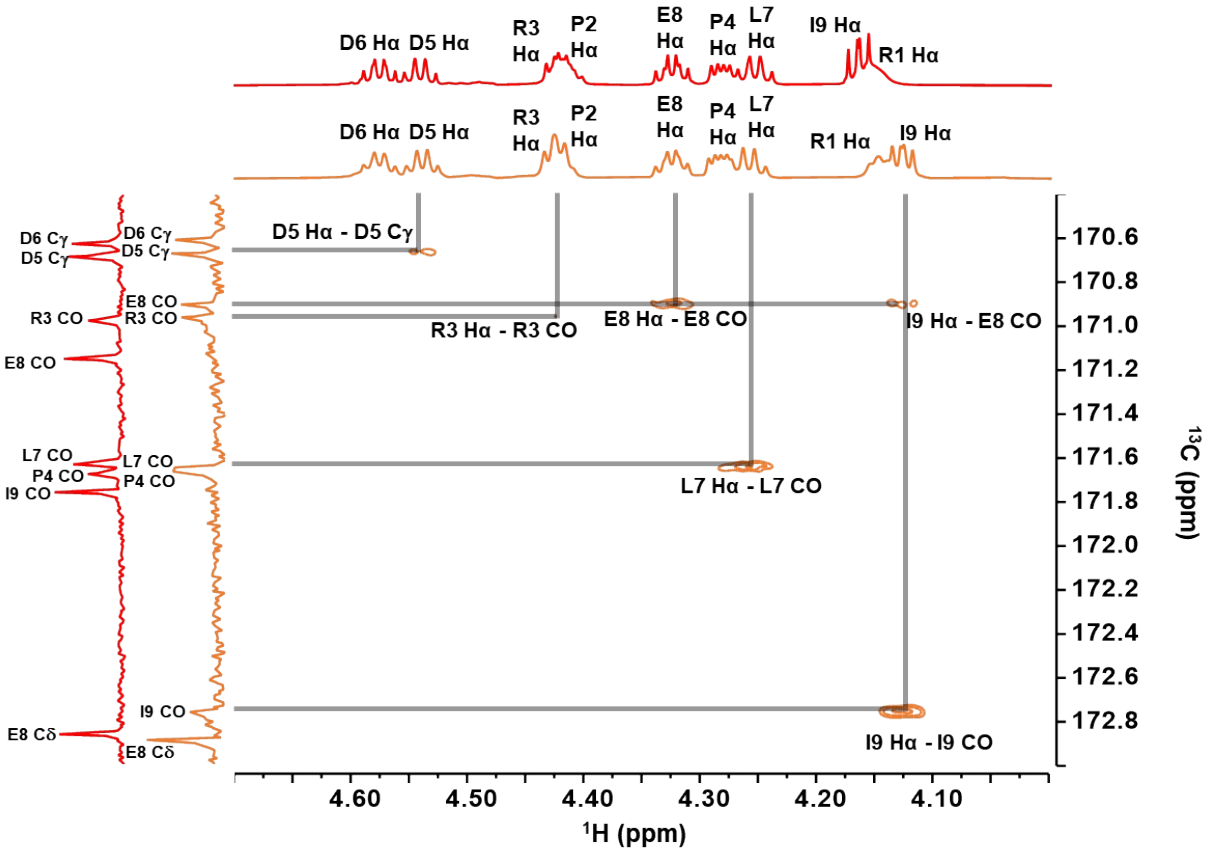

Figure S27. selHMBC of αCT11-3OMe(D5,D6,E8): Hα region (4.0 – 4.7 ppm) x carbonyl C region (170.4 – 173.2 ppm). Hα – C correlations and the D5 Hα - Cγ correlation were used to assign αCT11-3OMe(D5,D6,E8) carbonyl C resonances. Corresponding αCT11-4OMe ^{1}H and ^{13}C spectra (red) are stacked above the corresponding -3OMe(D5,D6,E8) spectra (orange) as a comparison, specifically highlighting the upfield shift in the I9 Hα resonance and the upfield/downfield shifts in the E8/I9 carbonyl C resonances observed in the -3OMe(D5,D6,E8) spectra relative to the 4OMe spectra.

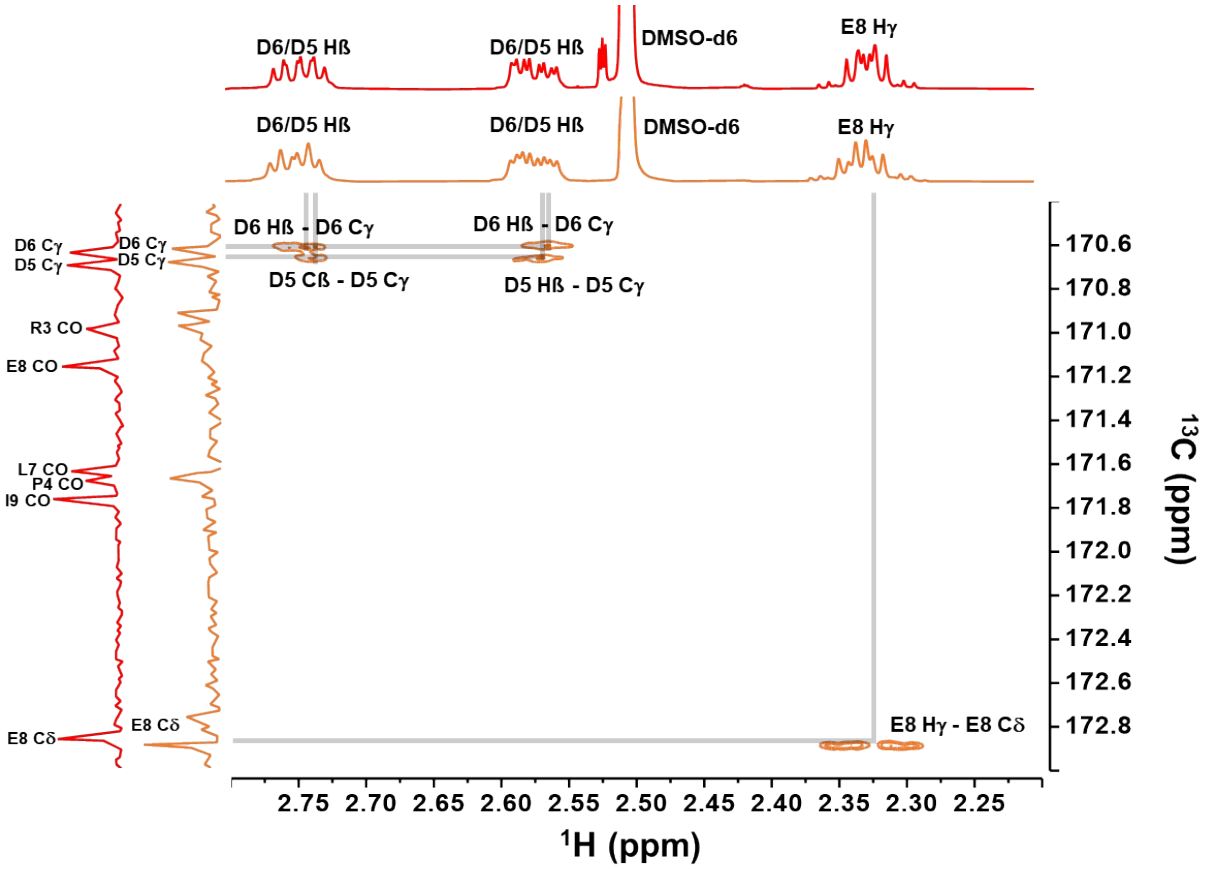

Figure S28. selHMBC of αCT11-3OMe(D5,D6,E8): D5/D6 Hß and E8 Hγ resonance region (2.2 – 2.8 ppm) x carbonyl C region (170.4 – 173.2 ppm). The D5/D6 Hß - Cγ and E8 Hγ - Cδ correlations were used to assign the D5/D6 Cγ and E8 Cδ resonances, respectively. Corresponding αCT11-4OMe ^{1}H and ^{13}C spectra (red) are stacked above the corresponding -3OMe(D5,D6,E8) spectra (orange), where shifts in the E8 C and its correlation with the E8 Hγ were observed.

Section S3: Hydrolysis of installed αCT11 methyl esters.

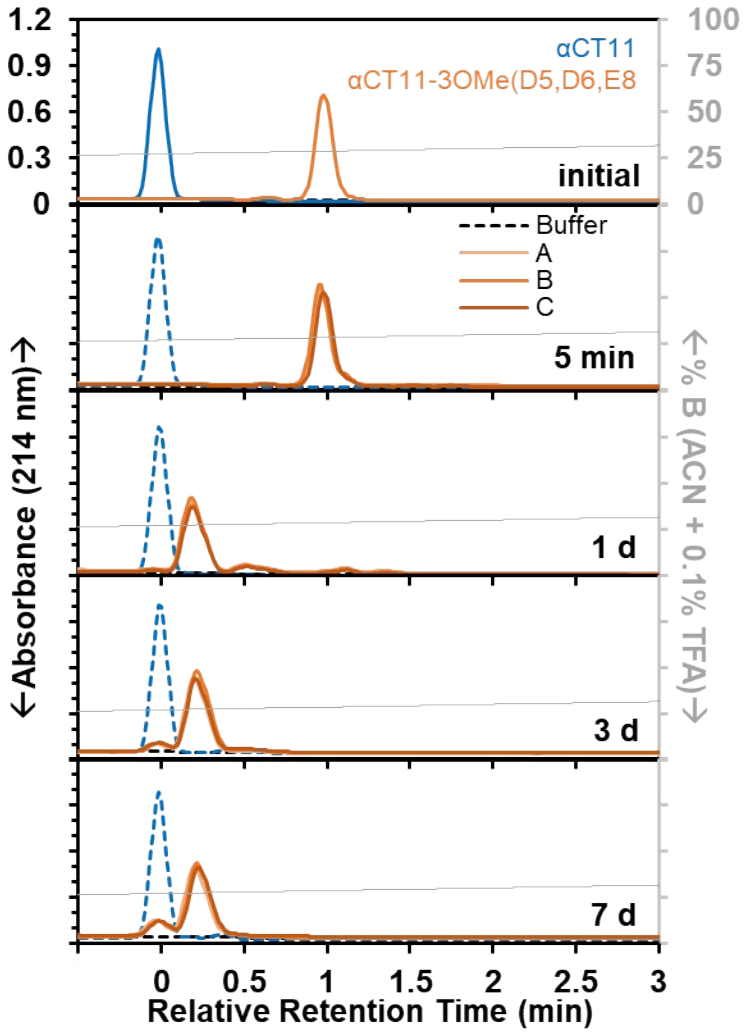

Figure S29. Hydrolysis of αCT11-3OMe(D5,D6,E8) in 1X PBS (pH 7.4). RP-HPLC chromatograms of αCT11-3OMe(D5,D6,E8) (orange solid lines) are shown compared to unmodified αCT11 (blue dashed lines) standards run at each timepoint. Standards were stored in 5 % ACN in which no hydrolysis was expected to occur. Significant hydrolysis in PBS was observed only in the first 24 h, but with little subsequent hydrolysis or activation occurring over the remainder of the 14-d experiment. This experiment was repeated in triplicate, with each replicate plotted as a solid line with varying shades of orange (A, B, C). Retention time for each esterified sample was reported relative to that of αCT11, which was set to a retention time of 0. Mobile phase composition (% ACN + 0.1% TFA, gray) was plotted against the retention time in each RP-HPLC chromatogram.

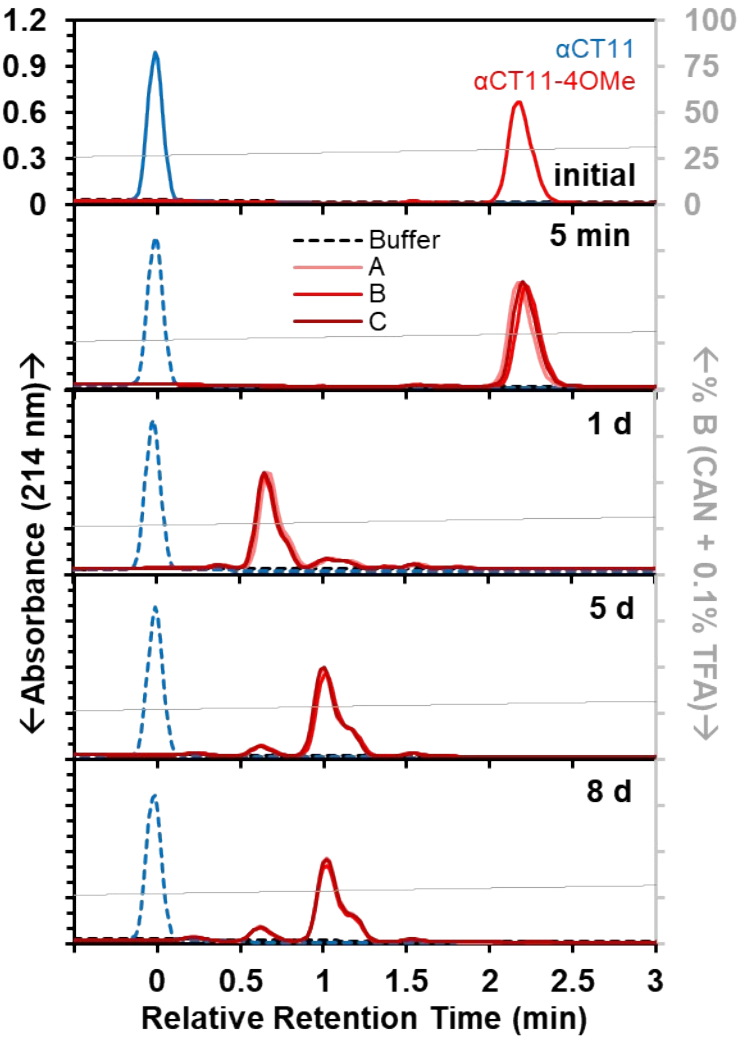

Figure S30. Hydrolysis of αCT11-4OMe in 1X PBS (pH 7.4). RP-HPLC chromatograms of αCT11-4OMe (red solid lines) are shown compared to unmodified αCT11 (blue dashed lines) standards run at each timepoint. Standards were stored in 5 % ACN in which no hydrolysis was expected to occur. Significant hydrolysis in PBS was observed only in the first 24 h, but with little subsequent hydrolysis or activation occurring over the remainder of the 8-d experiment. This experiment was repeated in triplicate, with each replicate plotted as a solid line with varying shades of red (A, B, C). Retention time for each esterified sample was reported relative to that of αCT11, which was set to a retention time of 0. Mobile phase composition (% ACN + 0.1% TFA, gray) was plotted against the retention time in each RP-HPLC chromatogram.

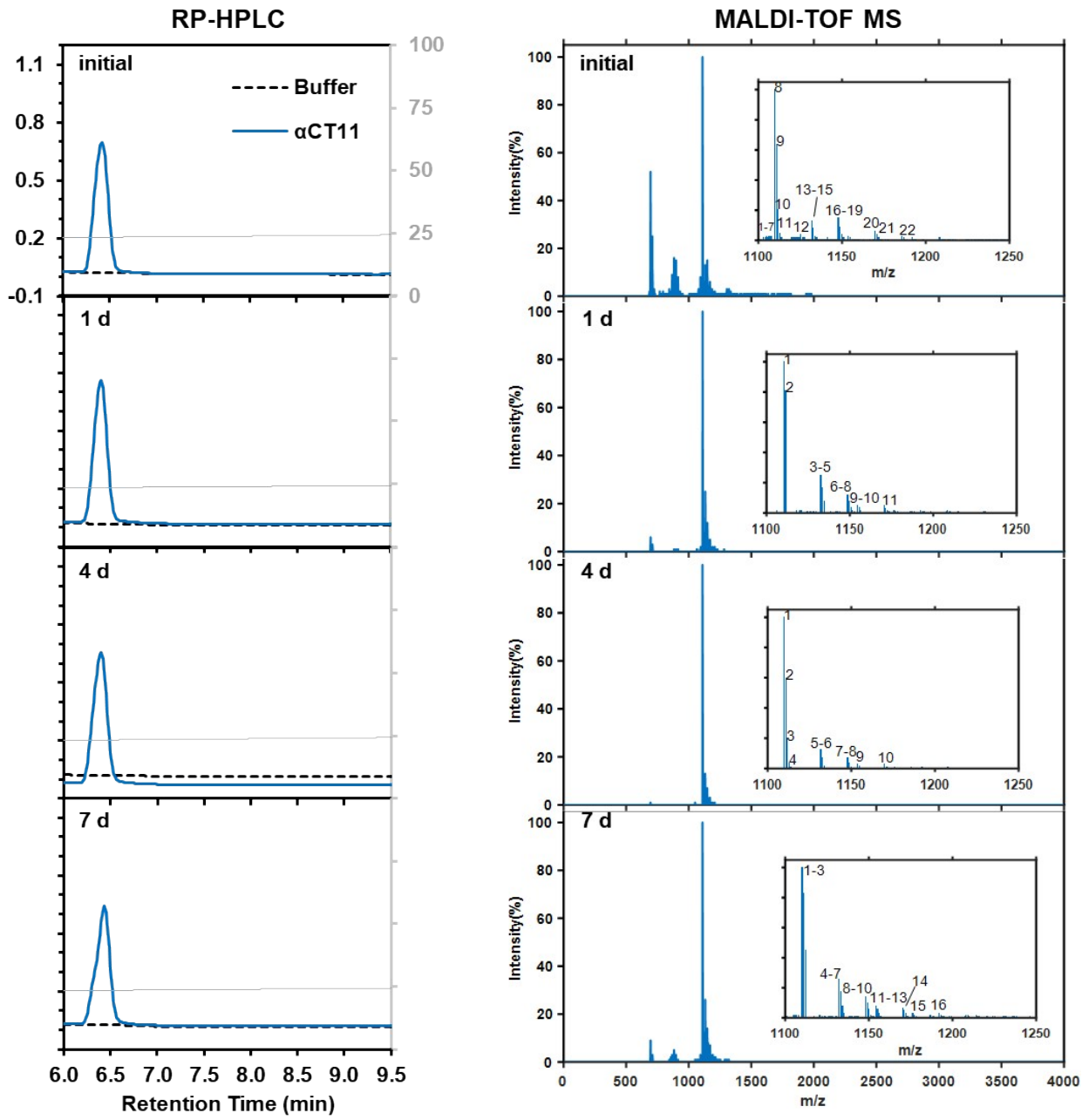

Figure S31. RP-HPLC chromatograms and MALDI-TOF spectra of αCT11 in 1X PBS (pH 7.4) over 1 week. No changes were seen in either the chromatograms or MALDI-TOF mass spec over 7 d. Mobile phase composition (% ACN + 0.1% TFA, gray) was plotted against the retention time in each RP-HPLC chromatogram. MALDI-TOF measurements were obtained through co-crystallization in a CHCA matrix. Data between 1100 and 1250 m/z are shown inset of each plot, with each peak is numerically labeled. Labels are defined in **Table S5**.

Table S5. Molecular weights of peaks observed in MALDI-TOF MS data measuring the incubation of αCT11 in 1X PBS, as shown in Figure S31.

Time	label	Mass (Da)	Intensity (%)	Species
initial	1	1104.742	3	?
	2	1104.897	3	?
	3	1106.055	3	?
	4	1106.595	3	?
	5	1107.136	3	?
	6	1107.6	3	?
	7	1107.909	3	?
	8	1109.919	100	[αCT11 + H]+
	9	1110.925	64	
	10	1111.931	21	
	11	1113.016	5	?
	12	1125.367	4	?
	13	1131.919	13	[αCT11 + Na]+
	14	1132.935	8	
	15	1133.951	3	
	16	1147.833	15	[αCT11 + K]+
	17	1148.856	9	
	18	1149.879	4	
	19	1153.898	3	[αCT11 + 2Na - H]+
	20	1169.806	6	[αCT11 + K + Na - H]+
	21	1170.839	4	[αCT11 + K + Na - H]+
	22	1185.743	3	?

	23	1321.423	3	?
1 d	1	1110.4	100	[αCT11 + H]+
	2	1111.5	81	
	3	1132.6	25	[αCT11 + Na]+
	4	1133.6	17	
	5	1134.6	8	
	6	1148.6	12	[αCT11 + K]+
	7	1149.6	8	
	8	1150.6	4	
	9	1154.7	5	[αCT11 + 2Na - H]+
	10	1155.6	4	
	11	1171.5	3	[αCT11 + K + Na - 2H]+
4 d	1	1109.8	100	[αCT11 + H]+
	2	1110.9	60	
	3	1111.9	20	
	4	1112.9	4	
	5	1131.8	13	[αCT11 + Na]+
	6	1132.9	7	
	7	1147.8	7	[αCT11 + K]+
	8	1148.9	4	
	9	1153.8	3	[αCT11 + 2Na - H]+
	10	1169.8	3	[αCT11 + K + 2Na - 2H]+
7 d	1	1110.1	100	[αCT11 + H]+
	2	1111.2	83	
	3	1112.2	45	

	4	1132.3	26	[αCT11 + Na]+
	5	1133.3	18	
	6	1134.2	8	
	7	1135.2	3	
	8	1148.2	14	[αCT11 + K]+
	9	1149.2	10	
	10	1150.2	6	
	11	1154.2	8	[αCT11 + 2Na - H]+
	12	1155.3	6	
	13	1156.218	3	
	14	1170.238	7	[αCT11 + K + Na - H]+
	15	1176.204	3	[αCT11 + 3Na - 2H]+
	16	1192.188	3	[αCT11 + K + 2Na - 2H]+

Table S6. Percent activation of αCT11-3OMe(D5,D6,E8) and -4OMe in 1X PBS (pH 7.4) and 100 mM carbonate buffer (pH 10.0) over 8 d.

Time (d)	**3OMe(D5,D6,E8)**				**4OMe**			
	1X PBS (pH 7.4)		100 mM carbonate buffer (pH 10)		1X PBS (pH 7.4)		100 mM carbonate buffer (pH 10)	
	Average	StDev	Average	StDev	Average	StDev	Average	StDev
0.00	0.0	0.0	0.22	0.11	0.00	0.00	0.62	0.08
0.25			54.65	2.42			15.20	0.36
0.50			66.94	0.87			35.81	0.32
1.00	3.4	1.0	88.14	0.46	0.00	0.00	62.33	1.09
1.50			96.15	0.74			76.36	0.55
2.00			98.33	0.27			84.41	0.13
3.00	5.8	1.9	100.32	0.08			93.82	0.18
5.00			99.99	0.15	0.00	0.00	98.50	0.28
7.00	10.5	2.3						
8.00					1.13	0.30		

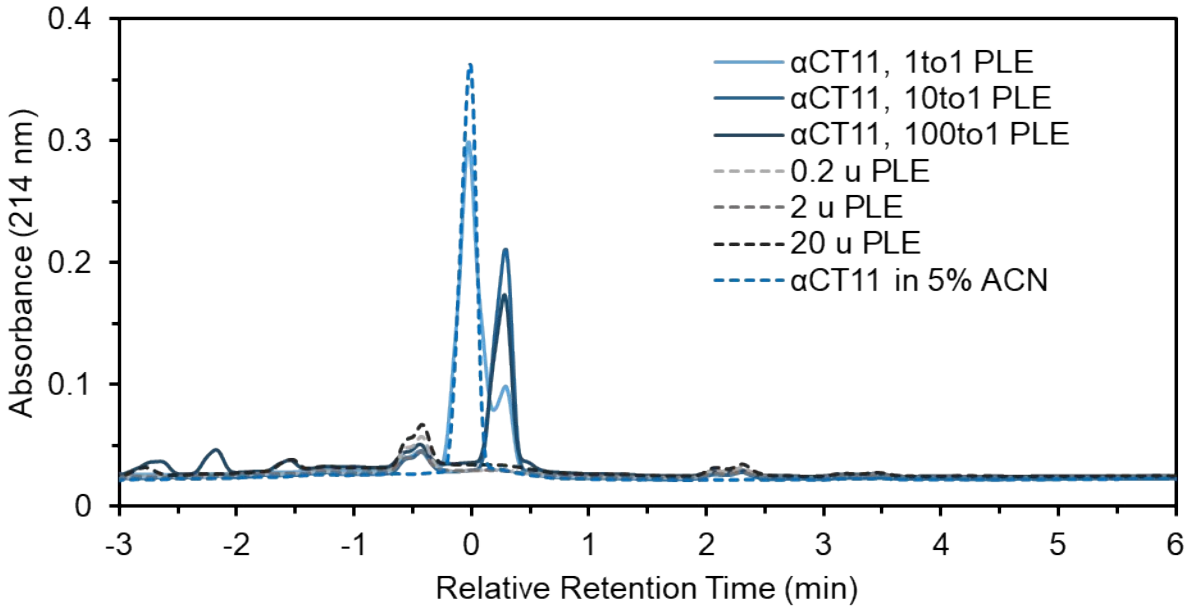

Figure S32. PLE-catalyzed hydrolysis of αCT11. Hydrolysis was performed at a 1:1 (light blue), 10:1 (blue), and 100:1 (navy blue) ratios of PLE enzyme units:μmol αCT11. PLE controls for each condition (gray, dashed lines) and an αCT11 only control (blue dashed line) is also pictured. The appearance of a second peak in αCT11 + PLE samples and the disappearance of αCT11 were observed with increasing PLE concentration. Retention time of each sample is reported relative to an αCT11 control, which was set to 0.

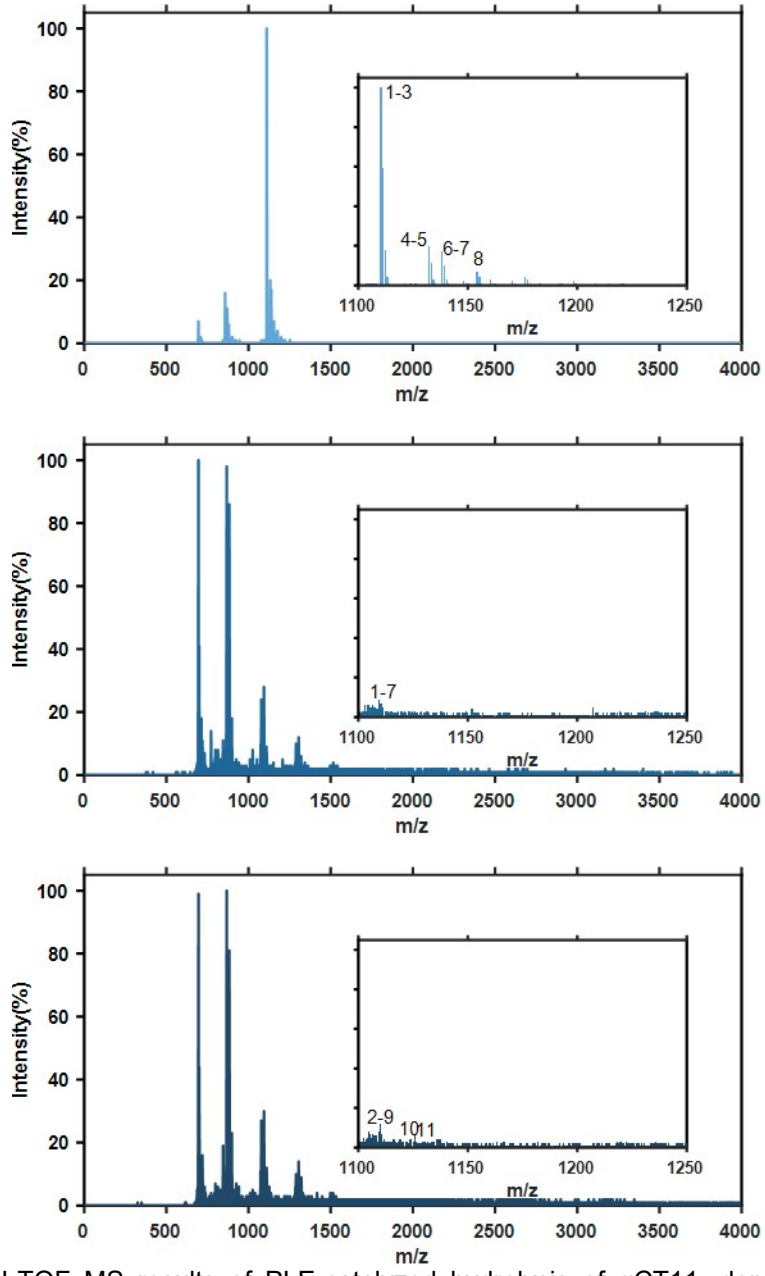

Figure S33. MALDI-TOF MS results of PLE-catalyzed hydrolysis of αCT11, depicted in Figure S32. Hydrolysis was performed at a 1:1 (light blue), 10:1 (blue), and 100:1 (navy blue) ratios of PLE enzyme units:μmol αCT11. Results between 1100-1250 m/z, where αCT11 is expected to appear in MALDI-TOF MS, is inset. αCT11-related peaks disappeared with increasing PLE concentration. Peak labels are defined in **Table S7**.

Table S7. MALDI-TOF MS results of PLE-catalyzed hydrolysis of αCT11.

PLE:αCT11 ratio (enzyme units: μmol peptide)	label	Mass (Da)	Intensity (%)	Species
1:1	1	1110.28	100	[αCT11 + H]+
	2	1111.28	59	[αCT11 + H]+
	3	1112.37	18	[αCT11 + H]+
	4	1132.36	20	[αCT11 + Na]+
	5	1133.38	11	[αCT11 + Na]+
	6	1138.31	17	[2OMe + H]+
	7	1139.32	10	[2OMe + H]+
	8	1154.34	7	[αCT11 + 2Na - H]+
10:1	1	1103.25	6	N/A
	2	1104.48	6	N/A
	3	1106.64	6	N/A
	4	1107.42	5	N/A
	5	1109.5	9	N/A
	6	1110.43	7	N/A
	7	1112.6	3	N/A
100:1	1	1100.86	3	N/A
	2	1104.64	8	N/A
	3	1105.25	7	N/A
	4	1106.64	7	N/A
	5	1106.95	6	N/A
	6	1107.96	6	N/A
	7	1109.5	8	N/A
	8	1109.97	12	N/A
	9	1110.82	7	N/A
	10	1118.65	3	N/A
	11	1125.81	6	N/A

*N/A refers to a sample that cannot be reliably attributed to either matrix or αCT11.

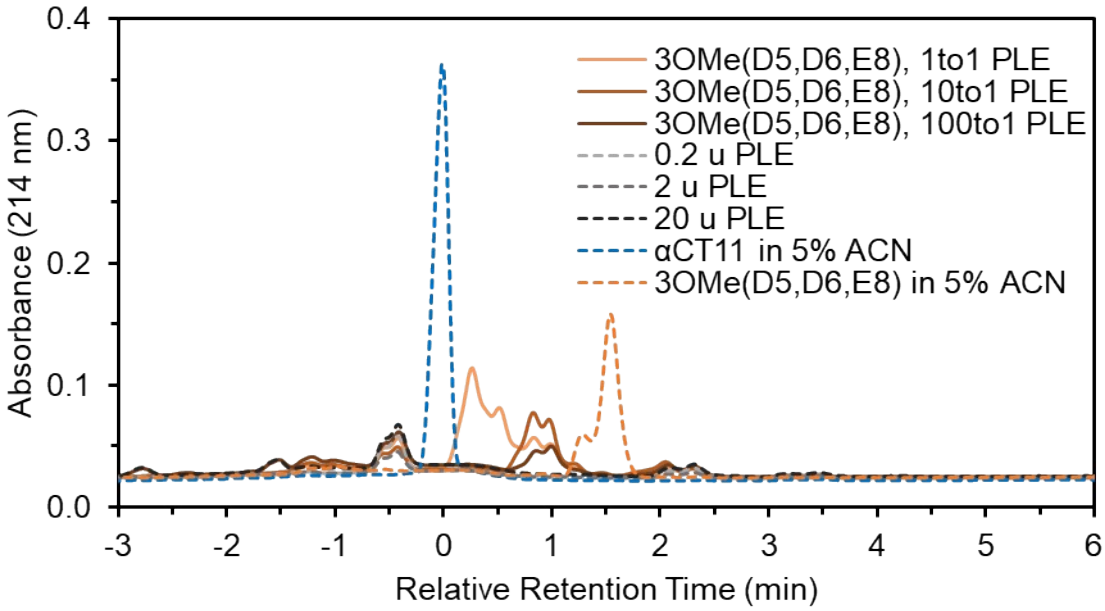

Figure S34. RP-HPLC chromatogram of PLE-catalyzed hydrolysis of αCT11-3OMe(D5,D6,E8). Hydrolysis was performed at a 1:1 (light orange), 10:1 (dark orange), and 100:1 (brown) ratios of PLE enzyme units:μmol αCT11. PLE controls for each condition (gray, dashed lines) and an αCT11-3OMe(D5,D6,E8) control (orange dashed line) and αCT11 control (blue dashed line) are also pictured. The appearance of an unaccounted-for peak in αCT11-3OMe(D5,D6,E8) + PLE samples and the disappearance of αCT11 were observed with increasing PLE concentration. Retention time of each sample is reported relative to an αCT11 control, which was set to 0.

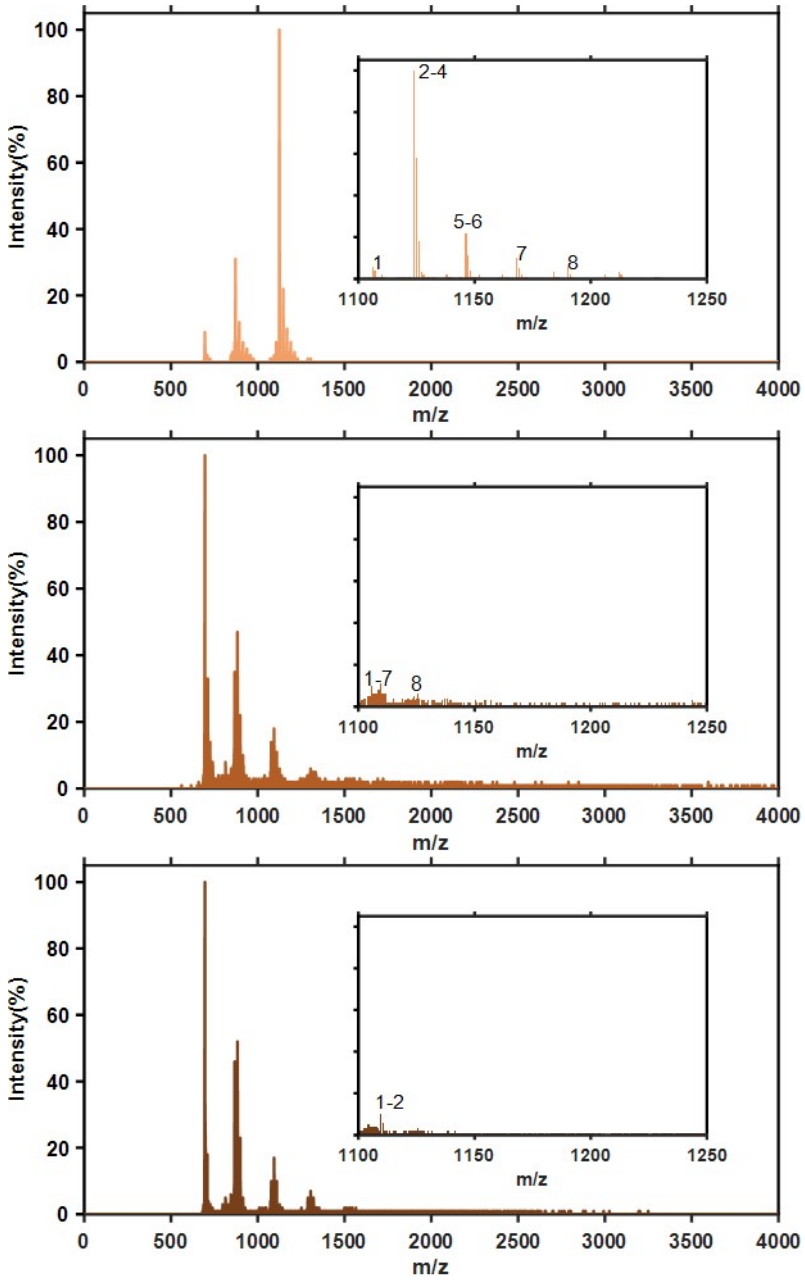

Figure S35. MALDI-TOF MS results of PLE-catalyzed hydrolysis of αCT11-3OMe(D5,D6,E8), depicted in Figure S34. Hydrolysis was performed at a 1:1 (light orange), 10:1 (dark orange), and 100:1 (brown) ratios of PLE enzyme units:μmol αCT11Results between 1100-1250 m/z, where αCT11 is expected to appear in MALDI-TOF MS, is inset. αCT11-related peaks disappeared with increasing PLE concentration. Peak labels are defined in **Table S8**.

Table S8. MALDI-TOF MS results of PLE-catalyzed hydrolysis of αCT11-3OMe(D5,D6,E8).

PLE:αCT11 ratio (enzyme units: μmol peptide)	label	Mass (Da)	Intensity (%)	Species
1:1	1	1106.103	6	[1OMe + 1 imide + H]+
	2	1124.092	100	[1OMe + H]+
	3	1125.104	58	[1OMe + H]+
	4	1126.117	18	[1OMe + H]+
	5	1146.152	22	[1OMe + Na]+
	6	1147.175	11	[1OMe + Na]+
	7	1168.19	10	[1OMe + 2Na - H]+
	8	1190.196	6	[3OMe + K]+
10:1	1	1105.794	10	N/A
	2	1106.489	6	[1OMe +1 imide + H]+
	3	1107.648	6	[1OMe +1 imide + H]+
	4	1108.653	8	[1OMe +1 imide + H]+
	5	1109.581	11	PLE
	6	1110.509	6	[αCT11 + H]+
	7	1111.593	6	[αCT11 + H]+
	8	1125.493	6	N/A
100:1	1	1109.735	10	PLE
	2	1110.741	6	PLE

*N/A refers to a sample that cannot be reliably attributed to either matrix or αCT11.

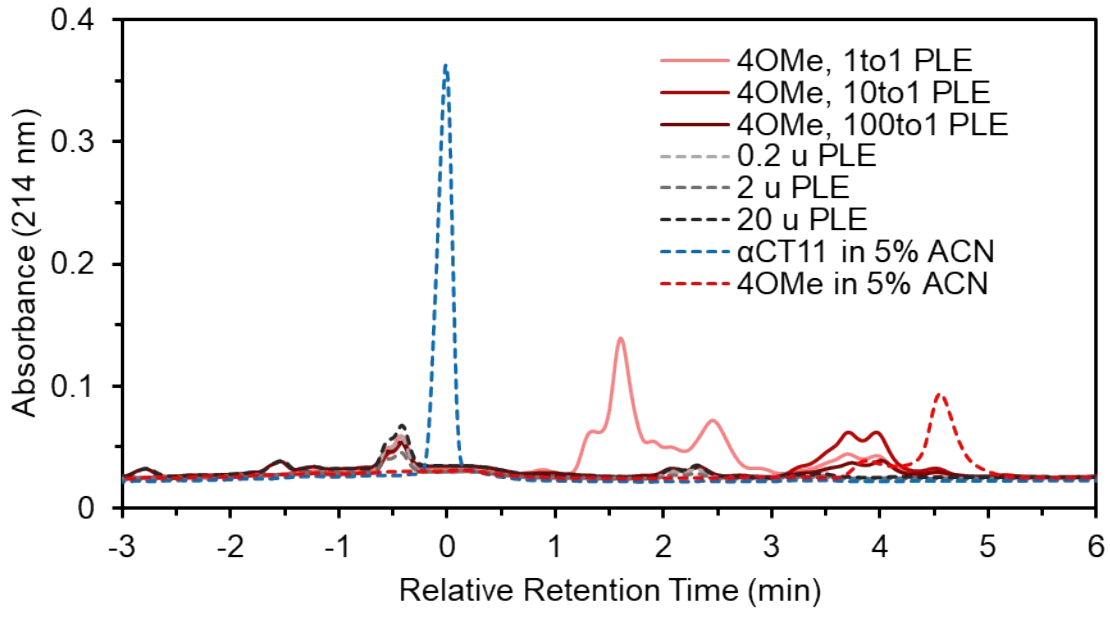

Figure S36. RP-HPLC chromatogram of PLE-catalyzed hydrolysis of αCT11-4OMe. Hydrolysis was performed at a 1:1 (pink), 10:1 (red), and 100:1 (dark red) ratios of PLE enzyme units:μmol αCT11. PLE controls for each condition (gray, dashed lines) and an αCT11-4OMe control (red dashed line) and αCT11 control (blue dashed line) are also pictured. The appearance of an unaccounted-for peak in αCT11-4OMe

+ PLE samples were observed with increasing PLE concentration. Retention time of each sample is reported relative to an αCT11 control, which was set to 0.

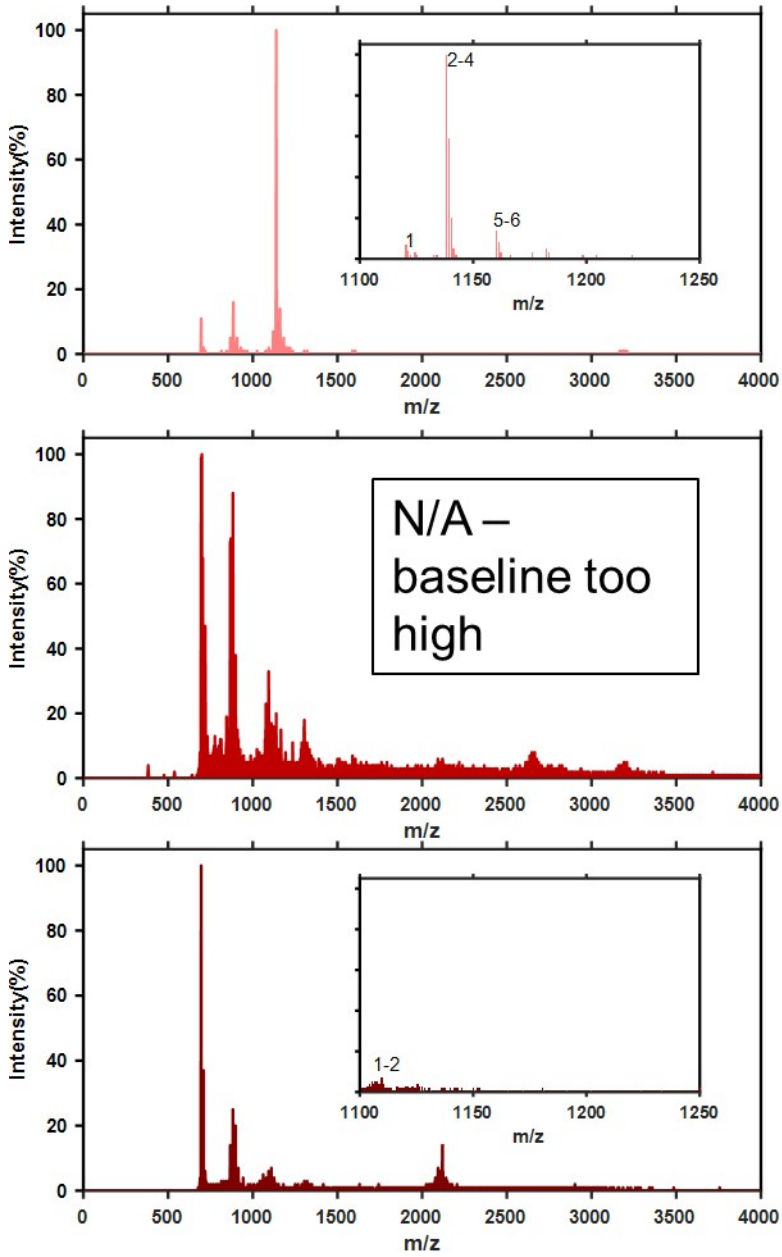

Figure S37. MALDI-TOF MS results of PLE-catalyzed hydrolysis of αCT11-4OMe, depicted in Figure S36. Hydrolysis was performed at a 1:1 (pink), 10:1 (red), and 100:1 (dark red) ratios of PLE enzyme units:μmol αCT11. Results between 1100-1250 m/z, where αCT11 is expected to appear in MALDI-TOF MS, is inset. αCT11-related peaks disappeared with increasing PLE concentration. Peak labels are defined in **Table S9**.

Table S9. MALDI-TOF MS results of PLE-catalyzed hydrolysis of αCT11-3OMe(D5,D6,E8).

PLE:αCT11 ratio (enzyme units: µmol peptide)	label	Mass (Da)	Intensity (%)	Species
1:1	1	1120.358	7	[2OMe + 1 imide + H]+
	2	1138.383	100	[2OMe + H]+
	3	1139.402	59	[2OMe + H]+
	4	1140.421	20	[2OMe + H]+
	5	1160.425	14	[2OMe + Na]+
	6	1161.454	8	[2OMe + Na]+
100:1	1	1107.493	5	?
	2	1109.658	7	PLE

*N/A refers to a sample that cannot be reliably attributed to either matrix or αCT11.

We varied the PLE concentration between 1:1, 10:1, and 100:1 enzyme units:µmol peptide and stirred the solution at 37 °C over 24 h. At all ratios, we observed the appearance of a new peak in the αCT11 RP-HPLC chromatogram, which eluted later (xxx) than the αCT11 peak, grew with increasing PLE concentration, and were not associated with any esterase peaks (**Figure S32**). Further, while MALDI-TOF MS confirmed the presence of αCT11 in the 1:1 PLE:αCT11 sample, we could identify no αCT11 peaks in the 10:1 and 100:1 MALDI-TOF spectra (**Figure S33, Table S7**). Similar trends were observed for the -3OMe(D5,D6,E8) and -4OMe samples, where the 1:1 PLE:peptide MALDI-TOF spectra revealed species similar to those present in samples incubated in only 1X PBS after 1 d (**Figures S34-S37, Table S8-S9**), but a loss of αCT11-related signal in both RP-HPLC chromatograms and MALDI-TOF MS spectra in both 10:1 and 100:1 PLE:peptide samples.

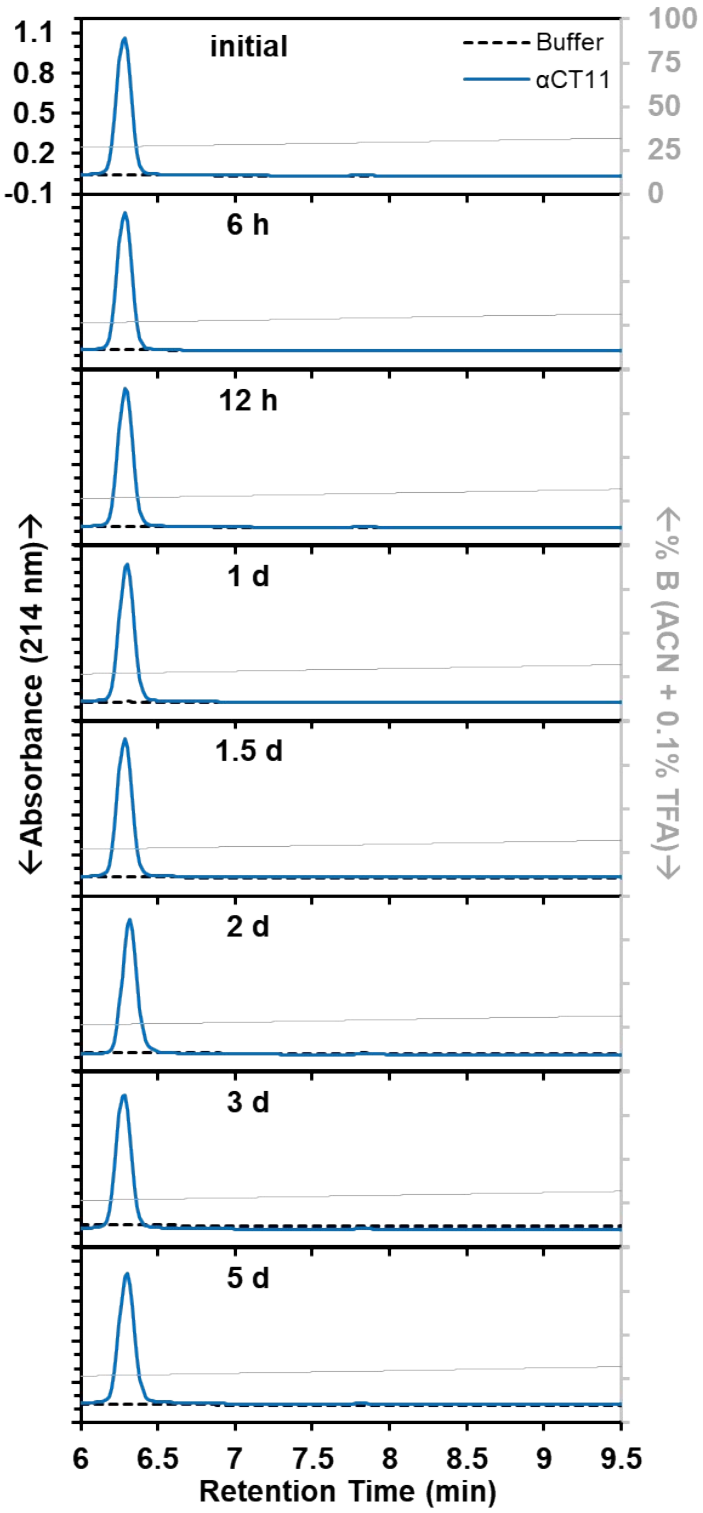

Figure S38. RP-HPLC chromatograms αCT11 in 100 mM carbonate buffer (pH 10) over 1 week. No changes were seen in RP-HPLC chromatograms at each tested timepoint, suggesting stability of αCT11 under the basic conditions tested. Mobile phase composition (% ACN + 0.1% TFA, gray) was plotted against the retention time in each RP-HPLC chromatogram.

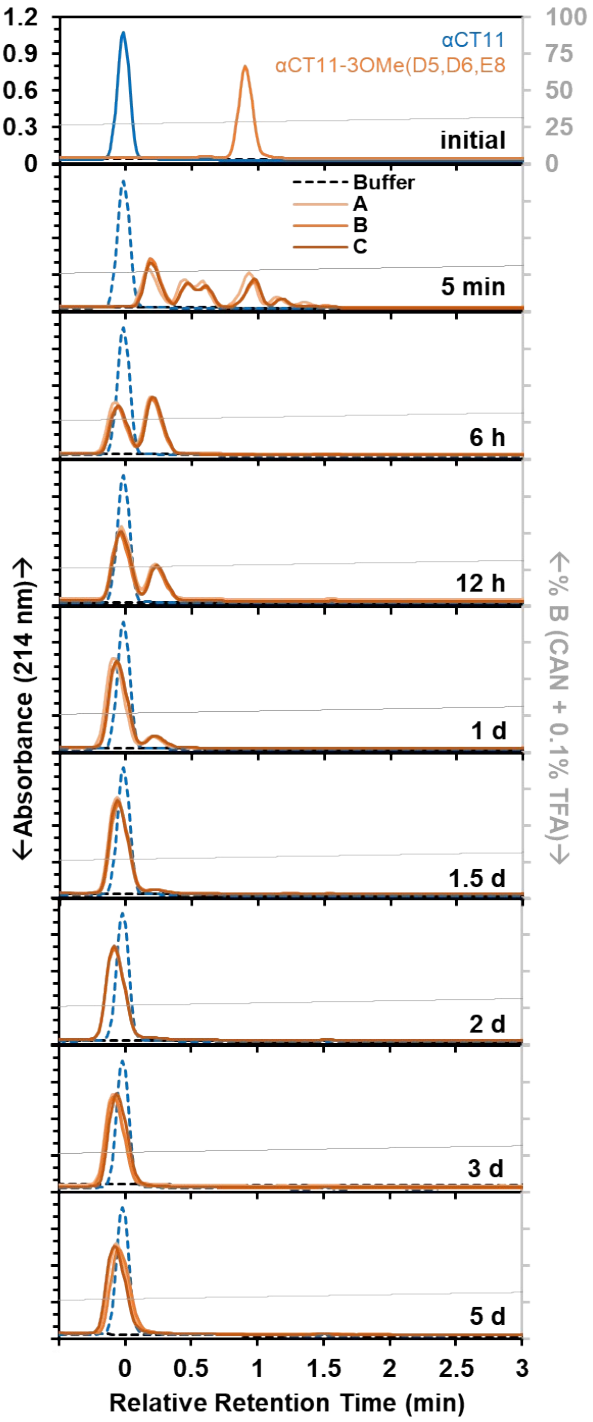

Figure S39. Hydrolysis of αCT11-3OMe(D5,D6,E8) in 100 mM carbonate buffer (pH 10.0). RP-HPLC chromatograms of αCT11-3OMe(D5,D6,E8) (orange solid lines) are shown compared to unmodified αCT11 (blue dashed lines) standards run at each timepoint. Standards were stored in 5 % ACN in which no hydrolysis was expected to occur. Full esterified peptide activation was observed after 3 d and was confirmed by LC-MS (**Figure S41**). The experiment was repeated in triplicate, with each replicate plotted as a solid line with varying shades of orange (A, B, C). Retention time for each esterified sample was reported relative to that of αCT11, which was set to a retention time of 0. Mobile phase composition (% ACN + 0.1% TFA, gray) was plotted against the retention time in each RP-HPLC chromatogram.

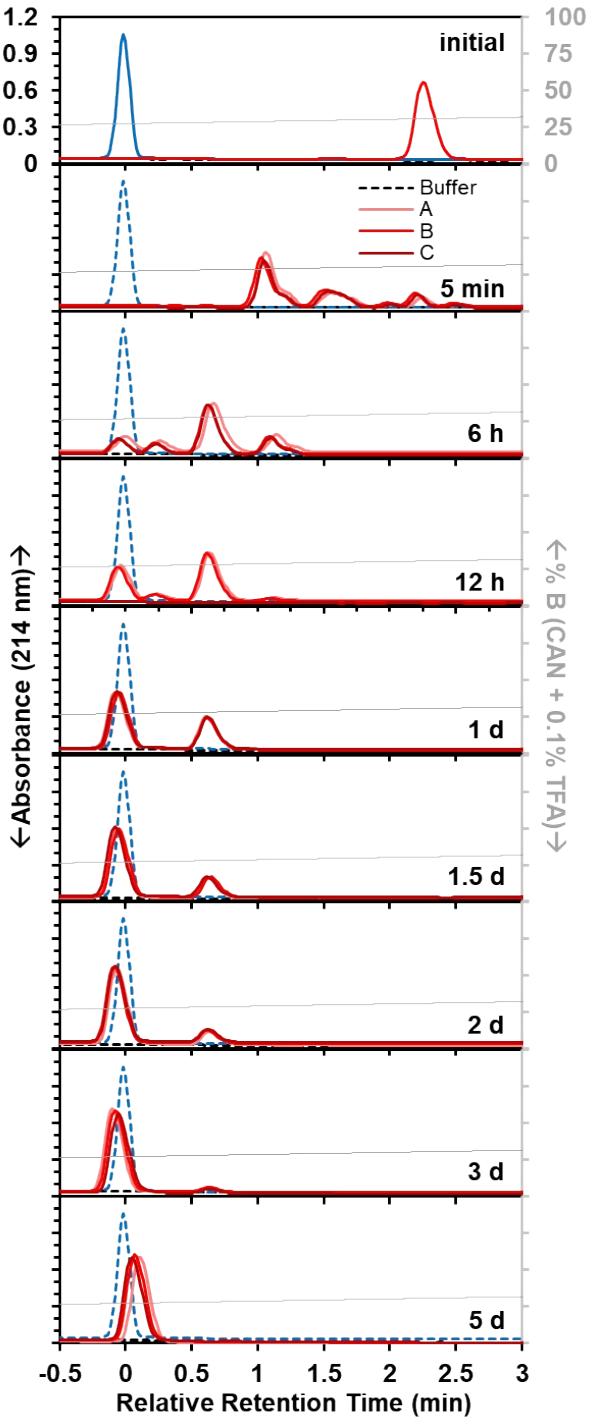

Figure S40. Hydrolysis of αCT11-4OMe in 100 mM carbonate buffer (pH 10.0). RP-HPLC chromatograms of αCT11-4OMe (red solid lines) are shown compared to unmodified αCT11 (blue dashed lines) standards run at each timepoint. Standards were stored in 5 % ACN in which no hydrolysis was expected to occur. Full esterified peptide activation was observed after 5 d and was confirmed by LC-MS (**Figure S42**). The experiment was repeated in triplicate, with each replicate plotted as a solid line with varying shades of red (A, B, C). Retention time for each esterified sample was reported relative to that of αCT11, which was set to a retention time of 0. Mobile phase composition (% ACN + 0.1% TFA, gray) was plotted against the retention time in each RP-HPLC chromatogram.

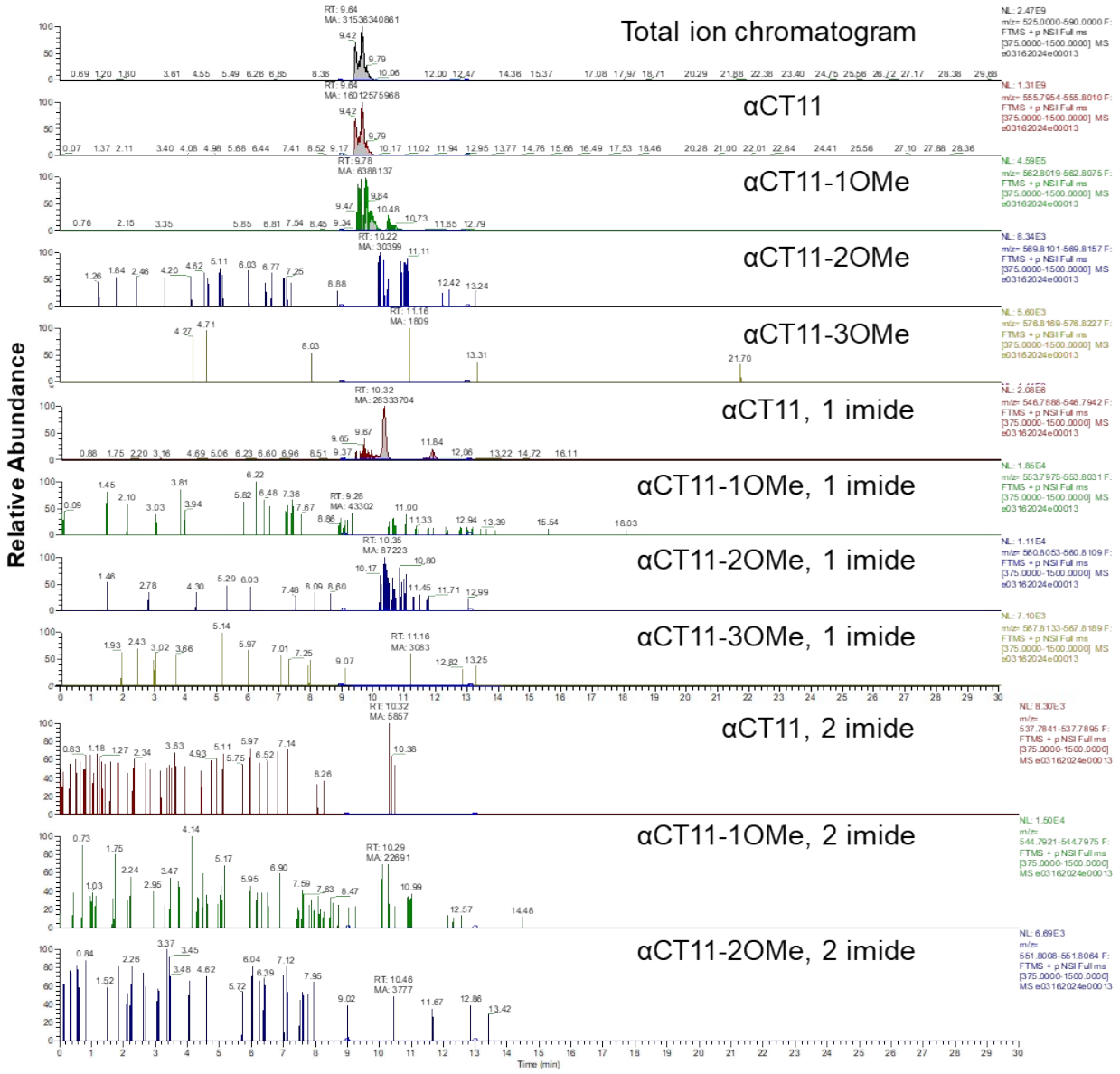

Figure S41. LC-MS chromatograms of αCT11-3OMe(D5,D6,E8) after 3 d of stirring in 100 mM carbonate buffer (pH 10.0) at 37 °C. Total ion chromatogram (top, gray) and selective ion chromatograms for αCT11 with different numbers of esters and/or imides.

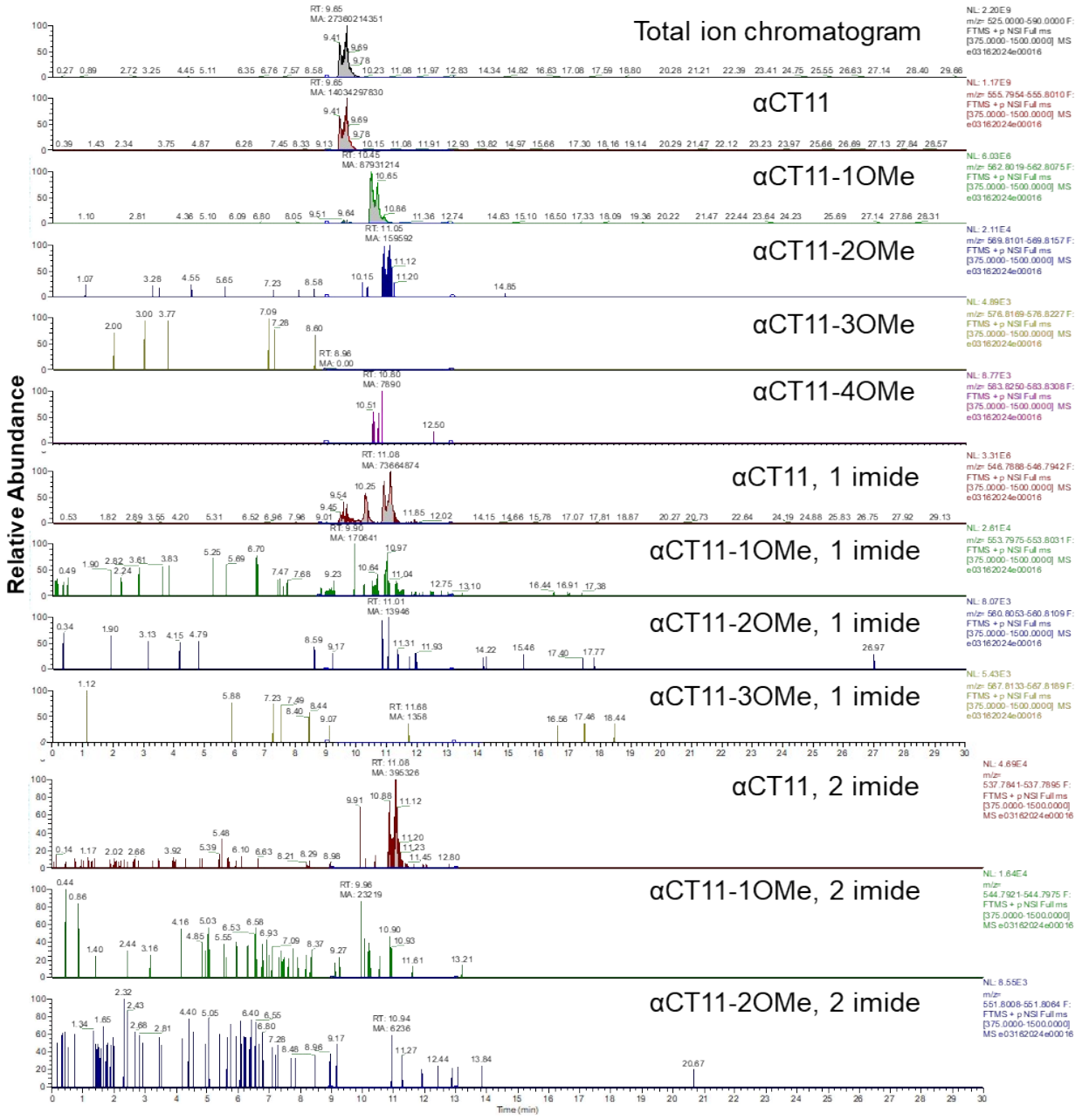

Figure S42. LC-MS chromatograms of αCT11-4OMe after 5 d of stirring in 100 mM carbonate buffer (pH 10.0) at 37 °C. Total ion chromatogram (top, gray) and selective ion chromatograms for αCT11 with different numbers of esters and/or imides.

Table S10. % Abundance and retention times (RT, min) of αCT11-based formulations produced by the hydrolysis of αCT11-3OMe(D5,D6,E8) in 100 mM carbonate buffer (pH 10) after 3 d, quantified by LC-MS.

		Ester #										Total
		0		1		2		3		4		
		% Abundance	RT (min)	% Abundance	RT (min)	% Abundance	RT (min)	% Abundance	RT (min)	% Abundance	RT (min)	% Abundance
3 d	no imides	96.47	9.42 9.64 9.79	0.04	-	0.00	-	0.00	-	N/A	N/A	**96.68**
	1 imide	0.17	-	0.00	-	0.00	-	0.00	-	N/A	N/A	**0.17**
	2 imides	0.00	-	0.00	-	0.00	-	N/A	N/A	N/A	N/A	**0.00**

Table S11. % Abundance and retention times (RT, min) of αCT11-based formulations produced by the hydrolysis of αCT11-4OMe in 100 mM carbonate buffer (pH 10) after 5 d, quantified by LC-MS.

		Ester #										Total
		0		1		2		3		4		
		% Abundance	RT (min)	% Abundance	RT (min)	% Abundance	RT (min)	% Abundance	RT (min)	% Abundance	RT (min)	% Abundance
5 d	no imides	97.46	9.41 9.65 9.69	0.61	-	0.00	-	0.00	-	0.00	-	**0.00**
	1 imide	0.51	-	0.00	-	0.00	-	0.00	-	N/A	N/A	**0.51**
	2 imides	0.00	-	0.00	-	0.00	-	N/A	N/A	N/A	N/A	**0.00**

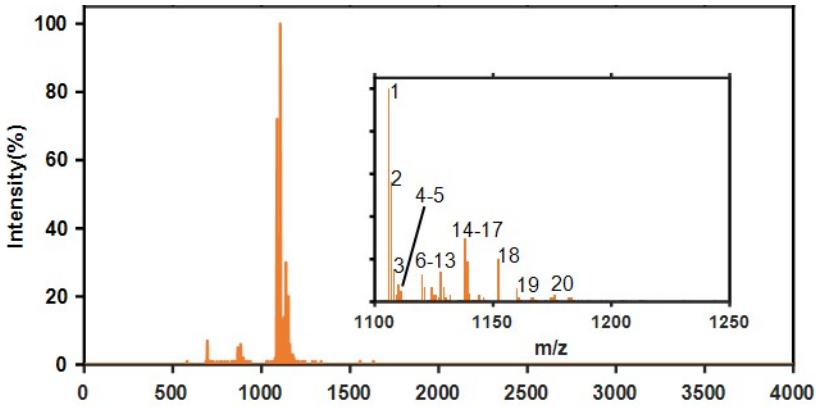

label	Mass (Da)	Intensity (%)	Species
1	1106.1	100	[αCT11-1OMe – H_2O + H]+
2	1107.1	56	
3	1108.1	15	
4	1110.1	8	[αCT11 + H]+
5	1111.1	5	
6	1120.2	13	[αCT11-2OMe – H_2O + H]+
7	1121.1	7	
8	1124.1	7	[αCT11-1OMe + H]+
9	1125.1	3	
10	1126.0	3	
11	1128.0	14	αCT11-1OMe – H_2O + Na]+
12	1129.1	7	
13	1132.0	3	[αCT11 + Na]+
14	1138.1	30	[αCT11-2OMe + H]+
15	1139.2	19	
16	1140.1	4	
17	1144.1	3	[αCT11-1OMe – H_2O + K]+
18	1152.2	20	[αCT11-3OMe + H]+
19	1160.1	6	[αCT11-2OMe + Na]+
20	1176.1	3	[αCT11-2OMe + K]+

Figure S43. MALDI-TOF MS of αCT11-3OMe(D5,D6,E8) after 2 h of incubation into 1X PBS. Peaks related to esterified αCT11 with the loss of either 1 or 2 H_2O molecules suggest the formation of intramolecular imides/amides.

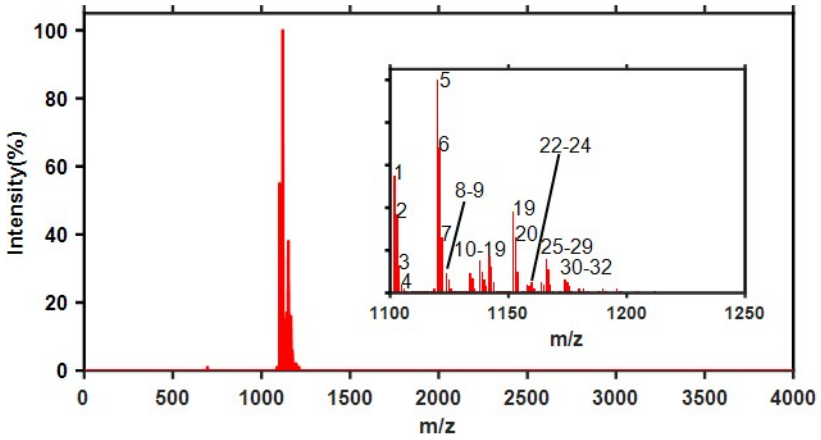

label	Mass (Da)	Intensity (%)	Species
1	1101.9	55	[αCT11-2OMe – 2 H_2O + H]+
2	1102.9	37	
3	1103.8	13	
4	1104.8	4	
5	1119.9	100	[αCT11-2OMe – H_2O + H]+
6	1120.9	68	
7	1121.9	26	
8	1123.9	9	[αCT11-1OMe H]+ or [αCT11-2OMe – 2 H_2O + Na]+
9	1124.8	6	
10	1133.9	9	[αCT11-3OMe – H_2O + H]+
11	1134.9	7	
12	1137.9	15	[αCT11-2OMe + H]+
13	1138.9	10	
14	1139.9	6	[αCT11-2OMe – 2 H_2O + K]+
15	1140.7	3	
16	1141.9	17	[αCT11-2OMe – H_2O + Na]+
17	1142.9	12	
18	1143.8	5	
19	1151.9	38	[αCT11-3OMe + H]+
20	1153.0	26	
21	1153.8	10	
22	1157.9	4	[αCT11-2OMe – H_2O + K]+
23	1158.8	3	
24	1159.9	5	[αCT11-2OMe + Na]+
25	1163.9	5	[αCT11-2OMe – H_2O + 2 Na - H]+
26	1164.9	4	
27	1166.0	16	[αCT11-4OMe + H]+
28	1166.9	11	
29	1167.8	4	
30	1173.9	6	[αCT11-3OMe + Na]+
31	1174.9	5	
32	1175.9	3	

Figure S44. MALDI-TOF MS of αCT11-4OMe after 2 h of incubation into 1X PBS. Peaks related to esterified αCT11 with the loss of either 1 or 2 H_2O molecules suggest the formation of intramolecular imides/amides.

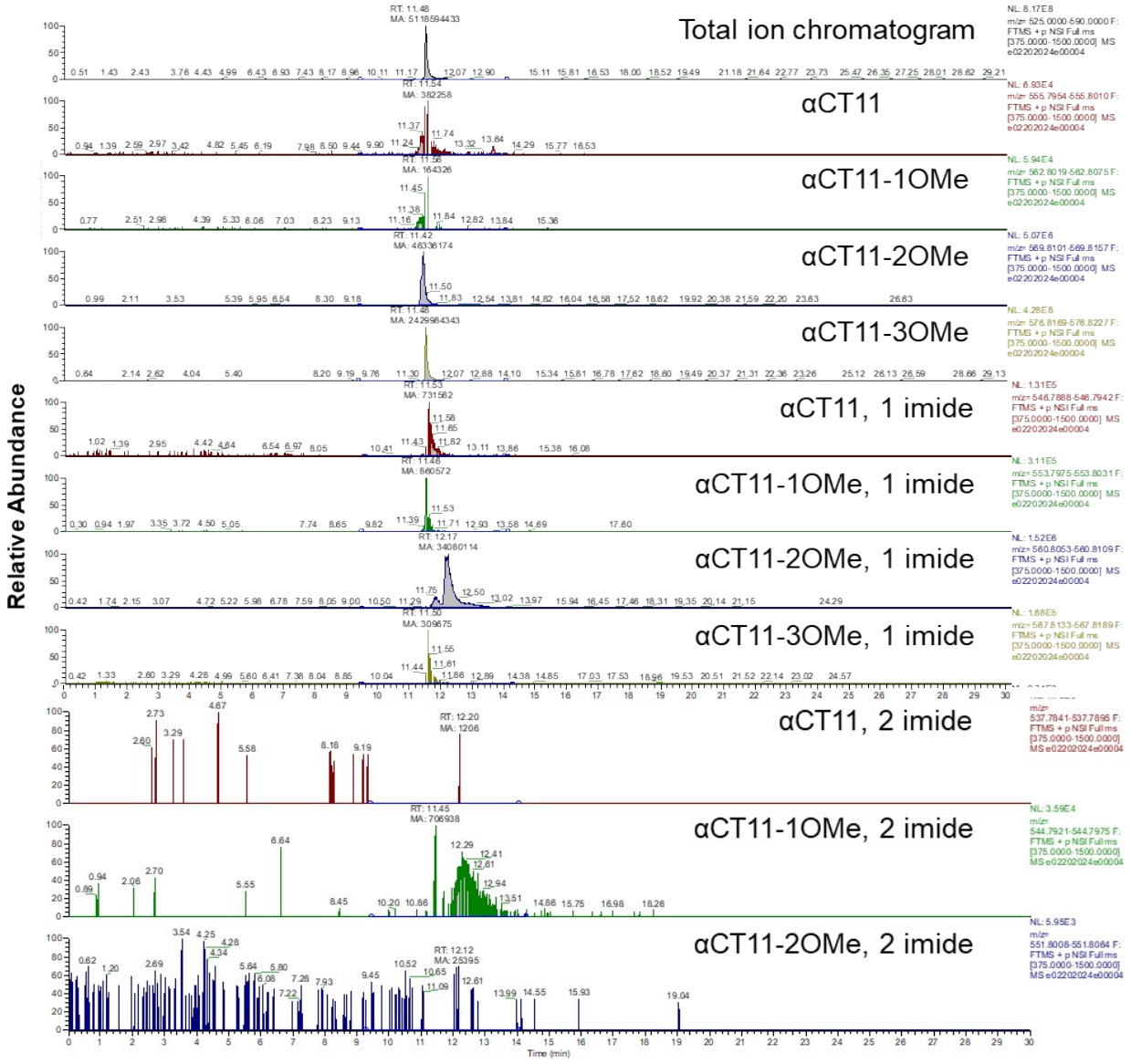

Figure S45. LC-MS chromatograms of αCT11-3OMe(D5,D6,E8) after 5 min of incubation in 37 °C 1X PBS (pH 7.4). Total ion chromatogram (top, gray) and selective ion chromatograms for αCT11 with different numbers of esters and/or imides.

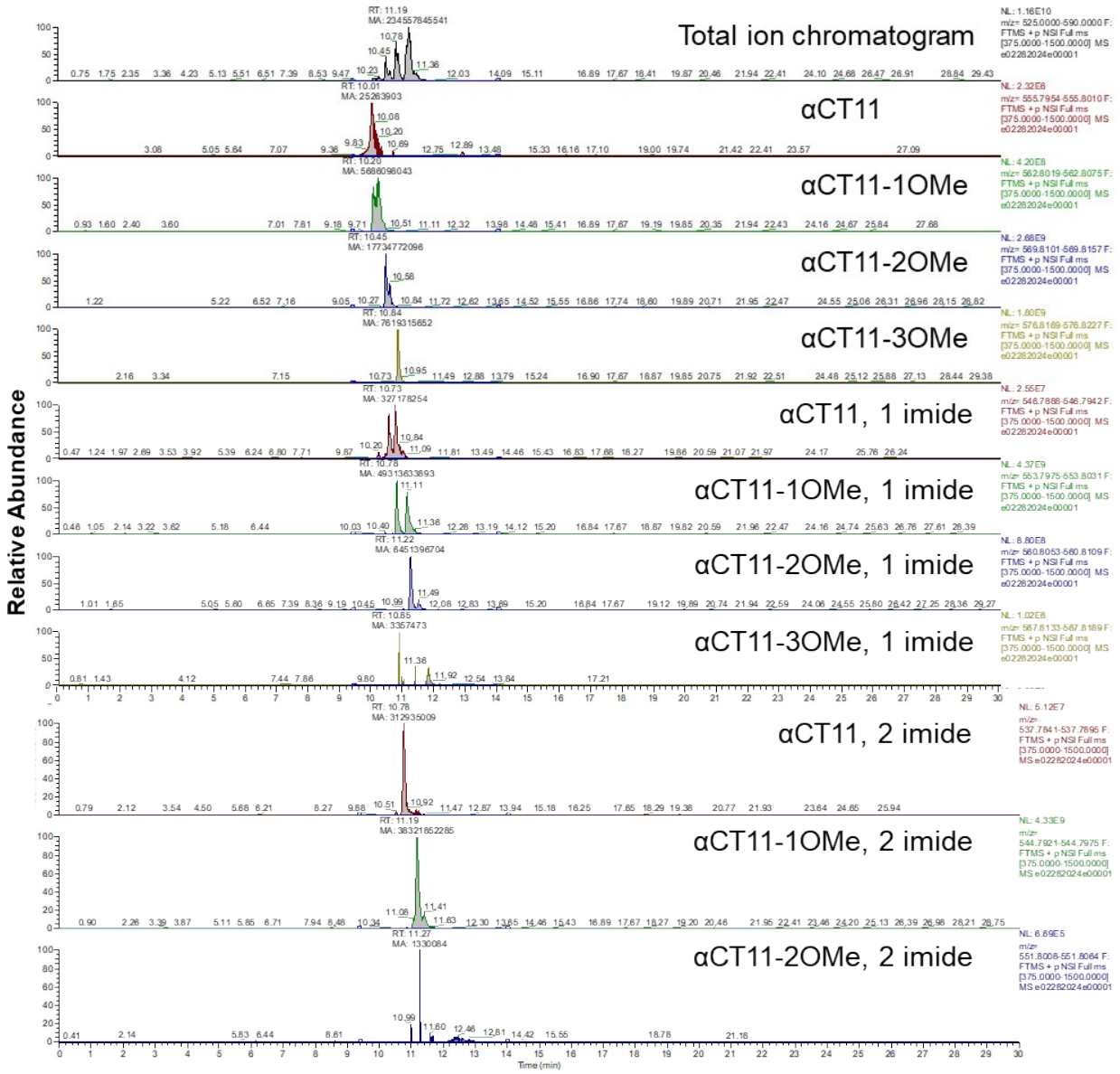

Figure S46. LC-MS chromatograms of αCT11-3OMe(D5,D6,E8) after 2 h of stirring in 1X PBS (pH 7.4) at 37 °C. Total ion chromatogram (top, gray) and selective ion chromatograms for αCT11 with different numbers of esters and/or imides.

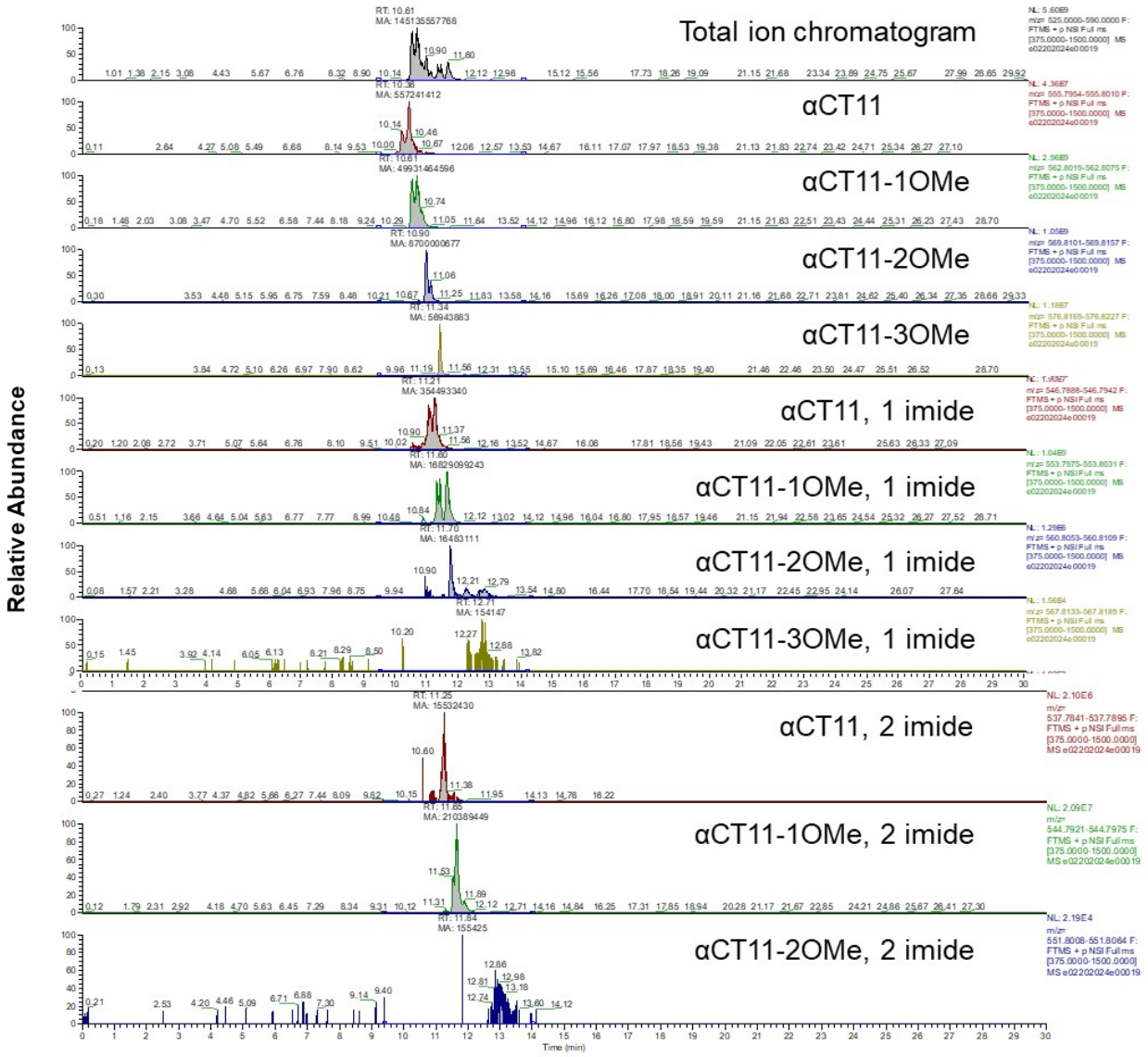

Figure S47. LC-MS chromatograms of αCT11-3OMe(D5,D6,E8) after 6 h of stirring in 1X PBS (pH 7.4) at 37 °C. Total ion chromatogram (top, gray) and selective ion chromatograms for αCT11 with different numbers of esters and/or imides.

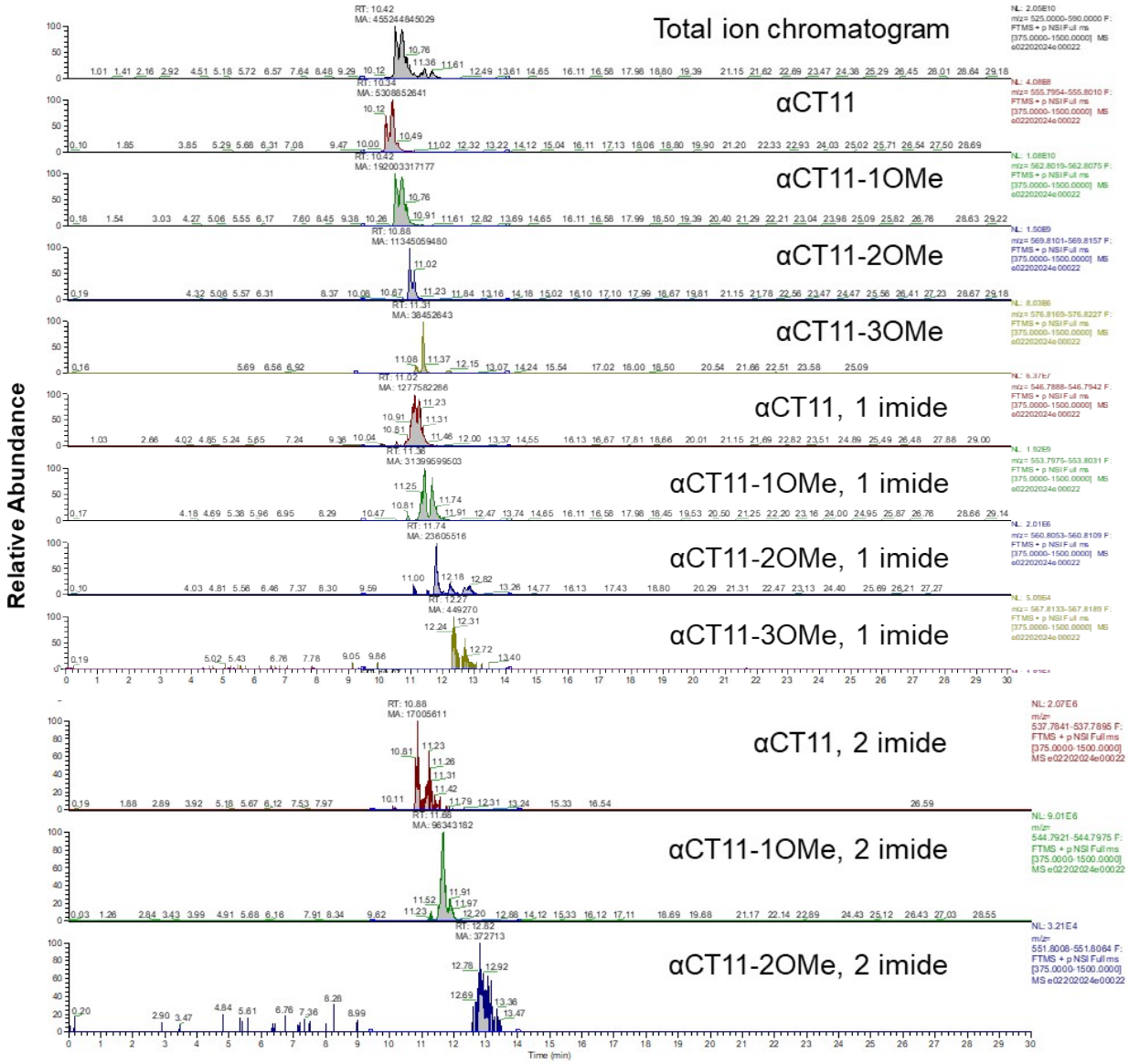

Figure S48. LC-MS chromatograms of αCT11-3OMe(D5,D6,E8) after 12 h of stirring in 1X PBS (pH 7.4) at 37 °C. Total ion chromatogram (top, gray) and selective ion chromatograms for αCT11 with different numbers of esters and/or imides.

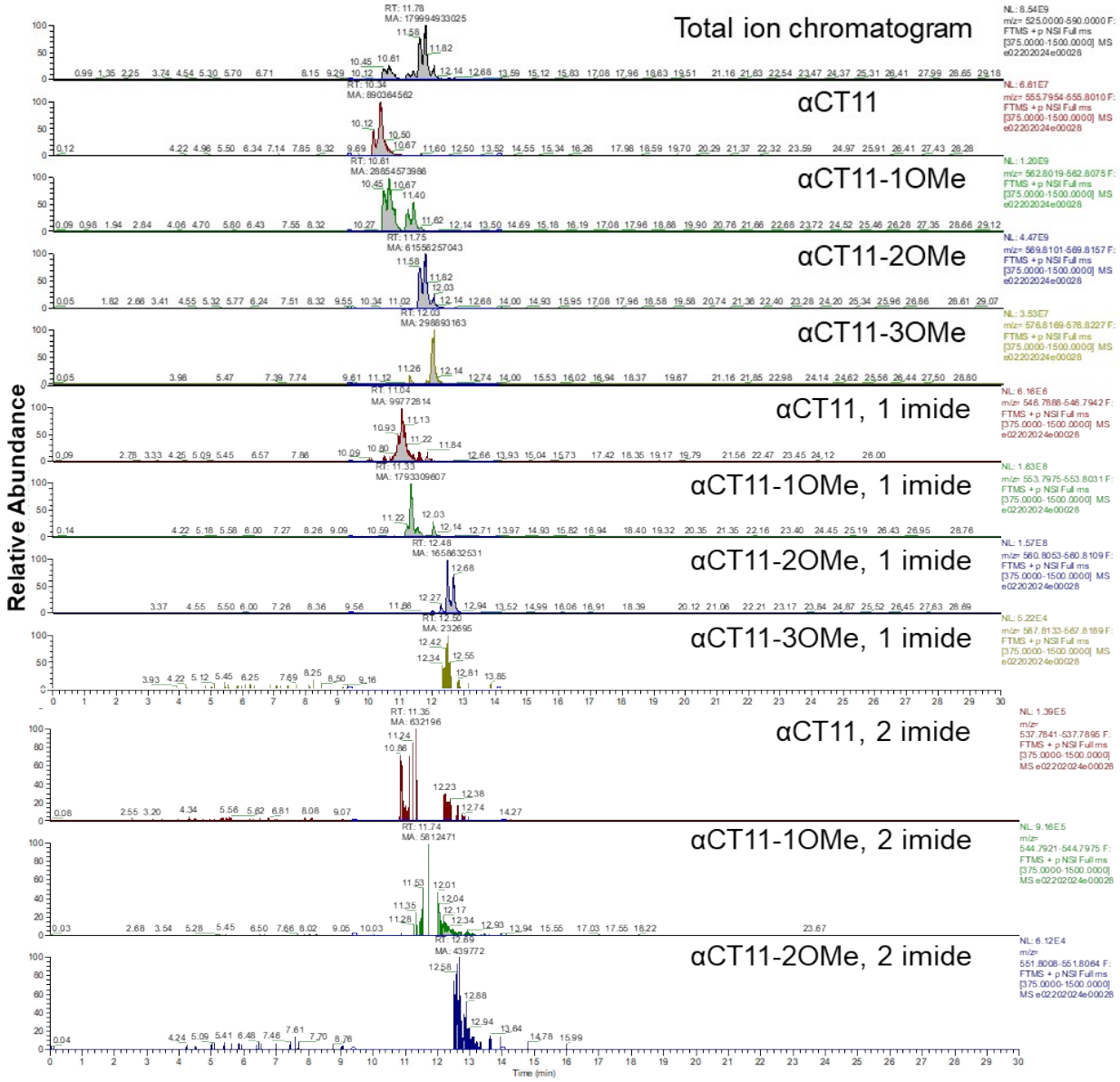

Figure S49. LC-MS chromatograms of αCT11-3OMe(D5,D6,E8) after 24 h of stirring in 1X PBS (pH 7.4) at 37 °C. Total ion chromatogram (top, gray) and selective ion chromatograms for αCT11 with different numbers of esters and/or imides.

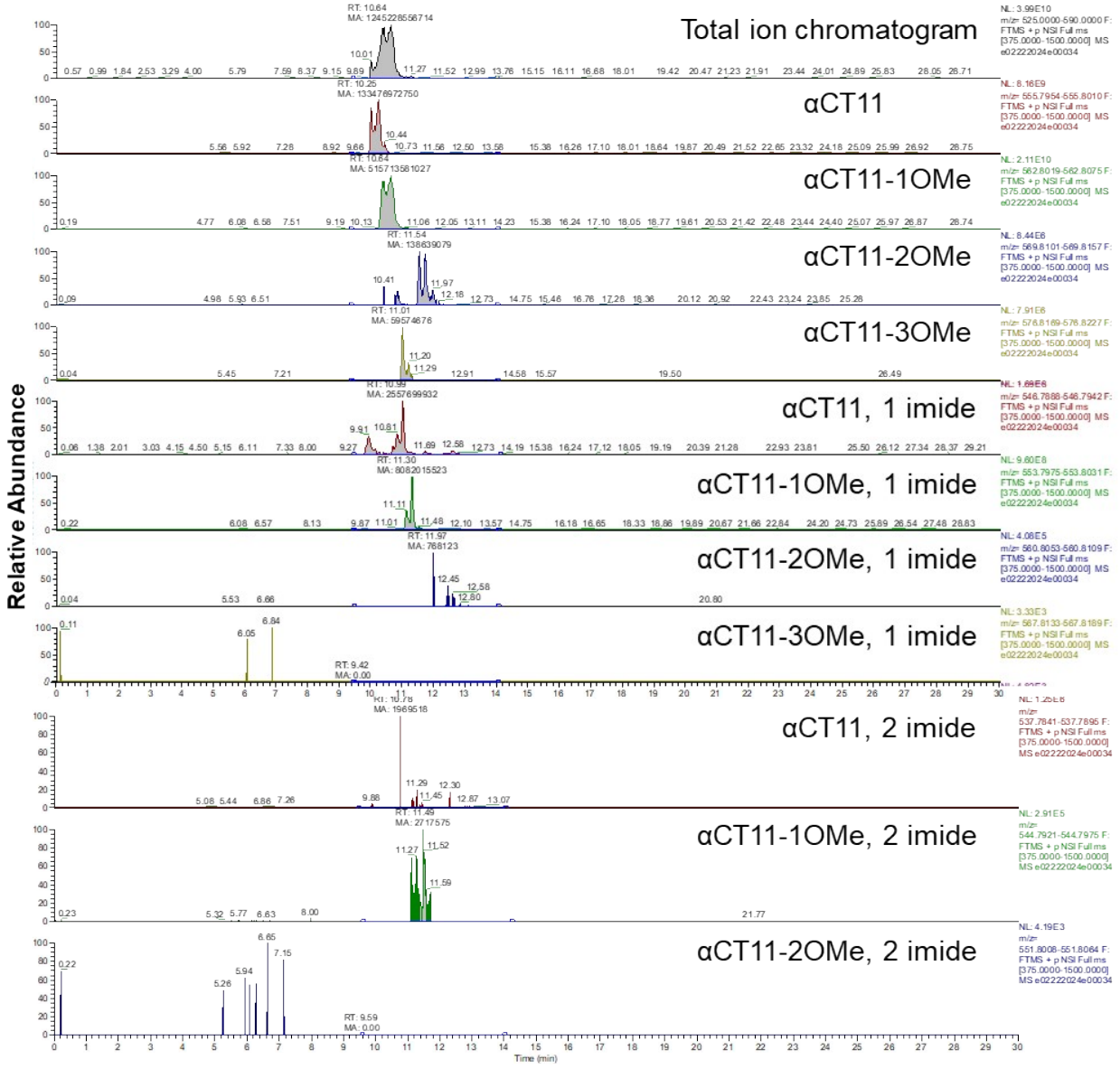

Figure S50. LC-MS chromatograms of αCT11-3OMe(D5,D6,E8) after 1 week of stirring in 1X PBS (pH 7.4) at 37 °C. Total ion chromatogram (top, gray) and selective ion chromatograms for αCT11 with different numbers of esters and/or imides.

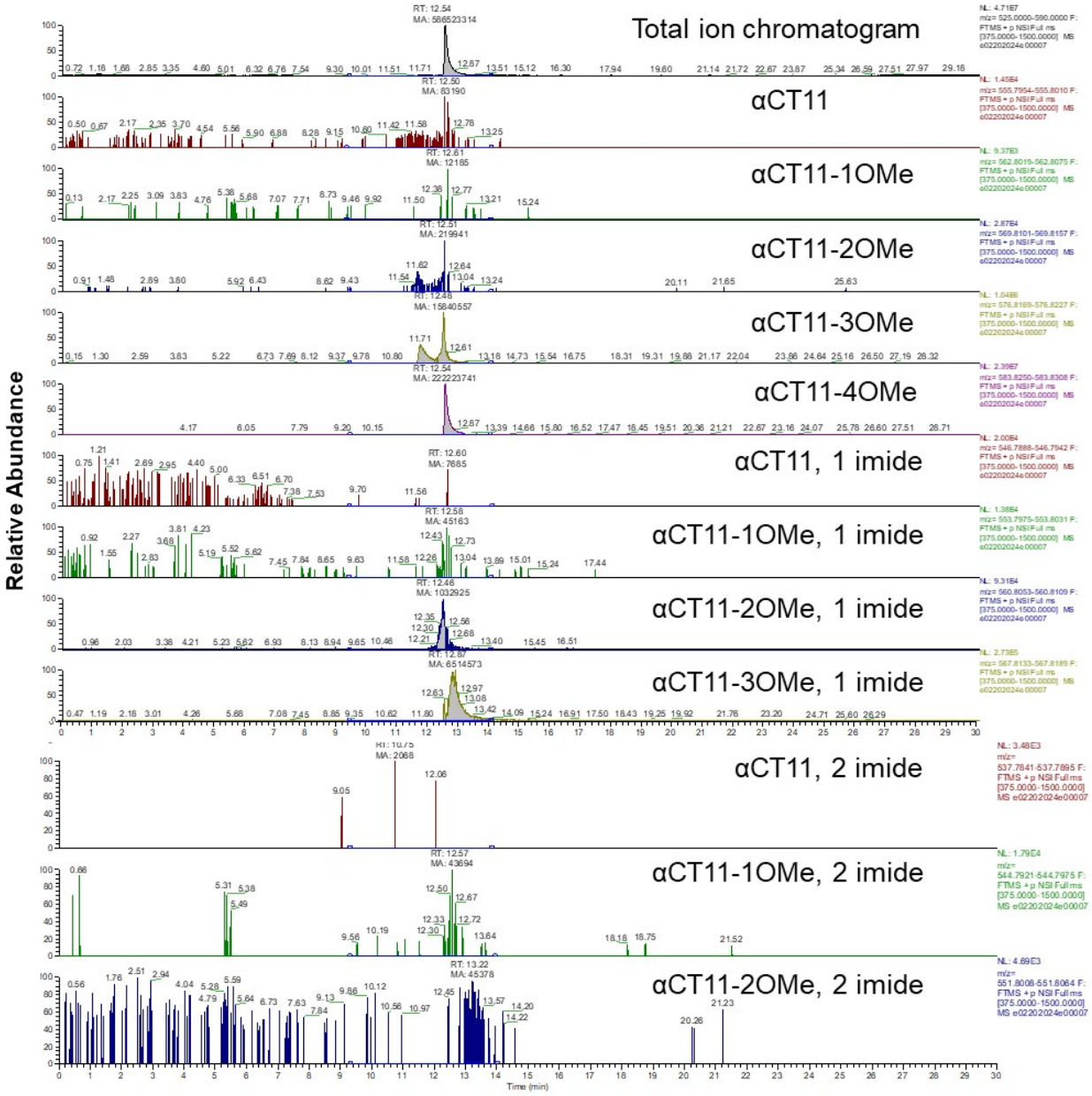

Figure S51. LC-MS chromatograms of αCT11-4OMe after 5 min of incubation in 37 °C 1X PBS (pH 7.4). Total ion chromatogram (top, gray) and selective ion chromatograms for αCT11 with different numbers of esters and/or imides.

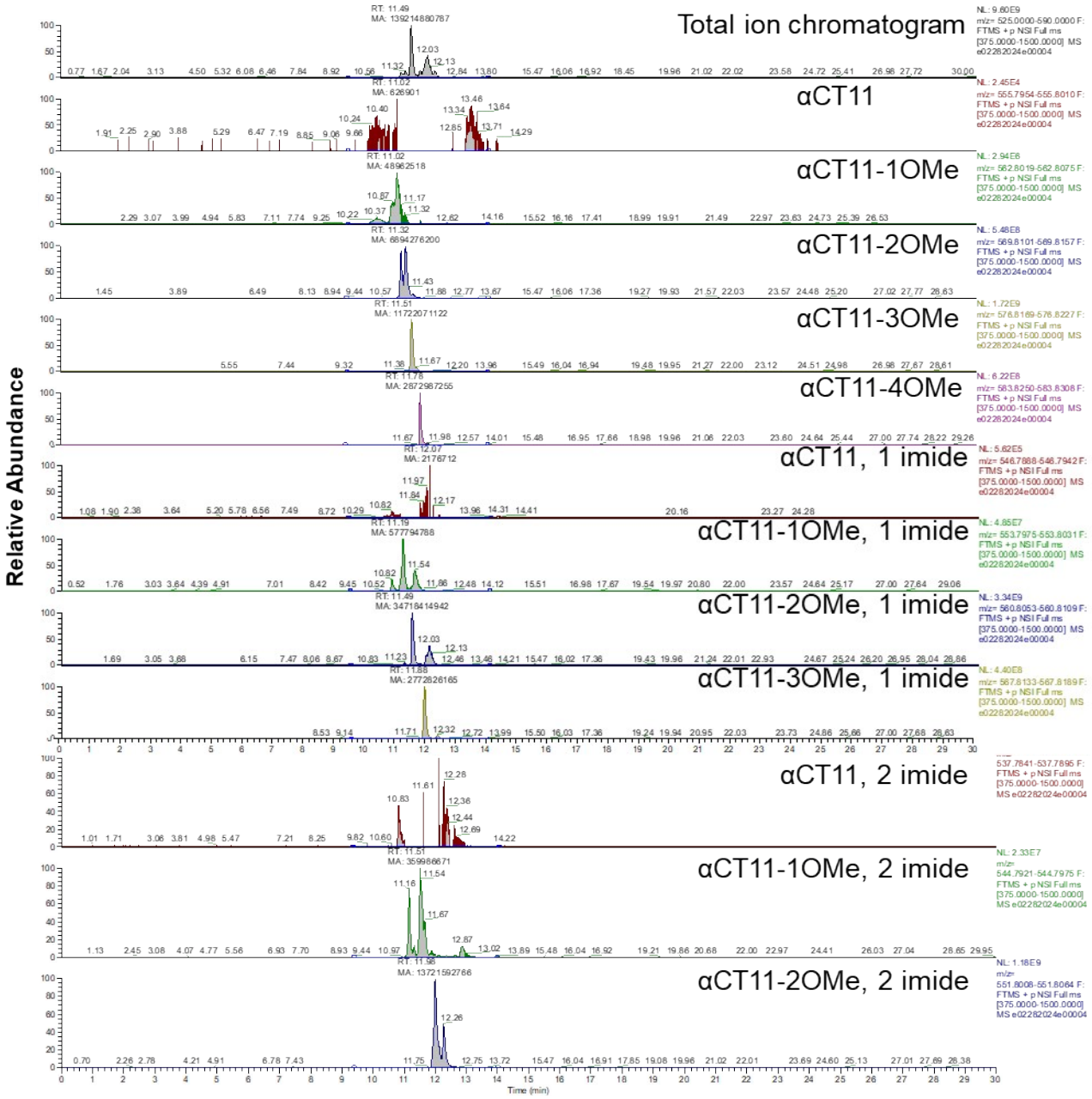

Figure S52. LC-MS chromatograms of αCT11-4OMe after 2 h of stirring in 1X PBS (pH 7.4) at 37 °C. Total ion chromatogram (top, gray) and selective ion chromatograms for αCT11 with different numbers of esters and/or imides.

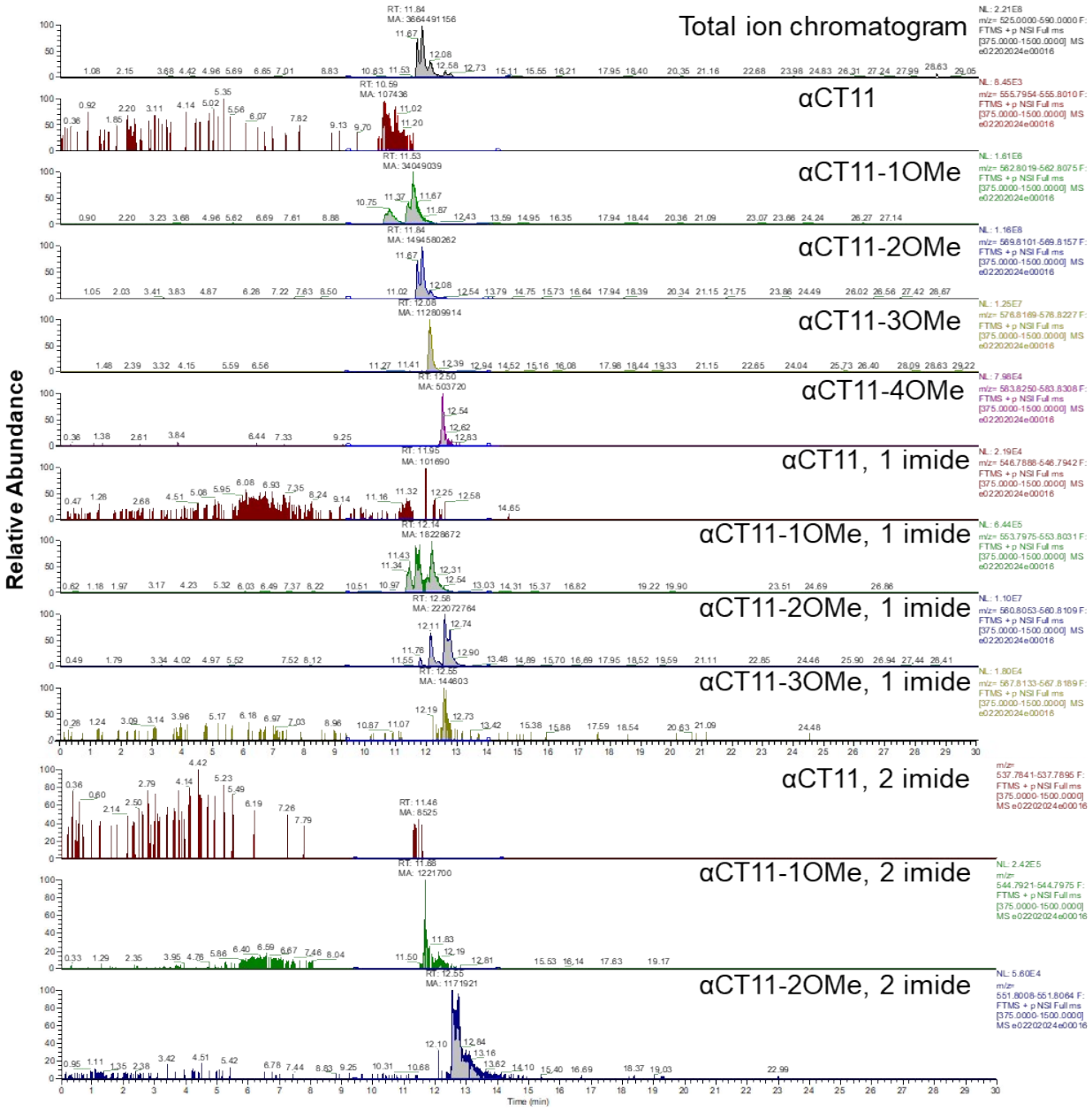

Figure S53. LC-MS chromatograms of αCT11-4OMe after 6 h of stirring in 1X PBS (pH 7.4) at 37 °C. Total ion chromatogram (top, gray) and selective ion chromatograms for αCT11 with different numbers of esters and/or imides.

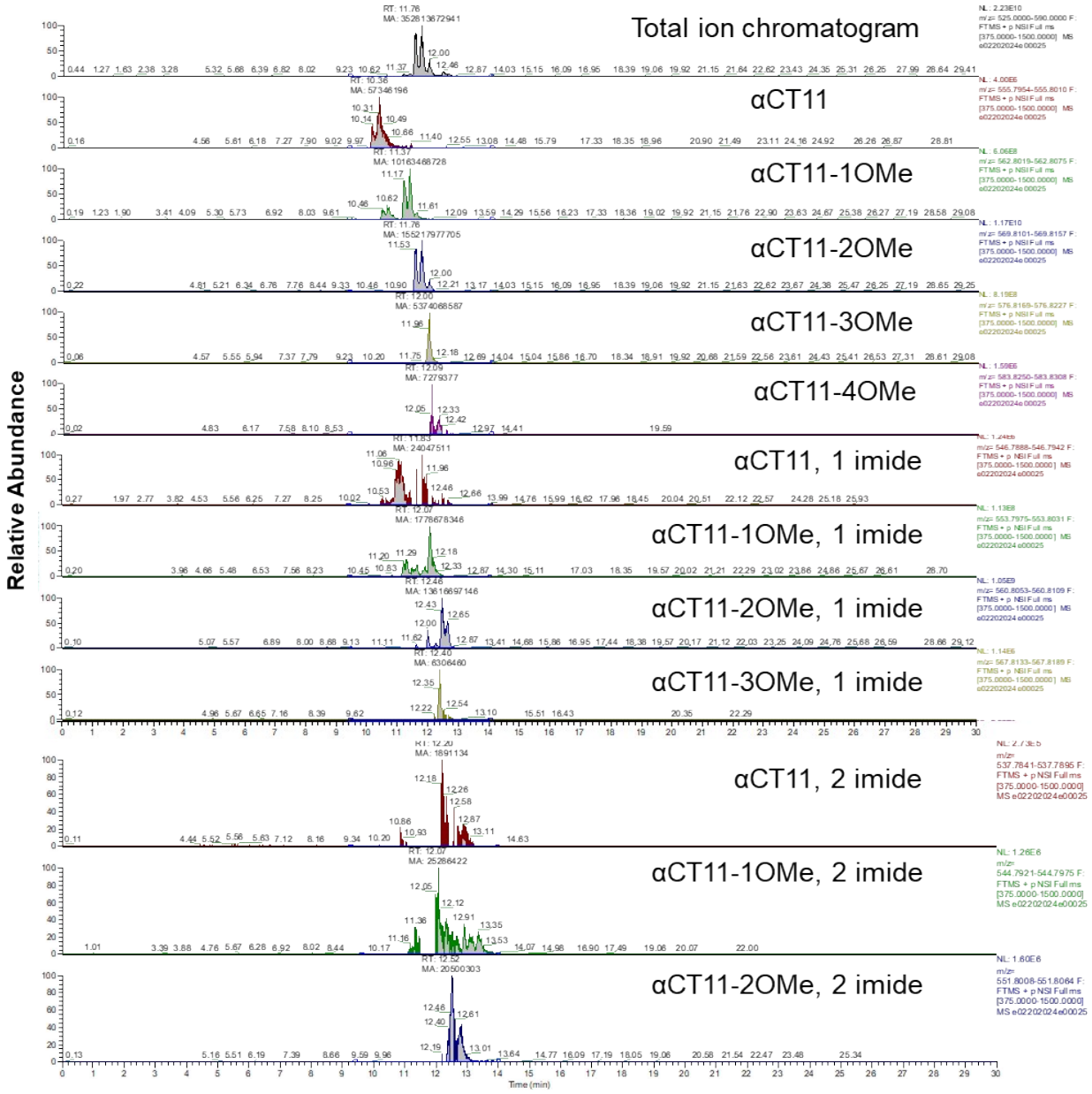

Figure S54. LC-MS chromatograms of αCT11-4OMe after 12 h of stirring in 1X PBS (pH 7.4) at 37 °C. Total ion chromatogram (top, gray) and selective ion chromatograms for αCT11 with different numbers of esters and/or imides.

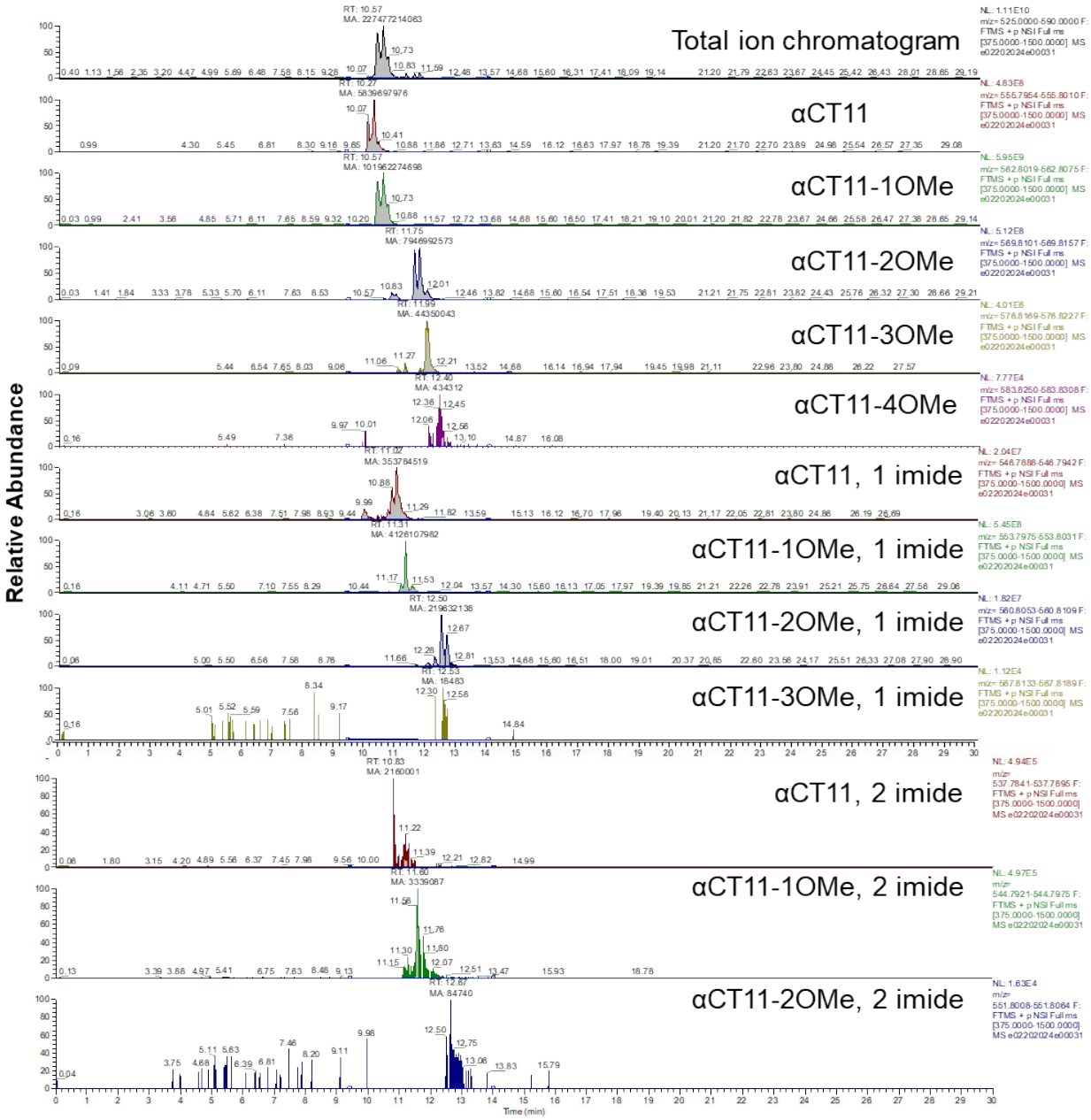

Figure S55. LC-MS chromatograms of αCT11-4OMe after 24 h of stirring in 1X PBS (pH 7.4) at 37 °C. Total ion chromatogram (top, gray) and selective ion chromatograms for αCT11 with different numbers of esters and/or imides.

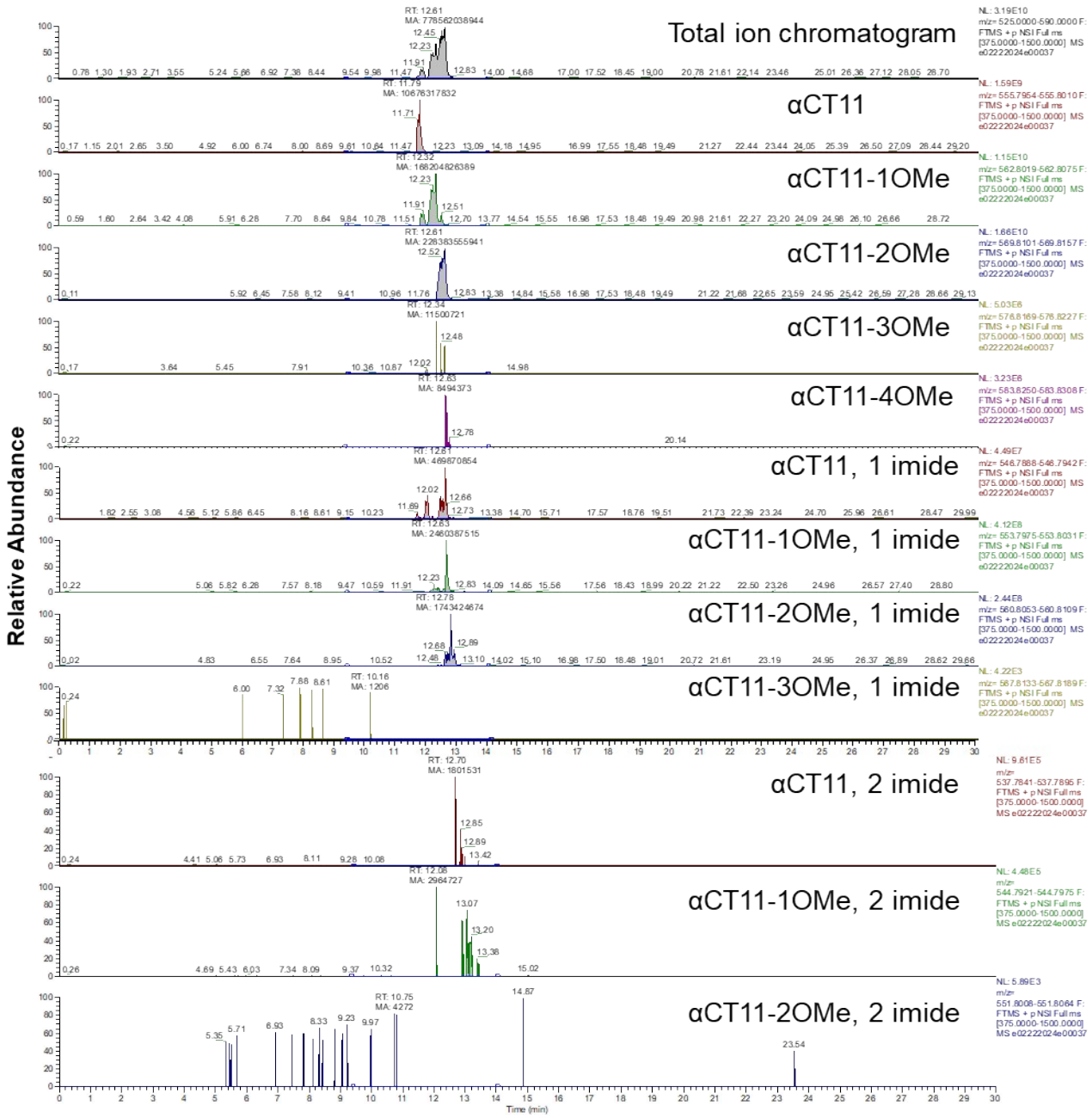

Figure S56. LC-MS chromatograms of αCT11-4OMe after 1 week of stirring in 1X PBS (pH 7.4) at 37 °C. Total ion chromatogram (top, gray) and selective ion chromatograms for αCT11 with different numbers of esters and/or imides.

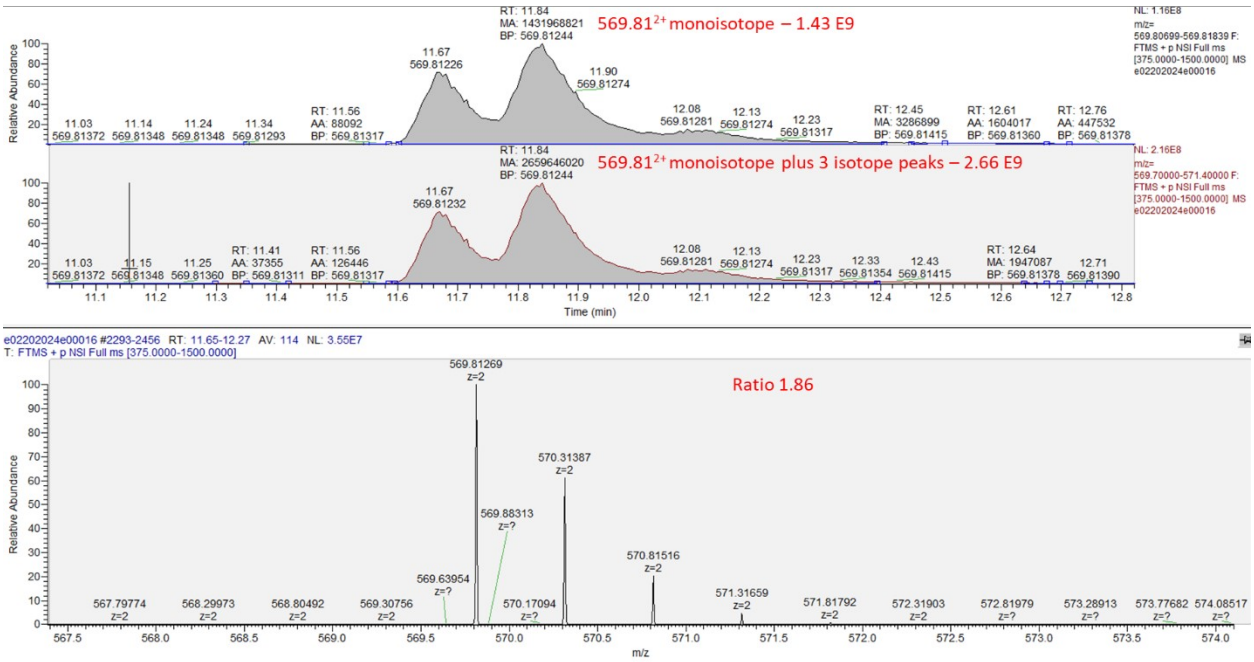

Figure S57. LC-MS chromatograms of relevant isotopes of αCT11-3OMe(D5,D6,E8) after 5 min of incubation in 37 °C 1X PBS (pH 7.4). The ratio of the area of the monoisotope (569.81) and 3 additional isotope peaks in the chromatogram to just the area of the monoisotope is 1.86; thus, all monoisotope selective ion chromatogram areas were multiplied by 1.9 to account for the additional isotopes.

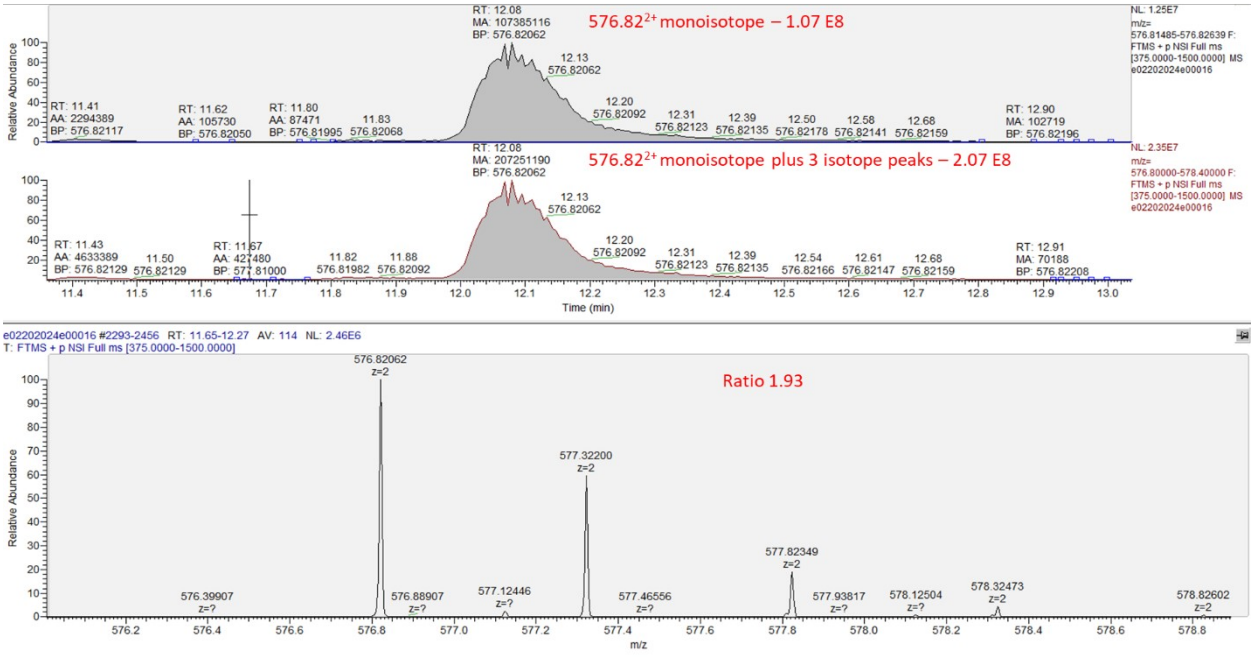

Figure S58. LC-MS chromatograms of relevant isotopes of αCT11-4OMe after 5 min of incubation in 37 °C 1X PBS (pH 7.4). The ratio of the area of the monoisotope (576.82) and 3 additional isotope peaks in the chromatogram to just the area of the monoisotope is 1.93; thus, all monoisotope selective ion chromatogram areas were multiplied by 1.9 to account for the additional isotopes.

Table S12. % Abundance and retention times (RT, min) of αCT11-based formulations produced by the hydrolysis of αCT11-3OMe(D5,D6,E8) in 37 °C 1X PBS over 7 d, quantified by LC-MS.

		Ester #										Total
		0		1		2		3		4		
		% Abundance	RT (min)	% Abundance	RT (min)	% Abundance	RT (min)	% Abundance	RT (min)	% Abundance	RT (min)	**% Abundance**
Initial	no imides	0.01	-	0.01	-	1.72	*11.40*	90.20	11.48	N/A	N/A	**91.94**
	1 imide	0.03	-	0.03	-	0.01	-	0.01	-	N/A	N/A	**0.08**
	2 imides	0.00	-	0.03	-	0.00	-	N/A	N/A	N/A	N/A	**0.03**
2 h	no imides	0.02	-	4.61	10.20 10.10	14.37	10.45 10.58	6.17	10.84	N/A	N/A	**25.16**
	1 imides	0.27	-	39.95	10.78 11.11	5.23	11.22 11.49	0.00	-	N/A	N/A	**45.44**
	2 imides	0.25	-	31.04	11.19	0.00	-	N/A	N/A	N/A	N/A	**31.30**
6 h	no imides	0.73	-	65.37	10.61 10.74	11.39	10.09 11.06	0.01	-	N/A	N/A	**77.49**
	1 imide	0.46	-	22.03	11.20 11.40 11.60	0.02	-	0.00	-	N/A	N/A	**22.52**
	2 imides	0.20	-	0.28	-	0.00	-	N/A	N/A	N/A	N/A	**0.48**
12 h	no imides	2.22	10.12 10.34	80.13	10.42 10.60	4.73	10.88 11.02	0.02	-	N/A	N/A	**87.10**
	1 imide	0.53	-	13.10	11.36 11.60	0.01	-	0.00	-	N/A	N/A	**13.65**
	2 imides	0.01	-	0.04	-	0.00	-	N/A	N/A	N/A	N/A	**0.05**
1 d	no imides	4.88	10.12 10.34	85.16	10.45 10.61 11.20	6.64	11.58 11.75 12.03	0.04	-	N/A	N/A	**96.72**
	1 imide	0.30	-	3.45	11.22 11.33 12.03	0.18	-	0.00	-	N/A	N/A	**3.93**
	2 imides	0.00	-	0.00	-	0.00	-	N/A	N/A	N/A	N/A	**0.00**
7 d	no imides	20.37	10 10.25	78.69	10.40 10.64	0.21	-	0.01	-	N/A	N/A	**99.28**
	1 imide	0.39	-	1.23	11.11 11.30	0.00	-	0.00	-	N/A	N/A	**1.62**
	2 imides	0.00		0.00		0.00		N/A	N/A	N/A	N/A	**0.00**

*Only retention times for products over 1% abundance were reported

Table S13. % Abundance and retention times (RT, min) of αCT11-based formulations produced by the hydrolysis of αCT11-4OMe in 37 °C 1X PBS over 7 d, quantified by LC-MS

		Ester #										Total
		0		1		2		3		4		
		% Abundance	RT (min)	% Abundance	RT (min)	% Abundance	RT (min)	% Abundance	RT (min)	% Abundance	RT (min)	**% Abundance**
Initial	no imides	0.03	-	0.00	-	0.07	-	5.13	12.48	71.99	12.54	**77.22**
	1 imide	0.00	-	0.01	-	0.33	-	2.11	12.87	N/A	N/A	**2.46**
	2 imides	0.00	-	0.01	-	0.01	-	N/A	N/A	N/A	N/A	**0.03**
2 h	no imides	0.00	-	0.07	-	9.41	11.20 11.32	16.00	11.51	3.92	11.78	**29.40**
	1 imides	0.00	-	0.79	-	47.38	11.49 12.03	3.78	11.88	N/A	N/A	**51.96**
	2 imides	0.00	-	0.49	11.19	18.73	11.98 12.26	N/A	N/A	N/A	N/A	**19.22**
6 h	no imides	0.01	-	1.77	10.75 11.37 11.53	77.49	11.87 11.84 12.08	5.85	12.08	0.03	-	**85.14**
	1 imide	0.01	-	0.95	-	11.51	12.11 12.58 12.74	0.01	-	N/A	N/A	**12.47**
	2 imides	0.00	-	0.06	-	0.06	-	N/A	N/A	N/A	N/A	**0.12**
12 h	no imides	0.03	-	5.47	11.17 11.37	83.59	11.53 11.76	2.89	12.00	0.00	-	**91.99**
	1 imide	0.01	-	0.96	-	7.33	12.46 12.65	0.00	-	N/A	N/A	**8.31**
	2 imides	0.00	-	0.01	-	0.01	-	N/A	N/A	N/A	N/A	**0.03**
1 d	no imides	0.94	-	30.46	10.40 10.57 10.73	64.98	11.60 11.75 12.01	0.32	-	0.01	-	**96.70**
	1 imide	0.11	-	1.89	11.17 11.31 11.53	1.75	12.50 12.67 12.81	0.00	-	N/A	N/A	**3.75**
	2 imides	0.00	-	0.01	-	0.00	-	N/A	N/A	N/A	N/A	**0.00**
7 d	no imides	2.61	11.79	41.05	11.91 12.23 12.32 12.51	55.73	12.52 12.61	0.00	-	0.00	-	**99.39**
	1 imide	0.11	-	0.60	-	0.43	-	0.00	-	N/A	N/A	**1.14**
	2 imides	0.00	-	0.00	-	0.00	-	N/A	N/A	N/A	N/A	

*Only retention times for products over 1% abundance were reported

Section S4: Activity of esterified αCT11

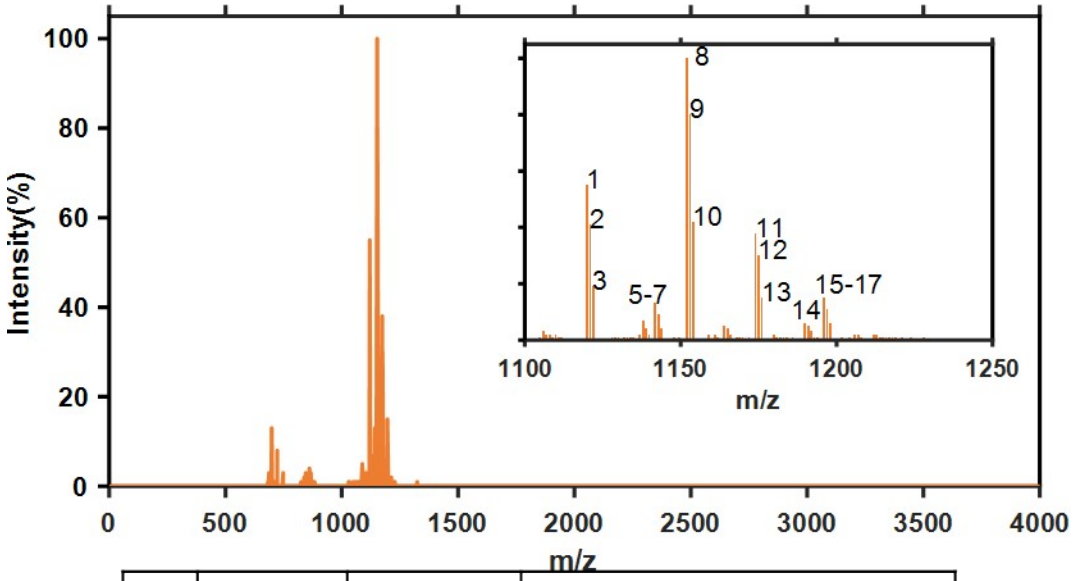

label	Mass (Da)	Intensity (%)	Species
1	1119.9	55	[αCT11-2OMe + 1 imide + H]+
2	1121	41	[αCT11-2OMe + 1 imide + H]+
3	1122	19	[αCT11-2OMe + 1 imide + H]+
4	1138	7	[αCT11-2OMe + H]+
5	1141.9	13	[αCT11-2OMe + 1 imide + Na]+
6	1142.8	9	[αCT11-2OMe + 1 imide + Na]+
7	1151.9	100	[αCT11-3OMe + H]+
8	1153	80	[αCT11-3OMe + H]+
9	1154	42	[αCT11-3OMe + H]+
10	1174	38	[αCT11-3OMe + Na]+
11	1174.9	30	[αCT11-3OMe + Na]+
12	1176	15	[αCT11-3OMe + Na]+
13	1189.9	6	[αCT11-3OMe + K]+
14	1196	15	[αCT11-3OMe + 2Na - H]+
15	1197	11	[αCT11-3OMe + 2Na - H]+
16	1198	6	[αCT11-3OMe + 2Na - H]+

Figure S59. MALDI-TOF MS of αCT11-3OMe(D5,D6,E8) after the trifluoroacetate counterion exchange. Multiple esterified αCT11 species, but no activated αCT11, were detected, suggesting a small amount of hydrolysis over the counterion exchange.

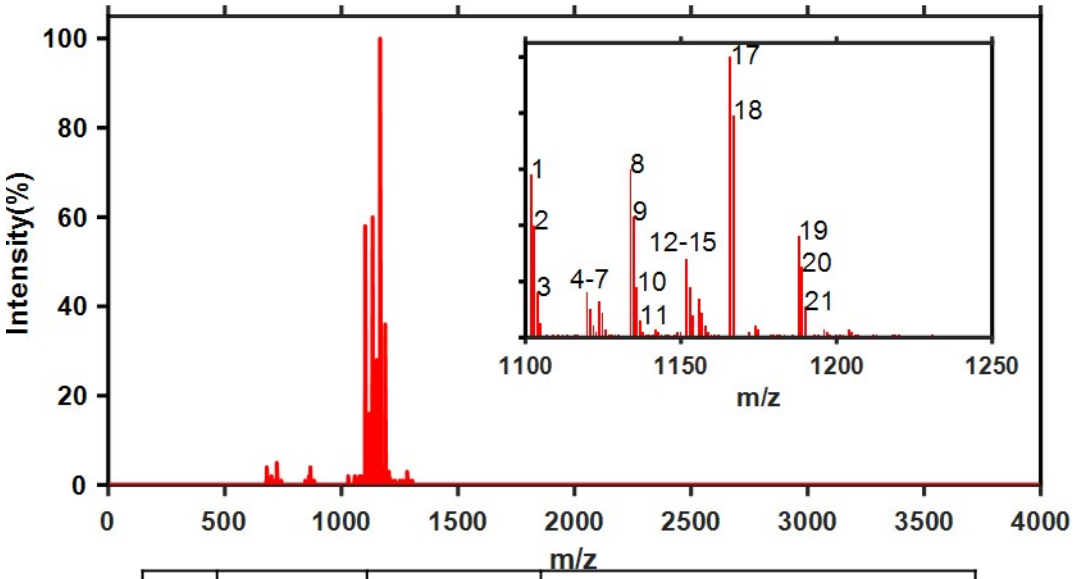

label	Mass (Da)	Intensity (%)	Species
1	1101.8	58	[αCT11-2OMe + 2 imide + H]+
2	1102.8	40	[αCT11-2OMe + 2 imide + H]+
3	1103.9	16	[αCT11-2OMe + 2 imide + H]+
4	1119.8	16	[αCT11-2OMe + 1 imide + H]+
5	1120.8	10	[αCT11-2OMe + 1 imide + H]+
6	1123.8	13	[αCT11-1OMe + H]+
7	1124.8	9	[αCT11-1OMe + H]+
8	1133.8	60	[αCT11-3OMe + 1 imide + H]+
9	1134.8	43	[αCT11-3OMe + 1 imide + H]+
10	1135.8	18	[αCT11-3OMe + 1 imide + H]+
11	1136.9	6	[αCT11-3OMe + 1 imide + H]+
12	1151.8	28	[αCT11-3OMe + H]+
13	1152.9	18	[αCT11-3OMe + H]+
14	1153.8	8	[αCT11-3OMe + H]+
15	1155.9	14	[αCT11-3OMe + 1 imide + Na]+
16	1156.8	9	[αCT11-3OMe + 1 imide + Na]+
17	1165.8	100	[αCT11-4OMe + H]+
18	1166.9	79	[αCT11-4OMe + H]+
19	1187.9	36	[αCT11-4OMe + Na]+
20	1188.9	25	[αCT11-4OMe + Na]+
21	1189.9	11	[αCT11-4OMe + Na]+

Figure S60. MALDI-TOF MS of αCT11-4OMe after the trifluoroacetate counterion exchange. Multiple esterified αCT11 species, but no activated αCT11, were detected, suggesting a small amount of hydrolysis over the counterion exchange.

Table S14. Scratch wound assay results: relative migration indices (Rel. Mis) and standard deviation for each individual scratched cell culture and their averages.

Cell Culture:	Vehicle		αCT11		3OMe(D5,D6,E8)		4OMe	
	Rel. MI	StDev	Rel. MI	StDev	Rel. MI	StDev	Rel. MI	StDev
1	1.0	0.3	1.7	1.2	6.0	1.7	8.1	0.9
2	1.0	0.3	1.4	0.5	5.3	1.4	6.6	0.7
3	1.0	0.8	1.0	0.4	3.1	0.5	4.0	0.5
Average	**1.0**	**0.0**	**1.4**	**0.4**	**4.8**	**1.5**	**6.2**	**2.1**

Table S15. Statistical analysis of scratch wound assays: one-tailed paired t-tests assuming unequal variances (confidence interval = 0.95).

Treatment	Vehicle	αCT11	3OMe(D5,D6,E8)	4OMe
Vehicle		0.11	0.02	0.02
αCT11			0.03	0.03
3OMe(D5,D6,E8)				0.19
4OMe				